The role of abnormal neutrophil activation in psoriasis

Vergnano, Marta

Awarding institution:
King's College London

THE ROLE OF ABNORMAL NEUTROPHIL ACTIVATION IN PSORIASIS

By

Marta Vergnano

A thesis submitted in fulfilment of the requirements for the degree of Doctor of Philosophy at King's College London

Department of Medical and Molecular Genetics

King's College London

9th floor, Tower Wing, Guy's Hospital

Great Maze Pond, London SE1 9RT

September 2019

ACKNOWLEDGEMENTS

It has been a privilege to work in Dr Francesca Capon's group and having her as my first supervisor. She probably doesn't know, but back in 2015 I almost chose a project with another supervisor: I am forever grateful I didn't! She has supported me and taught me a lot, from how to be thrifty with lab consumables to trouble-shooting experiments. She helped me grow as a scientist and a person, guiding me closely throughout my project. Shout out to her incredible memory, which has been life-saving whenever my notes were failing me! Although she often has the "Calimero syndrome", in the past 4 years Francesca has achieved a lot: the group has grown, more funding has come in together with important publications, and I am really thankful I was there to witness it.

I am also in debt with my second supervisor Prof Catherine Smith for the incredible chance she gave me to take a pick at the clinical aspect of the project. She has always been very supportive and in the last year she welcomed me as a member of her Skin Therapy Research Unit, where I can now see first-hand how our work can make a difference for patients affected by psoriasis. I am also grateful to Dr Paola Di Meglio for her guidance and help with my flow cytometry experiments.

Thank you to my fellow PhD students Marika Catapano, Satveer Mahil and Sophie Twelves for being great scientists and most of all friends over the past 4 years! It has also been a pleasure to work with the rest of the Capon lab members: if I am here now it's also because of your dedication and technical help.

I would like to thank my family for their affection and support despite the distance, and in particular my grandma Elena, who never failed to tell me that there is no cure for psoriasis as her friend had it for all her life (true story): I'd like to think my work will one day contribute to prove her wrong!

Finally, to Enrico, mio marito: I wouldn't be here without you (literally, I wouldn't have move to the UK if you hadn't started your PhD in 2012). Your faith in me, encouragements and love, accompanied by delicious risotti, a positive attitude towards

life and a contagious smile, are a constant reminder to look at bright side and be thankful for what we have achieved.

CONTRIBUTIONS

I declare that the work carried out in this thesis was performed by myself, with the following exceptions. Ms Marika Catapano developed the RNA sequencing analysis pipeline and adapted a published script to identify blood transcription modules. She also contributed to the assessment of IL-36R surface expression in innate immune cells as well as to the PBMC and pDC stimulations described in chapter 5. Whole-exome sequencing was performed by technical staff from the Genomics Core facility of Guy's and St Thomas' Hospital Biomedical Research Centre (BRC), while the raw sequence data was processed by the BRC Bioinformatics Core.

ABSTRACT

Psoriasis is a complex skin disorder that has been classified into several forms. These include common psoriasis vulgaris (PsV), a T-cell mediated disease, and Generalised Pustular Psoriasis (GPP), a rare condition associated with neutrophilic inflammation. While the genetic basis of PsV has been extensively studied, only a few innate immune genes have been associated with GPP.

Neutrophils are the first cells to migrate toward sites of infection, where they recruit and activate T cells, as well as keratinocytes, thus amplifying the cutaneous inflammatory response. Hence, the current project sought to investigate the role of abnormal neutrophil activation in psoriasis.

The initial focus of the study was the identification of new disease genes by means of whole-exome-sequencing. A Chinese-Malay family where several members suffered from PsV and/or GPP was first analysed, in order to identify new genetic determinants of neutrophilic skin inflammation. This uncovered a candidate disease variant in *PRR13*, with a second damaging change observed in an unrelated individual sequenced by the 100,000 Genomes Project. While the function of *PRR13* is poorly understood, alleles at this locus have been associated with neutrophil count variation in a genome-wide study.

Next, the analysis of 147 pustular psoriasis patients uncovered two individuals with a homozygous splicing variant in *MPO*, a gene that is crucial to the microbicidal activity of neutrophils. Importantly, the variant was associated with increased neutrophil counts.

In the final stage of the project, neutrophil RNA-sequencing was undertaken in 8 GPP cases vs. 11 controls. This identified an unexpected type-I IFN signature in patient neutrophils, an observation that was also validated in a PsV cohort. Mechanistic experiments demonstrated that the up-regulation of type-I IFN genes is driven by IL-36, which potentiates IFN-α production by enhancing TLR-9 activation in plasmacytoid dendritic cells.

Taken together, these findings identify new molecular pathways causing abnormal neutrophil activation in plaque and pustular forms of psoriasis.

TABLE OF CONTENTS

LIST OF TABLES

LIST OF FIGURES

ABBREVIATIONS

ACH	Acrodermatitis continua of Hallopeau
AP1S3	Adaptor related protein complex 1 subunit sigma 3 gene
APP	Acral pustular psoriasis
B2M	Beta-2-Microglobulin
BSA	Bovine serum albumin
BSA	Body surface area
CADD	Combined annotation dependent depletion
CANDLE	Chronic atypical neutrophilic dermatosis with lipodystrophy and elevated temperature syndrome
CAPS	Cryopyrin associated periodic syndrome
CARD14	Caspase recruitment domain family, member 14 gene
CCL	C-C motif ligand
CGD	Chronic granulomatous diseases
CXCL	C-X-C motif ligand
CyTOF	Mass cytometry by time-of-flight
DEG	Differentially expressed gene
DITRA	Deficiency of the IL-36 receptor antagonist disorder
EDC	Epidermal differentiation cluster
FAP	Functional annotation of psoriasis susceptibility alleles
FBS	Fetal bovine serum
FC	Fold change
FDR	False discovery rate
fMLP	N-Formylmethionyl-leucyl-phenylalanine
GPP	Generalised pustular psoriasis
GWAS	Genome wide association studies

HLA	Human leukocyte antigen
HSC	Hematopoietic stem cell
IFN	Interferon
IL	Interleukin
IL-1RAcP	Interleukin 1 receptor accessory protein
IL-36	Interleukin 36
IL-36R	Interleukin 36 receptor
IL-36Ra	Interleukin 36 receptor antagonist
IL36RN	Interleukin 36 receptor antagonist gene
IPA	Ingenuity pathway analysis
IRAK	Interleukin 1 receptor associated kinase
IS	Interferon score
ISGs	Interferon stimulated genes
JAK	Janus kinase
LDNs	Low-density neutrophils
MAF	Minor allele frequency
MAPK	Mitogen-activated protein kinase
mDC	Myeloid dendritic cell
MHC	Major histocompatibility complex
MMP9	Matrix metalloproteinase 9
MPO	Myeloperoxidase
MyD88	Myeloid differentiation primary response 88
MZB	Marginal zone B cells
NADPH	Nicotinamide adenine dinucleotide phosphate
NE or ELANE	Neutrophil elastase
NETs	Neutrophil extracellular traps
NF-κB	Nuclear factor-κB

NK	Natural killer (cells)
PASI	Psoriasis area severity index
PBMCs	Peripheral blood mononuclear cells
PBS	Phosphate buffered saline
PCR	Polymerase chain reaction
pDC	Plasmacytoid dendritic cell
PheWAS	Phenome-wide association scan
PLSCR1	Phospholipid scramblase 1
PLUM	Pustular psoriasis, eLucidating Underlying Mechanisms
PMNs	Polymorphonuclear leukocytes
PPP	Palmoplantar pustular psoriasis
PROVEAN	Protein variation effect analyser
PRP	Pityriasis rubra pilaris
PRR13	Proline rich protein 13
PsA	Psoriatic arthritis
PsV	Psoriasis vulgaris
RIN^e	RNA integrity number equivalent
ROS	Reactive oxygen species
RPL13A	Ribosomal protein L13a
RPKM	Reads per kilobase per million
RPMI	Roswell park memorial institute
SD	Standard deviation
SEM	Standard error of the mean
SIFT	Sorting intolerant from tolerant
SLE	Systemic lupus erythematosus
SNP	Single nucleotide polymorphism
TLR	Toll-like receptor

TNF	Tumor necrosis factor
Tollip	Toll interacting protein
TPM	Transcript per million
TSP1	Thrombospondin 1 gene
TYK2	Tyrosine Kinase 2
VEGF	Vascular endothelial growth factor
WES	Whole-exome sequencing

1 INTRODUCTION

1.1 Psoriasis

1.1.1 Overview

Psoriasis is a chronic inflammatory skin disease affecting around 2% of the population worldwide, and occurring with a prevalence as high as 4% in North-European countries[1]. Several studies report a bimodal distribution of age of onset, with peaks around 30–39 and 50–69 years of age. Conversely, no significant sex difference is observed in disease frequency[2].

Psoriasis is generally considered a multifactorial condition caused by the interaction of environmental triggers (e.g. mechanical skin trauma, stress, smoking, infections and drugs) and inherited susceptibility alleles[3,4].

Psoriasis is characterised by skin lesions varying from papules, macules, plaques to pustules and is classified into six clinical types (Table 1.1, Figure 1.1)[5]. As the focus of this thesis is on psoriasis vulgaris and on pustular forms of the disease, these two disease phenotypes will be discussed in more detail.

Table 1.1 Classification of psoriasis clinical variants

Subtype	Affected sites	Clinical manifestations
Psoriasis vulgaris	Scalp, limbs, trunk, genitalia, extensor surfaces	Dry, sharply demarcated oval plaques with adherent silvery scales
Guttate psoriasis	Trunk and extremities	Small, round erythematous plaques often preceded by streptococcal infection
Pustular psoriasis	Palms, soles and distal phalanxes (in localised disease) or trunk and limbs (in generalised pustular psoriasis)	Small, sterile pustules on normal or blotchy and inflamed skin
Erythrodermic psoriasis	Over 90% of the skin surface area	Generalized erythema
Flexural/Inverse psoriasis	Intertriginous and flexural areas	Well-defined plaques with minimal scale and a shiny surface
Nail psoriasis	Nails	Pitting, subungual hyperkeratosis, discoloration and onycholysis

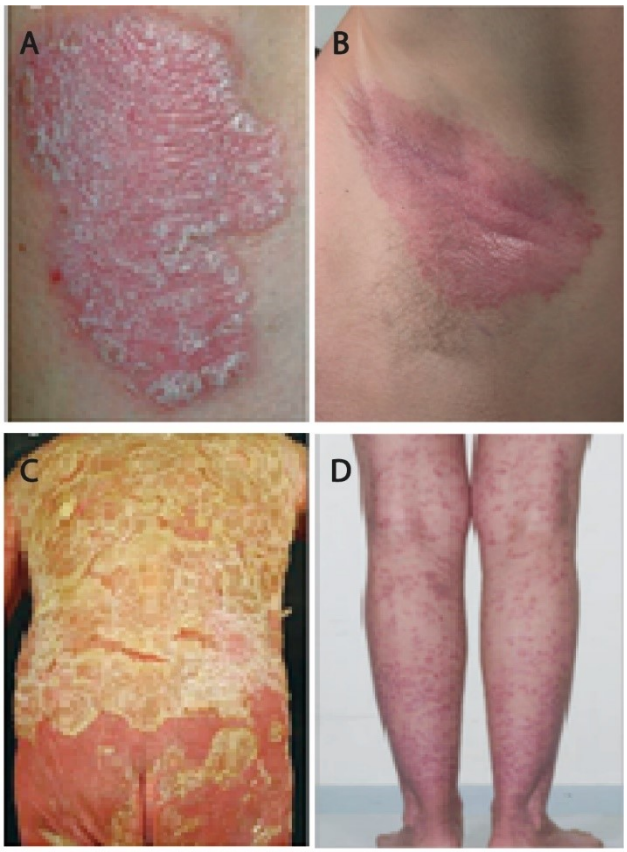

Figure 1.1 Clinical presentation of psoriasis

The heterogeneous spectrum of psoriasis includes psoriasis vulgaris (A), flexural psoriasis (B), erythrodermic psoriasis (C) and guttate psoriasis (D)[4,6]. Pustular variants are illustrated in Figure 1.4.

1.1.2 Psoriasis Vulgaris

1.1.2.1 Clinical features

Psoriasis vulgaris (PsV) is the most common form of the disease and accounts for approximately 90% of cases. It usually manifests with well-demarcated, red, scaly oval plaques that mostly affect the scalp, limbs, trunk, sacral region and extensor aspects of knees and elbows[6].

Histological staining of psoriatic lesions shows thickening of the epidermis (acanthosis), retention of keratinocyte nuclei in the stratum corneum (parakeratosis) and a mixed cellular infiltrate composed of T lymphocytes and dendritic cells[7]. Neutrophils collect within the stratum corneum and stratum spinosum of lesions, forming Munro's microabscesses and Kogoj pustules, respectively. Plaques are also highly vascularised, with tortuous capillaries surfacing and dilating, which causes skin redness[5].

Disease severity can be roughly evaluated as the percentage of body surface area (BSA) that is affected by lesions. In this context, BSA values >10% correspond to "moderate to severe" psoriasis. The Psoriasis Area Severity Index (PASI) is a more sophisticated scoring method, which takes into account the affected surface area as well as the intensity of erythema, desquamation and skin induration within plaques[8].

Severe PsV is also associated with several comorbidities[4], including type 2 diabetes, cardiovascular disorders, depression and psoriatic arthiritis[9–11]. The latter is observed in up to 30% of psoriatic patients[12]. It is a chronic inflammatory disorder affecting the spine, peripheral joints, tendon insertions and fingers[13,14]. All these concomitant illnesses can lead to occupational or functional disability, thus compounding the impact of the disease on the quality of life[15].

1.1.2.2 Genetics

It has long been recognised that psoriasis vulgaris is caused by the interplay between environmental and genetic factors, and can therefore be considered a complex trait[3,16]. Epidemiological studies have demonstrated that PsV has a higher incidence among relatives of affected individuals, particularly in early onset and childhood cases, compared to the general population[1,17]. Moreover, disease concordance is increased in monozygotic compared to dizygotic twins, with heritability estimates ranging between 60 and 90%[18].

While linkage studies identified 9 genomic regions (*PSORS 1-9*) co-segregating with psoriasis, only 3 could be reliably validated in wider patient cohorts and therefore considered genuine susceptibility loci[19,20].

PSORS1 maps to the Major Histocompatibility Complex (MHC) class I region on chromosome 6p21. The *HLA-Cw*0602* allele, which maps to this region, is the strongest genetic determinant of the disease (35-50% prevalence among patients) and has consistently been associated with odds ratios >2.0 [21–25]. While *CDSN* also maps to the MHC I region, subsequent studies have demonstrated that *CDSN* alleles are unlikely to play a causal pathogenic role[25,26].

The *PSORS2* locus on chromosome 17q25 encompasses *CARD14*, which encodes an adaptor protein activating NF-κB signalling in keratinocytes[27]. While common *CARD14* variants have been associated with sporadic disease, rare deleterious alleles cause monogenic forms of PsV[28]. However, these mutations are only found in a small number of extended pedigrees[29].

The *PSORS4* region on chromosome 1q21 spans the Epidermal Differentiation Cluster (EDC) and contains several genes involved in terminal keratinocyte differentiation[30,31]. Among these *LCE3B* and *LCE3C* (which encode late cornified envelope proteins) harbour variants associated with PsV and disruption of skin barrier function[32,33].

With technological advances in high-throughput genotyping and the advent of genome wide association studies (GWAS), the analysis of large case-control cohorts has

uncovered over 60 of psoriasis susceptibility loci. These include genes involved in antigen presentation (*HLA-C*, *ERAP1*), Th17 cell activation (*IL23R*, *IL23A*, *IL12B*, *TRAF3IP2*), innate antiviral responses (*IFIH1*, *RNF114*) and skin barrier function (*LCE3B/D*)[24,25,32,34–37]. Of note, evidence of a genetic interaction between *HLA-C* and *ERAP1* has been identified, as *ERAP1* variants confer disease susceptibility only in individuals carrying the *HLA-Cw*0602* allele[25].

Further susceptibility alleles have been identified through targeted studies, using platforms such as the immunochip (which affords deep coverage of susceptibility regions associated with immune diseases) and the exome chip (which only contains coding SNPs). These analyses have confirmed the fundamental pathogenic role of the IL23/Th17 axis and increased the number of known disease regions (now exceeding 60[38–40]). However, on average only 5% of autoimmune diseases susceptibility SNPs documented to date are likely to be causal[41], with only a small fraction of PsV heritability (~25%) accounted for by known loci[42]. Hence, there is still a clear need to uncover new genetic risks for psoriasis, as for other common, complex diseases[43–45].

1.1.2.3 Pathophysiology

The pathophysiology of PsV is multifactorial and involves epidermal hyperproliferation, abnormal keratinocyte differentiation and dysregulation of the immune system.

Skin trauma (Koebner phenomenon), infections (e.g. streptococcus) or medications (IFNα, corticosteroid) can all act as PsV triggers. These agents cause keratinocytes to produce the anti-microbial peptide LL37, which can bind self-RNA and self-DNA. The LL37/self nucleic acid complexes activate plasmacytoid dendritic cells (pDCs) through Toll-like receptor (TLR) -7 or -9, leading to the secretion of IFNα[46,47]. This can in turn activate myeloid dendritic cells (mDCs), which migrate into draining lymph nodes and produce TNFα, IL-12 and IL-23, triggering the differentiation of naïve T lymphocytes into Th17 and Th1 cells[47–50]. mDCs can also be activated through direct binding of LL37/RNA complexes to TLR-8[47].

Th17 cells infiltrate skin lesions and secrete IL-17, which binds its receptor on the surface of keratinocytes. The engagement of IL-17R leads to STAT1 and NF-κB activation and the production of several cytokines and chemokines, such as IL-36, CCL20 and IL-8. While IL-36 acts on DCs to promote the activation of further Th17 cells, CCL20 and IL-8 drive the recruitment of additional Th17 cells and neutrophils, contributing to the formation of a cutaneous plaque[51–53]. For an in-depth overview, I refer to excellent reviews on this subject[54,55]. Thus, IL-17 and IL-36 activate keratinocytes and Th17 cells, respectively, thereby promoting a positive feedback loop that leads to a sustained inflammatory state. Vascular endothelial growth factor (VEGF) is also secreted by keratinocytes: it induces angiogenesis and vascular dilation, facilitating the flux of inflammatory cytokines and infiltrating leukocytes[56].

The identity of the antigens presented to T cells by activated mDCs remains poorly understood. However, recent studies have shown that peptides derived from LL37 may act as autoantigens and be recognised by T lymphocytes in an *HLA-Cw*0602* restricted manner[57,58]. A potential role for lipid antigens generated by phospholipase A2 and presented by skin-resident Langerhans cells has also been suggested[59].

In conclusion, genetic and immunological studies have demonstrated that the pathogenesis of PsV is driven by a cross-talk between immune activation and skin barrier disruption (Figure 1.2)[60].

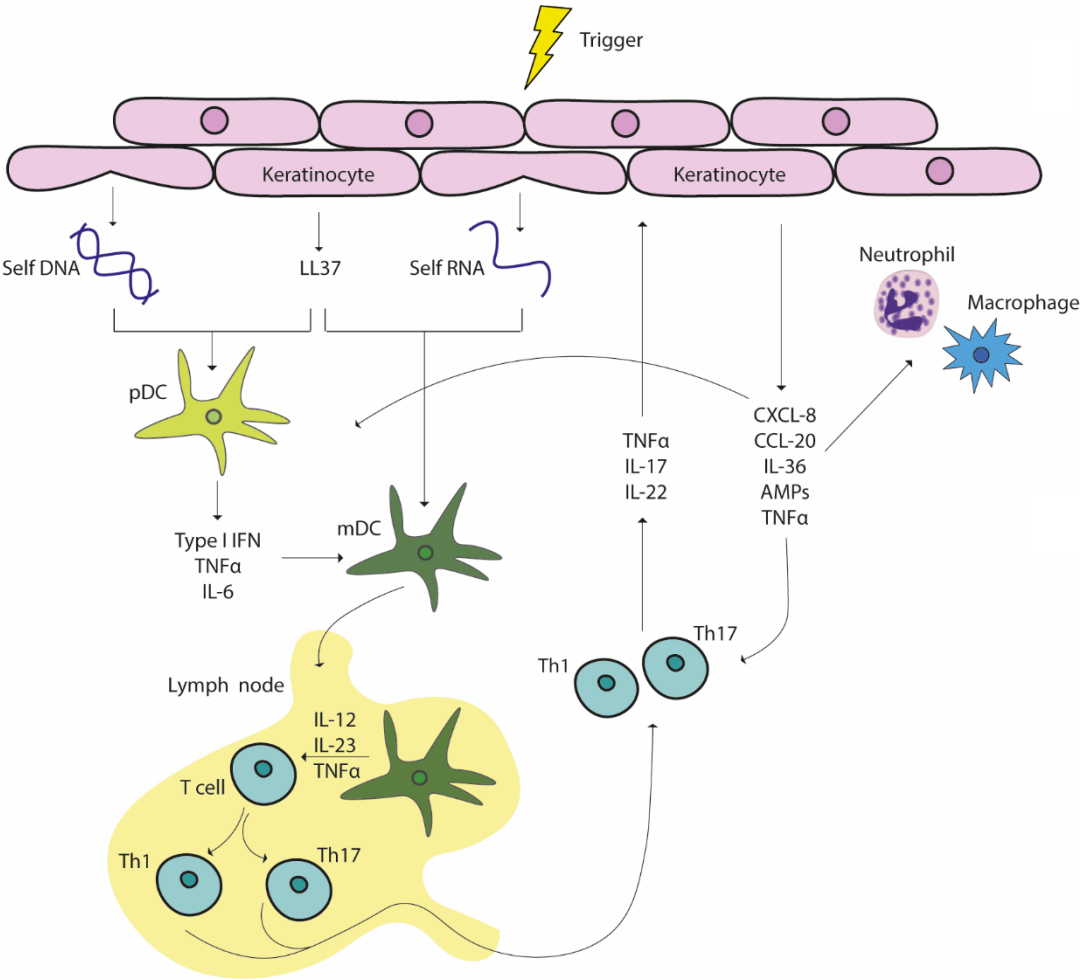

Figure 1.2 Current understanding of PsV pathogenesis

Environmental triggers and loss of tolerance to self nucleic acids lead to activation of pDCs, which in turn activate mDCs. The latter secrete IL-23 and present psoriasis autoantigens, triggering T cells differentiation. Activated Th1 and Th17 produce IL-17 and TNFα that act on keratinocytes to promote the production of further antimicrobial peptides, cytokines and chemokines. This drives the recruitment of additional T lymphocytes, neutrophils and macrophages, to promote a state of chronic inflammation[55].

pDC, plasmacytoid dendritic cell; mDC, myeloid dendritic cell; AMPs, Antimicrobial peptides. Adapted from Mahil et al. 2016[61].

1.1.2.4 Treatment

The best treatment for PsV will depend on disease severity and the presence of any co-morbidities[62].

Topical corticosteroids are the first-line therapy: they are often used in conjunction with vitamin D analogues in patients with mild to moderate psoriasis (<10% BSA) and no concurrent psoriatic arthritis. Short term phototherapy, which works by inhibiting T cell activation, is recommended for patients with moderate to severe psoriasis[63].

The most commonly prescribed systemic medications for severe psoriasis are methotrexate (MTX), cyclosporine and acitretin. These act by inhibiting T cell activation and (in the case of MTX) neutrophil chemotaxis[64–66]. The use of these agents however, is associated with risks of organ toxicity and drug-drug interactions.

As recent studies have started to uncover the mechanisms underlying the pathogenesis of PsV, new therapeutics which inhibit specific inflammatory cytokines (biologics) have been developed[67].

The first biologic agents showing efficacy in PsV were TNFα antagonists (adalimumab, etanercept and infliximab), which block the production of IL-23 by mDCs and the subsequent differentiation of Th17 cells [68,69]. However, the risk of serious adverse events such as opportunistic infections (tuberculosis), demyelination and a higher incidence of certain skin cancers, cannot be disregarded when prescribing these drugs[70,71].

Following the success of genetic studies carried in recent years, the IL-23/Th17 axis has become the key target for the development of new biologics (Figure 1.3).

Ustekinumab, an inhibitor of the p40 subunit shared by IL-12 and IL-23, has shown remarkable safety and efficacy, with >60% of patients achieving a 75% reduction in their baseline PASI (PASI75)[72,73]. While a superior clinical effect compared to etanercept has also been reported, monitoring of long term adverse events is still ongoing[74,75].

Selective IL-17 inhibitors have also been extensively studied. Both secukinumab and ixekizumab are monoclonal antibodies that bind IL-17A and have shown higher efficacy than etanercept and ustekinumab[76–78]. Brodalumab, which blocks the common IL-17 receptor and therefore antagonises IL-17F as well as IL- 17A, has also shown superior efficacy to ustekinumab[79,80]. In keeping with the indirect role of IL-17 in neutrophil activation, secukinumab induces a rapid reduction in cutaneous neutrophil numbers. However, it can also cause mild neutropenia[81,82]. IL-17 inhibitors are also associated with greater incidence of *Candida* and upper respiratory tract infections, likely due to the important role of IL-17A in anti-fungal immunity[76]. Moreover, increased suicide rates have been reported in patients treated with IL-17 inhibitors[77,78].

Building on the success of ustekinumab, three selective IL-23p19 blockers have been recently approved. Risankizumab, tildrakizumab and guselkumab, all lead to rapid and sustained improvement of disease symptoms, in the absence of major safety concerns[83,84].

A number of small molecule therapeutics have also been developed in the last few years. Apremilast, an oral phosphodiesterase-4 (PDE-4) inhibitor that prevents the conversion of cyclic adenosine monophosphate (cAMP) to AMP, is now used for the treatment of moderate-to-severe psoriasis. Higher cAMP levels help reduce inflammation by downregulating TNFα and IL-23 while increasing the production of the anti-inflammatory molecule IL-10[85]. While apremilast is less efficacious than biologic injectable agents (PASI75 is only achieved by 33% of patients), its oral administration and safety are favoured by patients and prescribers[86].

Lastly, Janus kinase (JAK) inhibitors are a new class of small molecules inhibitors acting on the tyrosine kinases that mediate the activation of STAT proteins, downstream of IL-23R. Tofacitinib (an oral JAK1 and JAK3 inhibitor) has demonstrated a PASI75 response in 67% of patients with moderate to severe plaque psoriasis, and sustained efficacy over 1 year[87,88]. Ruxolitinib, a JAK1 and JAK2 inhibitor, has also shown encouraging clinical results and has been tested as a topical formulation[89]. Trials of selective inhibitors of tyrosine kinase 2 (TYK2, another JAK family member), are underway[90].

In conclusion, the recent advances in elucidating the pathogenesis of PsV have led to the development of more successful and targeted drugs. However, current therapies are still not sufficient to treat all PsV cases due to the heterogeneity of the disease, the presence of concomitant illnesses and individual variation in response rates[91]. Therefore, the pathogenesis of PsV needs to be further investigated to better understand the disease and ultimately benefit patients.

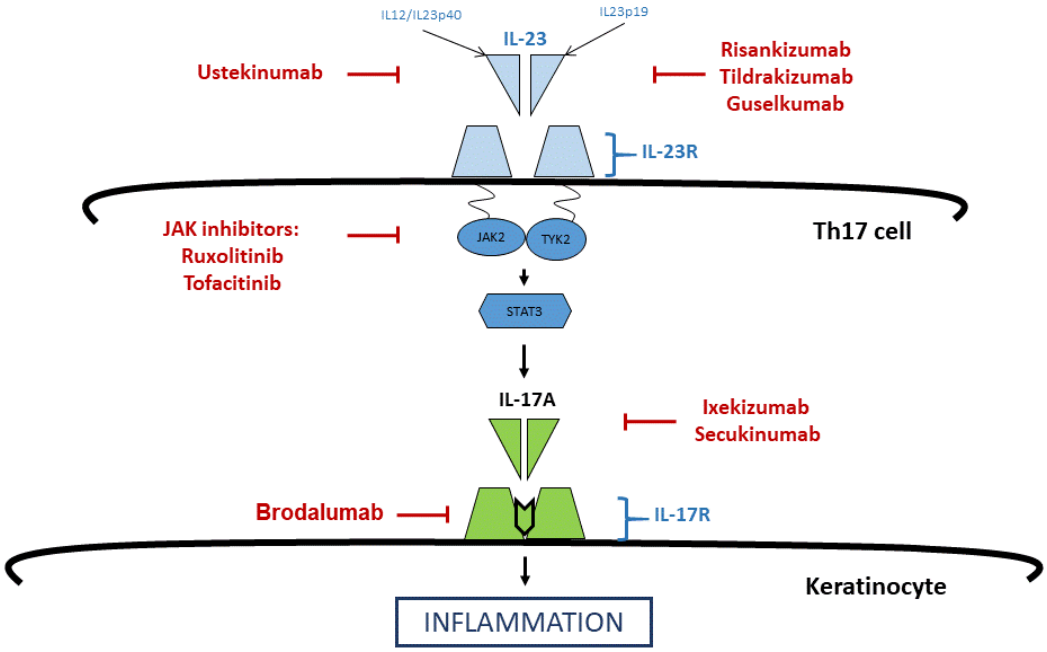

Figure 1.3 The IL23/Th17 axis as a therapeutic target for psoriasis

Diagram illustrating the molecules that can be targeted to treat PsV. The most effective agents inhibit IL-23 signalling at the receptor complex level (ustekinumab, tildrakizumab and guselkumab) or immediately downstream (JAK inhibitors). Ixekizumab and secukinumab inhibit Th17 activity by targeting IL-17, while brodalumab blocks IL-17R. Adapted from Mahil et al. 2016[61].

1.1.3 Pustular psoriasis

1.1.3.1 Clinical features

Pustular psoriasis is a rare disease variant characterised by the eruption of sterile, neutrophil-filled pustules appearing on normal or erythematous skin. It can be classified into generalised and localised forms (Figure 1.4)[5,92,93].

Generalised pustular psoriasis (GPP) is the most severe form of the disease and affects around 2 to 7 individuals per million[94,95]. It presents with acute and potentially life-threatening episodes of widespread skin pustulation and systemic upset (e.g. fever, malaise, elevated levels of acute phase reactants, neutrophilia). Around 30% of affected individuals suffer from concomitants PsV[96]. The course of the disease can be persistent (>3 months) or relapsing (>1 episode), and often requires intensive care admission. Flares can be triggered by infection, drugs (e.g. terbinafine and nonsteroidal anti-inflammatory drugs (NSAIDs)), sunburns, steroid withdrawal, stress or pregnancy[97–99].

Localised or acral pustular psoriasis (APP) is further classified into two subtypes. Acrodermatitis continua of Hallopeau (ACH) affects fingers and/or toes, leading to osteolysis of the distal phalanx and destruction of the nail apparatus. Conversely, palmoplantar pustulosis (PPP) affects palms and soles, where pustules develop on erythematous skin[92,99]. Both disease forms are chronic (>3 months), painful and disabling, but not life-threatening.

As ACH is even rarer than GPP, very little is known about its epidemiology. PPP, on the contrary, has a higher incidence (1200/million) and a distinctive demographic distribution[100–102]. The disease shows a marked sex bias, with female to male ratios often exceeding 3:1[103]. Patients typically present with disease symptoms after the age of 40 and almost invariably report an history of cigarette smoking[104,105]. Other triggering factors are similar to those seen in GPP, with the addition of skin trauma, thyroid dysfunction and metal sensitivity[98,99].

Figure 1.4 Clinical presentation of pustular psoriasis

Pustular psoriasis can present as generalised (GPP: left) or localised disease (PPP: middle; ACH: right)[97,106].

1.1.3.2 Genetics

The rarity and heterogeneous nature of pustular psoriasis has hindered the recruitment of sizeable patient cohorts, so that the identification of disease loci has been challenging. An analysis of two North-European PPP cohorts was carried out in 2003. This showed a lack of association with *PSORS1* markers, suggesting the existence of pathogenic pathways that are distinct from those that underlie PsV[107].

This notion was confirmed following the identification of pustular psoriasis alleles in three innate immune genes (*IL36RN*, *AP1S3* and *CARD14)*.

Autosomal recessive loss of function mutations in *IL36RN* were first identified in GPP through linkage studies of consanguineous pedigrees and whole exome sequencing of isolated cases[108,109].

IL36RN encodes the IL-36 receptor antagonist (IL-36Ra). This molecule competes with three agonists (IL-36α, IL-36β and IL-36γ) for binding to the IL-36 receptor (IL-36R). Once IL-36 cytokines have engaged with IL-36R, this dimerises with IL-1RAcP, a membrane-bound accessory protein composed of an extracellular ligand-binding domain, a transmembrane sequence and a cytoplasmic Toll/IL-1 receptor (TIR) domain. The complex then recruits MyD88, Tollip and IRAK, leading to the activation of NF-κB and mitogen-activated protein (MAP) kinase pathways. This, in turn, causes the transcription of several innate immune genes (such as *IL8*, *IL1*, *IL6* and *TNFA)*, which then mediate inflammatory responses (Figure 1.5, left).

When IL-36Ra binds to IL-36R, however, the receptor does not dimerise, preventing any downstream signalling (Figure 1.5, middle)[110,111]. In this context, *IL36RN* mutations disrupt the immune modulatory activity of IL-36Ra, causing unrestrained IL-36 signalling, excessive IL-1β, IL-6 and IL-8 production, and an enhanced inflammatory response (Figure 1.5, right)[108,112].

A total of 20 deleterious alleles have now been identified in *IL36RN*, including missense, stop-gain, splice site and deletion variants[113]. *IL36RN* defects have been reported in all ethnic groups, with distinct changes dominating the mutational landscape in Asian

(c.115+6T>C), European (p.Ser113Leu) and North-African (p.Leu27Pro) populations[109,114].

While *IL36RN* defects are typically recessive, GPP patients harbouring a single deleterious change have also been described. Interestingly, these individuals tend to show a delayed disease onset[115].

IL36RN alleles account for approximately 25% of GPP cases[115] and are more frequent among individuals suffering from severe disease (early-onset GPP with high risk of systemic inflammation). While homozygous, compound heterozygous, and single heterozygous *IL36RN* mutations have also been observed in subjects with localised pustular psoriasis, their frequency is much lower in this patient group (<5%), where they tend to occur in heterozygosity[114].

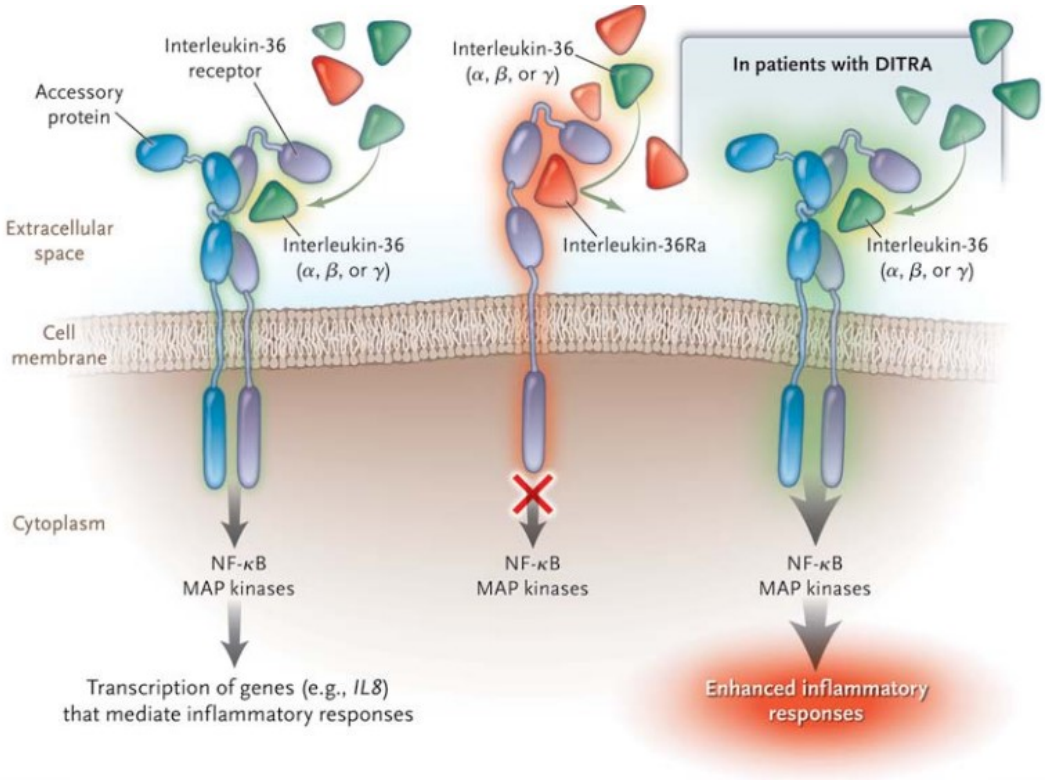

Figure 1.5 Disruption of IL-36 signalling in GPP

The cytokines IL-36α, -β and -γ (green) bind to the interleukin-36 receptor (IL36R, purple), which enables the recruitment of the IL-1R accessory protein (IL-1RAcP, blue), leading to an NF-κB and MAPK mediated inflammatory response. The IL-36Ra (red) also binds to IL-36R, which then fails to recruit the accessory protein, therefore inhibiting downstream signalling. Patients with *IL36RN* mutations experience exacerbated inflammatory responses due to lack of receptor antagonist. DITRA, deficiency of the IL-36 receptor antagonist. From Marrakchi et al. 2011[109].

Following the identification of *IL36RN* as a disease gene, further studies were undertaken to uncover other susceptibility loci. Two founder alleles in *AP1S3*, p.Phe4Cys and p.Arg33Trp, were discovered through exome sequencing of pustular psoriasis cases and found to be significantly more frequent in affected individuals compared to controls[116].

AP1S3 encodes the σ1 subunit of AP-1, an intracellular trafficking complex facilitating vesicular transport of proteins and autophagosome formation[117]. Disease alleles cause impaired autophagy, abnormal accumulation of p62 (an NF-kB adaptor) and increased production of IL-36 by keratinocytes[118].

Finally, Sugiura et al. described Japanese GPP patients harbouring a missense variant in *CARD14,* a gene that is also mutated in familial PsV (*PSORS2*) and pityriasis rubra pilaris (PRP)[27,119,120]. The allele described by Sugiura (p.Asp176His) was then uncovered in an extended Chinese cohort and in 2 PPP cases[29,121], confirming the association with pustular psoriasis. The change is a gain-of-function mutation, which causes abnormal TRAF-2 dependent activation of NF-κB signalling[28,122], which is thought to lead to excessive IL-6, IL-8 and IL-36 production. Thus, the effects of disease alleles seem to converge on the up-regulation of IL-36 activity.

In conclusion, genetic studies have shown that pustular psoriasis is mostly associated with rare and deleterious alleles. This near-monogenic genetic architecture differentiates it from PsV, which is caused by common variants of small effect. While there is some overlap between the genetic determinants of GPP and PPP, substantial genetic heterogeneity has also been observed, as known genes account for less than 10% of PPP cases[103].

1.1.3.3 Pathophysiology

Nearly all studies of disease pathogenesis have been carried out in GPP. Due to the rarity of the disease, however, progress has been slow.

The transcription profiling of GPP skin biopsies revealed a distinctive pattern of differential gene expression, with limited similarities to PsV. In keeping with the results of genetic studies, IL-1 and IL-36 were found to be significantly upregulated, together with several neutrophil chemokines (IL-8, CXCL1 and CXCL2) and neutrophil-derived proteases, such as neutrophil elastase and cathepsin G and S. Of note, the latter are responsible for processing IL-36 precursors into their active forms, which further validates the fundamental role that IL-36 plays in the pathogenesis of GPP[123–126].

Two studies have also demonstrated that the pathways that are induced in keratinocytes stimulated with IL-36 significantly overlap with those that are abnormally active in GPP skin[123,127]. A notable example of this phenomenon is the infiltration of neutrophils into inflamed skin, a hallmark of GPP, which is mediated by genes that are up-regulated by IL-36.

Taken together, these findings suggest that high levels of IL-1 and IL-36 cause the activation of GPP keratinocytes. These then produce chemokines (IL-8, CXCL1 and CXCL2) that attract neutrophils to the site of inflammation. As neutrophil proteases can process IL-36 into its bioactive form, their recruitment sustains and propagates inflammation in GPP skin.

While systemic inflammation is a key feature of GPP, its causes remain poorly understood, so that further research is required in this area.

1.1.3.4 Treatment

Treatment options for pustular psoriasis are profoundly limited, owing to the limited understanding of disease pathways and the difficulty of running clinical trials for such a rare condition. There is therefore a clear unmet need for effective therapeutics[128].

First line treatments for GPP include acitretin, cyclosporin, methotrexate and the TNF blocker infliximab, which has been reported to rapidly improve fever and skin symptoms. Second line therapies include the TNF inhibitors adalimumab and etanercept, topical agents and phototherapy[97]. However, the efficacy of these agents (which are used to good effect in PsV) is limited. Conversely, promising results have been obtained with the IL-17A antagonist secukinumab[129,130].

IL-1 blockers (e.g. anakinra) have also been used in the treatment of GPP, based on their efficacy in other autoinflammatory conditions presenting with recurrent fevers and skin rashes[131,132]. Anakinra initially caused rapid clinical improvement, but full disease remission was not observed. This is in keeping with the notion that IL-1 is not the dominant disease driver, but is rather involved in a pro-inflammatory feedback loop driven by IL-36[133].

Therapies for acral pustular psoriasis include psoralen/UVA photochemotherapy (PUVA) and topical corticosteroids. In more severe cases, where multiple digits/nails are involved, dermatologists might prescribe cyclosporin and retinoids[97]. Successful treatment of ACH with TNF antagonists has been reported[106,134], while there are conflicting reports regarding the use of ustekinumab in acral pustular psoriasis[135,136].

Finally, the results of genetic studies are driving the clinical development of two IL-36 inhibitors. These agents, which act by blocking the IL-36 receptor, have shown a favourable safety profile, with one trial also reporting substantial improvement of GPP symptoms[137,138]. Such progresses highlight the translational potential of gene identification studies in the development of novel therapies for orphan diseases.

1.2 Neutrophils

1.2.1 Life cycle

Neutrophils, also known as polymorphonuclear leukocytes (PMNs) or neutrophilic granulocytes, are an essential part of the innate and adaptive immune system, protecting the host from bacterial and fungal pathogens. They provide the first line of defence of the innate immune system by phagocytosing, killing and digesting bacteria and fungi. In addition, they recruit and activate other cells of the immune system. Neutrophils are the most abundant cell type in human blood, comprising 60-70% of all circulating white blood cells[139].

Every day more than 10^{11} neutrophils are produced in the bone marrow, in a process called granulopoiesis[140]. Hematopoietic stem cells (HSC) differentiate into multipotent progenitor cells (MPP) and then into lymphoid-primed multipotent progenitors (LMPP). These become granulocyte-monocyte progenitors (GMP), which, in the presence of the granulocyte colony-stimulating factor (G-CSF), differentiate into myeloblasts. These cells then follow a multi-step maturation process that includes the stages of promyelocyte (characterised by a round nucleus and relatively dark cytoplasm), myelocyte (round nucleus with initial dents and less-dark cytoplasm), metamyelocyte (kidney-shaped nucleus and clear cytoplasm), band cell (horseshoe-shaped nucleus and clear cytoplasm), leading to a mature neutrophil with its characteristic segmented nucleus (Figure 1.6)[141,142].

Granulopoiesis is under the control of several transcription factors, such as Runx1 (AML1), PU.1, CCAAT/enhancer-binding proteins (C/EBP)α–ζ and Gfi-1[143,144].

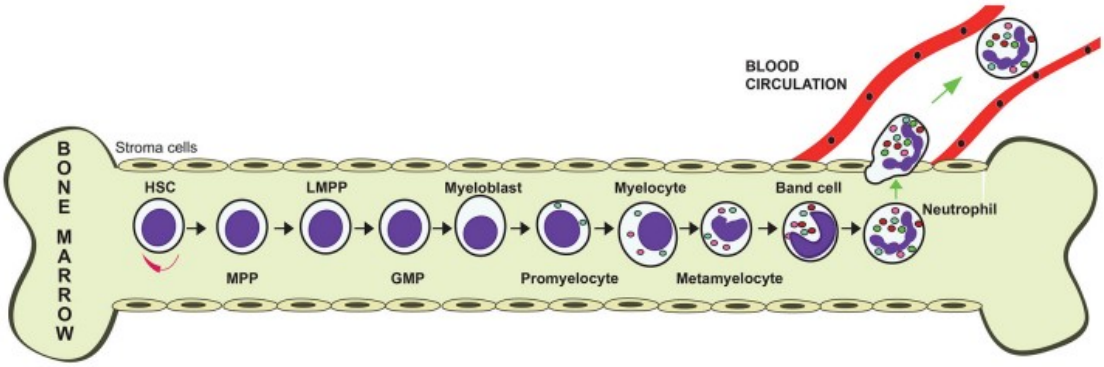

Figure 1.6 The stages of granulopoiesis

Neutrophils are produced in the bone marrow. A multipotent progenitor (MPP) cell originates from a hematopoietic stem cell (HSC). MPPs generate lymphoid-primed multipotent progenitors (LMPPs), which differentiate into granulocyte-monocyte progenitors (GMPs). In the presence of the granulocyte colony-stimulating factor (G-CSF), GMPs turn into myeloblasts, which then follow a maturation process that comprises the stages of promyelocyte, myelocyte, metamyelocyte, band cell, and mature neutrophil. Primary granules appear at the myeloblast to promyelocyte stage, secondary granules at the myelocyte and metamyelocyte stages, tertiary granules at the band cell stage, while secretory vesicle only present in mature PMNs. Once mature, neutrophils are released in the blood stream. From Rosales 2018[142].

The secretory vesicles and granules found within mature neutrophils are also formed during granulopoiesis[145].

Primary (azurophilic) granules, containing myeloperoxidase (MPO) and serine proteases (proteinase 3, cathepsin G and neutrophil elastase (NE)), appear at the myeloblast to promyelocyte stage. Secondary (specific) granules, which contain high levels of the iron-binding protein lactoferrin, are detected at myelocyte and metamyelocyte stages. Tertiary (gelatinase) granules, containing matrix metalloproteinase 9 (MMP9, also known as gelatinase B) are formed at the band cell stage. Finally, secretory vesicles, which contain plasma-derived proteins such as albumin, are only present in mature neutrophils (Figure 1.6)[146,147].

Once neutrophils mature, they are released into the circulation in a process that is tightly regulated by chemokines. These include CXCL12 and CXCL1/CXCL2, which act through their respective receptors, CXCR4 and CXCR2, to modulate the release of neutrophils from the bone marrow. Thus, CXCR4–CXCL12 signalling promotes neutrophil retention, as opposed to CXCL2–CXCR2, which stimulates PMNs release into the circulation [139,148].

1.2.2 Activation

Quiescent neutrophils are short-lived cells, which continuously probe their microenvironment, seeking signs of infection and inflammation. They typically die within a day of entering the circulation[149]. PMNs can however be recruited to sites of infection or inflammation, where their lifespan is extended by local cytokines and microbial products[150].

Neutrophils become activated through a two-stage process. First, bacterial products, cytokines and chemokines (e.g. IL-8, IFN-γ TNF- α and GM-CSF) prime resting cells, and these are then mobilised to the site of infection or inflammation, where they encounter the signals that trigger microbial killing[151].

Bacterial compounds (e.g. lipopolysaccharide (LPS) and N-Formylmethionyl-leucyl-phenylalanine (fMLP)) and cytokines (e.g. TNF-α and IL-1β) also stimulate vascular endothelial cells to produce E- and P-selectins. As neutrophils come into contact with these adhesion receptors, they "roll" along the endothelium, causing the partial activation of surface β2 integrin (also known as CD11/CD18). Binding of integrins to intercellular adhesion molecule-1 (ICAM-1) and ICAM-2 stops the rolling and promotes the adhesion of neutrophils to the endothelium. Crawling along the vessel wall, PMNs then reach endothelial cell junctions and extravasate into tissues (Figure 1.7). There, they move towards sites of inflammation following a chemotactic gradient driven by host-produced (e.g. IL-8) and pathogen-derived (e.g. fMLP) molecules. As they near their target, neutrophils become fully activated and finally release their antimicrobial arsenal once they have reached the site of infection[142,148,151].

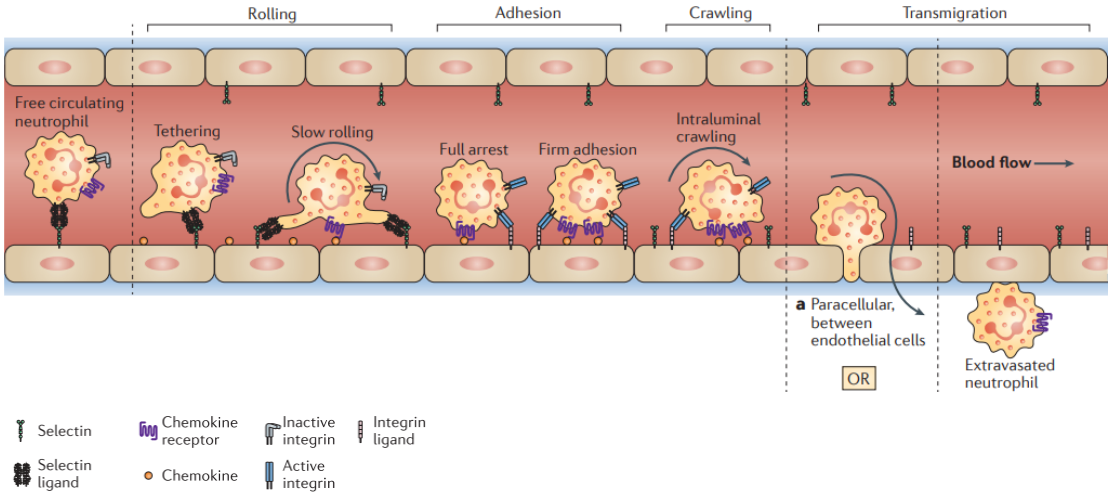

Figure 1.7 Neutrophil recruitment cascade

The figure shows the steps mediating neutrophil extravasation from blood vessel to sites of inflammation. Neutrophils adhere to the vascular endothelial wall using selectins, integrins and adhesion molecules. They then roll, arrest (adhesion) and transmigrate through endothelial cell junctions into peripheral tissues. Adapted from Kolaczkowska et al. 2013[146].

1.2.3 Functions

1.2.3.1 Elimination of microbes

Neutrophils can eliminate microbes through degranulation, phagocytosis or the release of neutrophil extracellular traps (NETosis, Figure 1.8). All three processes are tightly regulated.

1.2.3.1.1 Degranulation

Neutrophil granules contain a plethora of antimicrobial proteins and peptides. These can be divided into three main classes: i) cationic peptides and proteins binding to microbial membranes, ii) enzymes and iii) proteins that deplete microorganisms of essential nutrients[152]. The first group comprises defensins, cathelicidins, bactericidal/permeability-increasing protein (BPI) and histones. Apart from histones, which act through poorly understood mechanisms, all exert their function by permeabilising the bacterial membrane, hydrolysing bacterial phospholipids or inhibiting nucleic acid, protein and cell wall synthesis[153]. Of note, the LL37 cathelicidin may also potentiate the activation of plasmacytoid dendritic cells, as described in section 1.1.2.3[46].

The second group of antimicrobial proteins includes lysozymes and proteolytic enzymes such as serine proteases (proteinase 3, cathepsin G and neutrophil elastase). While lysozymes destroy the bacterial wall, serine proteases can cleave bacterial virulence factors and bind the bacterial membrane[152].

Finally, the third group encompasses metal chelator proteins such as lactoferrin and calprotectin, which sequester essential nutrients (iron, manganese and zinc) and/or bind LPS causing increased membrane permeability[148,154].

As PMNs become activated, granules are gradually mobilised. They then fuse with the phagosome (see section 1.2.3.1.2) or neutrophil plasma membrane, thus releasing their toxic content. Interestingly, several granule proteins (e.g. azurocidin, proteinase 3,

cathepsin G and LL37) can also mediate the recruitment of other cells involved in the inflammatory response[155].

Secretory vesicles are the first to be released, followed by gelatinase, secondary and azurophilic granules. While the mechanisms underlying this differential mobilisation are not fully understood, changes in cytosolic calcium levels are thought to be necessary for granule secretion[156,157]. Of note, the engagement of secretory vesicles also sustains PMN activation, as the secretion of membrane-bound proteins (β2 integrin, FcγR, complement and fMLP receptors) promotes the transition to firm endothelium adhesion[158–160]. Likewise, metalloproteases contained in tertiary granules may help neutrophils cross the endothelial membrane[161].

Another component of the degranulation process is the oxidative burst. Neutrophils produce reactive oxygen species (ROS) through a process mediated by the nicotinamide adenine dinucleotide phosphate (NADPH) oxidase complex. When this is assembled on the phagosomal and PMN plasma membranes, it reduces molecular oxygen to superoxide. Superoxide alone is not a strong oxidant, but it can either dismutate and form hydrogen peroxide, or react with nitric oxide to form peroxynitrite. Once myeloperoxidase (MPO) is released by azurophilic granules, it reacts with hydrogen peroxide and Cl^- to produce hypohalous acids that have direct antimicrobial effects[148,162]. Of note, loss of function NADPH oxidase mutations cause chronic granulomatous diseases (CGD), a condition characterised by poor neutrophil antimicrobial activity[163].

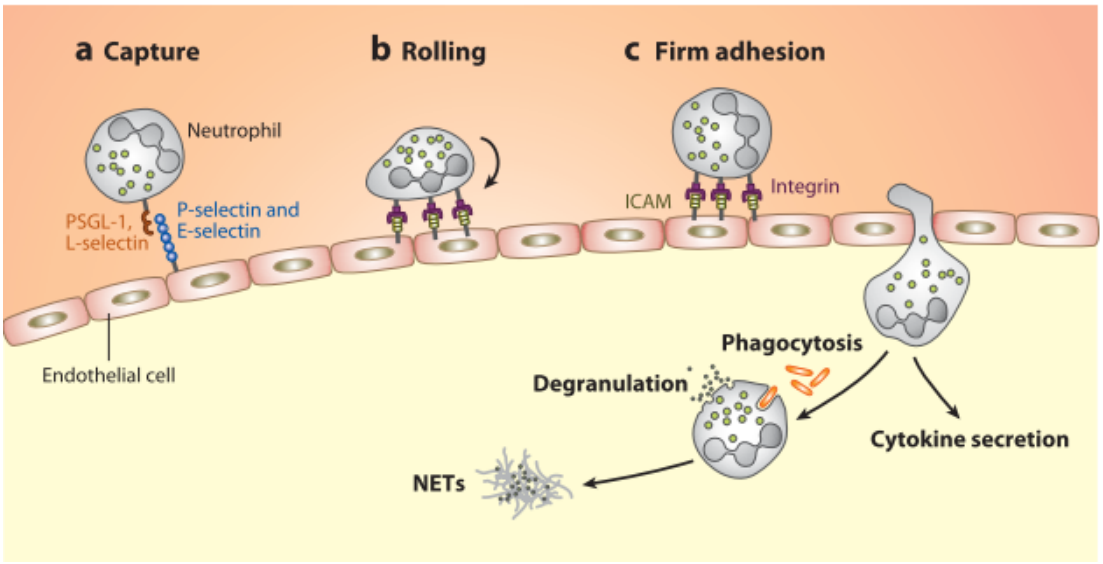

Figure 1.8 Neutrophil antimicrobial functions

Once neutrophils migrate to the site of inflammation, they phagocytose and digest their target. They then release granules and neutrophil extracellular traps (NETs) to kill invading pathogens. PMNs also produce pro-inflammatory cytokines. From Amulic et al. 2012[148].

1.2.3.1.2 Phagocytosis

Phagocytosis is the main method to eliminate pathogens and cell debris[148].

Neutrophils can internalise both opsonised and non-opsonised particles. Opsonins are pattern-recognition receptors that facilitate the attachment of particles to professional phagocytic cell, enhancing the efficacy of the phagocytic process[148]. Once activated, neutrophil opsonic receptors such as FcγR, β2 integrin, C-type lectins or complement receptors, situated on PMN membrane, bind to IgG or complement-coated particles, which are then engulfed. During this process, protein and lipid kinases promote actin polymerization, leading to the formation and sealing of a phagosomal cup[164].

The nascent phagosome subsequently acquires its antimicrobial effects through calcium-dependent fusion with secretory vesicles and granules[156]. The SNARE (soluble N-ethylmaleimide-sensitive-fusion-protein attachment protein receptor) family of proteins also contributes to this process, as a v-SNARE on the target membrane interacts with a similar protein on the phagosome[154].

Once primary and secondary granules have fused with the phagosome, they unload their antimicrobial enzyme content. Meanwhile, the NADPH oxidase complex is assembled on the phagosomal membrane, leading to the production of ROS (see section 1.2.3.1.1). Together, granule fusion and ROS formation create a toxic, alkaline environment (despite the entry of acidic granule contents) for the pathogens engulfed in the phagosome, resulting in rapid microbial killing[148,164,165].

1.2.3.1.3 NETosis

Neutrophil extracellular traps (NETs) are fibrous structures containing histones as well as antimicrobial proteins, such as LL37, neutrophil elastase (NE), cathepsin G, MPO and lactoferrin. In inflammatory conditions, neutrophils can release NETs into the extracellular space through a cell-death program called NETosis.

While the mechanism of NET formation is poorly understood, ROS are likely to play an important role, given that NETosis can be inhibited by NADPH oxidase blockade[166].

NETosis starts when activated neutrophils attach to their microbial targets. This causes nuclear and granular membranes to dissolve and release their content in the cytoplasm, leading to histone decondensation. Finally, PMN cell membrane ruptures, allowing the extracellular release of chromatin decorated with granular proteins.

NETs are sticky and voluminous. This enables them to trap microbes and expose them to the synergistic action of antimicrobial agents[167,168]. Thus, NETs contribute to the fight against parasites, Gram-positive and Gram-negative bacteria. They also play a role in eliminating pathogens such as fungi ,which are too large to be phagocytosed[168]. At the same time, NETs contain the systemic spread of antimicrobial agents and prevent them from damaging the surrounding tissue.

While neutrophils initiate phagocytosis within moments of engaging their targets, degranulation occurs approximately 10 minutes later and NETosis is a more prolonged process. This suggests that that the three defence strategies may be activated sequentially to maximise microbe killing.

1.2.3.2 Cross talk with other immune cells

Although neutrophils have a short lifespan, several signals (e.g. cytokines and microbial products) can extend their survival, allowing them to efficiently eliminate pathogens, release immunoregulatory molecules and recruit other cells. In fact, once neutrophils reach inflamed tissues, they participate in complex interactions with DCs, macrophages, natural killer (NK) cells, lymphocytes and mesenchymal stem cells, as summarised in Figure 1.9[148,169].

Even though neutrophils have a limited range of expression at the transcriptional level, their abundance within inflammatory sites means that they significantly contribute to cytokine production[148,170]. IL-8, which is released in the largest quantities, serves to recruit further PMNs, while TNF-α and IL-1β stimulate other leukocytes to produce neutrophil chemoattractants[171,172]. Neutrophil serine proteases can also activate cytokines produced by epithelial cells, such as IL-1α and, notably, IL-36[124–126,173].

Neutrophils can promote monocyte recruitment by expressing MIP (macrophage inflammatory protein) family chemokines and inducing monocyte extravasation through LL37, azurocidin and cathepsin G release[174–177].

Neutrophils can also affect the function of DCs (Figure 1.9C). For example, supernatants of neutrophil cultures exposed to *Toxoplasma gondii* induced DC maturation and activation, as demonstrated by the up-regulation of TNF-α and IL-12[178]. The DC-SIGN and Mac-1 (CD11b) receptors are thought to be responsible for the interaction between PMNs and DCs[179,180].

Neutrophils influence the responses of marginal zone B cells (MZB) by sequestering and transporting bacteria to the splenic marginal zone (Figure 1.9A)[181]. Activated neutrophils also express B-Cell-Activating Factor (BAFF) and produce APRIL (A proliferation-inducing ligand), a B cell-stimulating cytokine[182,183]. In keeping with these observations, Puga et al. showed that splenic PMNs boosted B cell survival, antibody production and MZB activation[184].

Neutrophils can regulate T cell function indirectly through pDCs or directly, by releasing chemoattractants (CCL2, CXCL9,CXCL10 and CCL20)[169,185,186]. Of note, neutrophils also express molecules required for antigen processing and presentation to T cells[187].

Neutrophils can influence cytokine production by NK cells. For example, *Legionella pneumophila* infection up-regulates IFN-γ production by murine NK cells, in a process that is dependent on neutrophil-derived IL-18 and DC-derived IL-12 (Figure 1.9D)[188,189]. Likewise, depletion of PMNs by anti-Ly6G antibodies reduces NK cells responsiveness[190,191].

Neutrophils are in turn influenced by cytokines produced by other leukocytes. For example, IFN-γ, GM-CSF and TNF (all released by T cells) control survival and expression of activation markers[192,193]. In addition, IL-17 cytokines can promote the release of granulopoietic factors and neutrophil chemoattractants by epithelial cells, thus augmenting PMN recruitment and activation[169]. Finally, type-I-IFN can exert multiple effects on neutrophils. It can delay apoptosis[194] and modulate neutrophil differentiation, activation, and migration. It has also been reported to drive CXCL10 production, thus promoting the recruitment of activated CXCR3-expressing neutrophils[195].

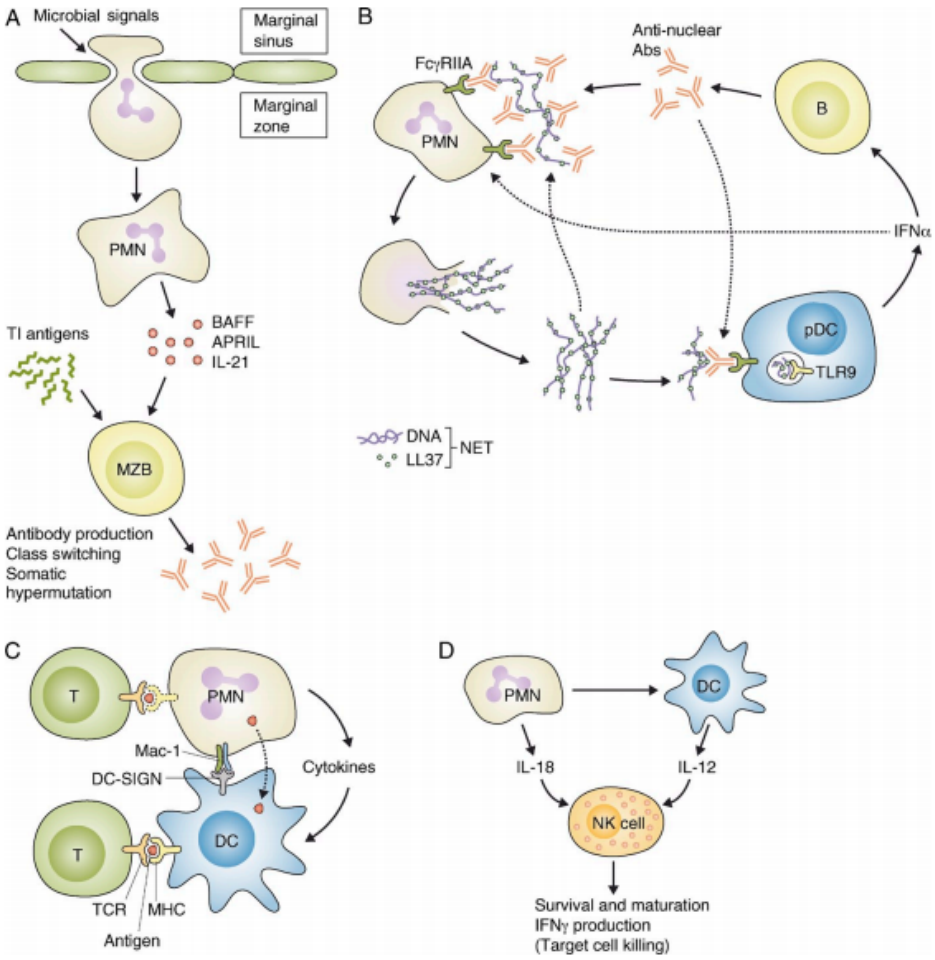

Figure 1.9 Interactions of neutrophils with other immune cells

A) Neutrophils (PMN) in the splenic marginal zone promote the activation and maturation of marginal zone B cells (MZB); B) Netting neutrophils stimulate pDCs to release IFN-α, which in turn up-regulates antibody production by B cells and causes further NET release; C) Neutrophils present antigens to T cells directly or through DCs; D) Neutrophils and DCs jointly activate NK cells. From Mocsai 2013[149].

PMN, polymorphonuclear cells; NET, neutrophil extracellular traps; MZB, marginal zone B cells; BAFF, B-cell activating factor; APRIL, a proliferation-inducing ligand; pDC, plasmacytoid dendritic cells; TLR9, toll-like receptor 9; TCR, T-cell receptor; MHC, major histocompatibility complex; DC-SIGN, Dendritic Cell-Specific Intercellular adhesion molecule-3-Grabbing Non-integrin; Mac-1, Macrophage-1 antigen; NK, natural killer.

1.2.3.3 Resolution of inflammation

During the late phases of inflammation, PMNs start to produce lipoxins, resolvins, and protectins. These lipids enhance monocyte and macrophage activation while limiting neutrophil migration[196–198]. Lipoxin also reduces neutrophil adhesion to the endothelium by inhibiting L-selectin shedding and β2 integrin production. At the same time, it modulates neutrophil activation by down-regulating ROS production, IL-8 expression and NF-κB activation[199–201].

Neutrophils also limit inflammation by expressing decoy receptors for several inflammatory chemokines and cytokines, including IL-1[202,203].

Aging neutrophils undergo apoptosis, a cell-death program which controls the numbers of PMNs in the circulation[204,205]. Apoptosis is tightly controlled by intrinsic and extrinsic signalling pathways, which are mediated by caspases 9 and 8, respectively[151]. Given that the prolonged release of proinflammatory molecules from dying PMNs can cause tissue damage, apoptotic neutrophils are promptly recognised and removed by macrophages[206–208]. This process is up-regulated by lipid mediators[197,201] and requires the presence of thrombospondin (TSP-1). The latter is thought to function as a bridge between the proteins expressed on the surface of macrophages (CD36) and neutrophils (integrins)[209,210].

1.2.3.4 Anti-tumour functions

Neutrophils are essential components of the tumour microenvironment and have been implicated in both the progression and resolution of several solid tumours[169,211].

Tumour-associated macrophages (TAMs) and chemokines released by tumour cells can recruit tumour-associated neutrophils (TANs). These are different from naïve bone marrow neutrophils, and two distinct subsets have been identified, N1 and N2[212].

N1 neutrophils have anti-tumoural functions: they are characterised by increased expression of TNF-α and reduced production of VEGF and MMP9. The latter are key angiogenic factors, contributing to tumour growth and progression[211]. Conversely, N2 neutrophils release MMP9, stimulating tumour growth and metastasis[211,213].

1.2.4 Disorders of neutrophil function

Diseases caused by inherited neutrophil defects are classified into four categories, as summarised in Table 1.2[214].

Severe combined neutropenia is the only condition that is considered a disorder of neutrophil homeostasis. It is caused by dominant mutations in *NE* or recessive mutations in *VPS45*, *HAX1* or *G6PC3*, leading to neutropenia and arrested neutrophil maturation[215].

PMN recruitment disorders (also known as leukocyte adhesion deficiencies) form a distinct disease group. They are caused by defective extravasation and impaired migration to inflammatory sites, due to abnormalities in selectin and integrin genes[216,217].

Neutrophil activation disorders are associated with disease alleles in four distinct genes. Recessive mutations in *MYD88* and *IRAK4* affect adhesion molecule expression, ROS formation, PMN survival and cytokine production in response to TLR agonists[218,219]. Conversely, deficiencies in Dectin-1 (*CLEC7A*) have a more restricted effect, as they disrupt a receptor that specifically recognises β -glucans in the fungal cell wall[220,221]. Likewise, recessive mutations in *CARD9* cause recurrent fungal infections, since they affect an adapter molecule that mediates Dectin-1 signalling.

Table 1.2 Congenital disorders of neutrophil function[214]

Disease	Causes	Neutrophil defects	Clinical manifestations
Disorder of neutrophil homeostasis			
Severe combined neutropenia	Mutations in *NE*, *VPS45*, *HAX1* or *G6PC3*	Prominent neutropenia and arrested neutrophil maturation	Recurrence of bacterial and fungal infections; leukaemia incidence ~25% after 20 years
Disorders of neutrophil recruitment			
Leukocyte adhesion deficiency I	*ITGB2* mutations resulting in integrin (CD18) deficiency	Abnormalities in diapedesis and complement-dependent phagocytosis	Leucocytosis and neutrophilia, recurrent severe infections, periodontal disease
Leukocyte adhesion deficiency II	Mutations in *SLC35C1* resulting in defective fucose metabolism	Absence of neutrophil rolling on selectins	
Leukocyte adhesion deficiency III	Mutations in *FERMT3*	Absence of integrin–mediated neutrophil adhesion and migration	
Disorders of neutrophil activation			
MyD88 and IRAK-4 deficiency	Mutations in *MYD88* and *IRAK4*	Defects in adhesion molecule expression, oxidative burst, cytokine production and cell survival in response to TLR agonists. Impaired NADPH oxidase activation	Recurrent pyogenic infections; invasive (meningitis and septicaemia) and localized (skin and upper respiratory tract) bacterial disease
Dectin-1 deficiency	Mutations in *CLEC7A*	Defective cytokine production	Mucocutaneous fungal infections
CARD9 deficiency	Mutations in *CARD9*	Not determined	Mucocutaneous fungal infections, possible occurrence of fatal candidal meningitis
Disorders of pathogen killing			
Chronic granulomatous diseases (CGD)	Mutations in NADPH oxidase components	Absence of oxidative burst	Severe bacterial (*S. aureus*) and fungal (*Aspergillus* and *Candida*) infections; excessive inflammation, pus, granulomas
Chédiak-Higashi syndrome	Loss-of-function mutations in *LYST*	Abnormally large granules due to lysosomal trafficking defects	Neutropenia, susceptibility to pyogenic infections (*S. aureus*), periodontal disease
Neutrophil-specific granule deficiency	Mutations in *CEBPE* or *GFI1*	Defective chemotaxis; reduced release of MPO and other granule proteins	Recurrence of cutaneous, ear, and sinopulmonary bacterial infections
MPO deficiency	Mutations in *MPO*	Absent MPO	Negligible, unless combined with another defect; fungal infections (*Candida*)

Chronic granulomatous diseases (CGD) are the most common defects of pathogen killing. They are caused by mutations in NADPH oxidase subunits, which lead to defective ROS production and microbial killing abnormalities[163]. Other disorders can result from defects in granule formation and/or loss of granule enzymes. For example, Chédiak-Higashi syndrome is characterised by the presence of abnormally large granules, due to mutations in the *LYST* lysosomal trafficking regulator[222]. Likewise, loss of function alleles in the *CEBPE* or *GFI1* transcription factors cause defective neutrophil chemotaxis and reduced release of granule proteins (neutrophil-specific granule deficiency). Finally, MPO deficiency causes enhanced phagocytosis and degranulation[223–225].

The majority of patients affected by congenital neutrophil abnormalities present with recurrent bacterial and fungal infections, mostly caused by *Staphylococcus aureus*, *Aspergillus fumigatus* and *Candida albicans*. The impact of disease alleles is highly variable. While individuals with MPO deficiency do not necessarily present with any clinical symptoms, patients bearing *CARD9* or *MYD88* mutations can suffer from life-threatening systemic diseases such as meningitis and septicaemia[214].

1.2.5 Role of neutrophils in psoriasis

The accumulation of neutrophils in the stratum corneum and the consequent formation of Munro's microabscesses are key features of plaque and pustular psoriasis. PMNs are recruited to the lesional epidermis by several chemokines secreted by hyperproliferating keratinocytes (e.g. CXCL1, CXCL2, IL-8 and IL-18)[226]. In turn, these activated neutrophils release pro-inflammatory mediators (e.g. IL-1, IL-8, IFN-α, MIP-1, LL37) and proteases through degranulation and NETosis, as described in section 1.2.3.1[227–229].

Some of the proteases released by degranulating blood neutrophils cleave IL-36 cytokines into their active forms. Cathepsin G can process IL-36α and -β, while NE recognizes IL-36α and -γ. Finally proteinase 3 cleaves IL-36γ and to a lesser extent, IL-36β[124–126,230]. Given the role of IL-36 cytokines in propagating the effects of abnormal IL-17 signalling (see 1.1.2.3), their activation by neutrophil proteases is critical to disease pathogenesis. Proteinase 3 was also shown to cleave hCAP-18 to generate LL37, while NE can promote keratinocyte proliferation by proteolytic activation of EGFR signalling[231,232].

Epidermal neutrophils are major producers of VEGF and IL-18, which contribute to angiogenesis and vascular dilation, thus facilitating the recruitment of further leukocytes to skin lesions. Moreover, neutrophil gelatinase granules contain MMP9, an enzyme that has been associated with new vessel formation[227,233].

PMNs are particularly important in pustular forms of psoriasis, which are characterised by IL-36 driven neutrophilic skin inflammation[93]. In GPP, unrestrained IL-36R signalling also causes systemic inflammation and peripheral neutrophilia[234]. The underlying pathways, however, remain poorly understood.

Of note, the IL-17 blocker secukinumab, which has shown efficacy in both plaque and pustular psoriasis, reduces neutrophil infiltration and down-regulates the production of keratinocyte-derived neutrophil chemoattractants[81].

While these data suggest that activated neutrophils have a prominent role in the pathogenesis of psoriasis, many of the genes that mediate these effects remain to be identified.

1.3 Aim and overview of the study

The hypotheses underlying this study are:

i) the identification of novel genetic determinants for psoriasis can uncover new immune pathogenic pathways;
ii) neutrophils are inappropriately activated in psoriasis.

The aim of the PhD was to validate these propositions by uncovering new disease genes and investigating the immunological pathways that mediate abnormal neutrophil function in psoriasis. Particular attention was paid to pustular forms of the disease, given that neutrophilic inflammation is especially prominent in these clinical variants.

Thus, the objectives of my project were:

- To carry out whole-exome sequencing in an extended pedigree and in a collection of unrelated cases in order to uncover novel disease variants;
- To investigate the function of the newly identified disease genes, through *ex-vivo* and *in-silico* studies;

as well as:

- To analyse the neutrophil transcriptome of patients with GPP and compare it with that of healthy individuals and disease controls;
- To investigate the link between excessive IL-36 signalling and neutrophil activation in GPP.

2 MATERIALS AND METHODS

2.1 Materials

Reagent	Manufacturer
5 ml round-bottom polystyrene tubes	Corning
7-AAD (7-Aminoactinomycin D)	BioLegend
100bp DNA Ladder	New England BioLabs
1kb DNA Ladder	New England BioLabs
10X DreamTaq buffer	Thermo Scientific
2-Mercaptoethanol	Sigma-Aldrich
Agarose	Severn Biotech
Agencourt AMPure XP	Beckman Coulter
B2M (Beta-2-Microglobulin, human)	PrimerDesign
Big Dye Terminator v3.1 Cycle Sequencing Kit	Applied Biosystems
Bovine Serum Albumin (BSA)	New England Biolabs
Brefeldin A	BioLegend
Bromophenol blue	Sigma-Aldrich
dNTP nucleotides	Fisher Scientific
DreamTaq DNA polymerase	Thermo Scientific
Ethanol	VWR
Ethidium bromide	Sigma-Aldrich
Ficoll	GE
FIX & PERM™ Cell Permeabilization Kit	Invitrogen
FBS (Foetal Bovine Serum)	Gibco
GeneJET RNA Purification Kit	Thermo Fisher Scientific
GeneScan 500 TAMRA Size Standard	Life Technologies
Herculase II Fusion DNA Polymerase Kit	Agilent Technologies
Hi-Di™ Formamide	Applied Biosystems
IL-1β	Miltenyi
IL-6	PeproTech
Illustra ExoProStar 1-Step	GE Healthcare/Fisher

LIVE/DEAD™ Fixable Near-IR (APC-Cy7)	Thermo Fisher Scientific
Loading dye	3% Glycerol, 2.5% (w/v) Bromophenol blue, ddH20
MACSxpress® Neutrophil Isolation Kit for human	Miltenyi
NaOAc (Sodium Acetate)	Sigma-Aldrich
ODN-A CpG	InVivoGen
Oragene DNA kit DNA	Genotek
PBS	Gibco
Penicillin-Streptomycin (P/S)	Life technologies
Plasmacytoid Dendritic Cell Isolation Kit II for human	Miltenyi
Precipitation solution	95% Ethanol, 0.12M NaOAc (pH 4.6)
Precision nanoScript2 Reverse Transcription kit	PrimerDesign
PrecisionPlus SYBR and ROX qPCR Mix	PrimerDesign
Recombinant Human IL-36 alpha/IL-1F6 (aa 6-158) Protein	R&D Systems
Red Blood Cell lysis solution	Miltenyi
RNA TapeStation kit	Agilent
RNaseZap™ RNase Decontamination Solution	Invitrogen
NaOAc (Sodium Acetate)	Hettich
RPL13A (Ribosomal Protein L13a, human)	PrimerDesign
RPMI 1640 Medium	Gibco
RPMI Medium 1640 - GlutaMAX™	Gibco
SB-203580	VWR
Staining buffer	Phosphate-buffered saline (PBS) pH 7.2, 2% FBS, and 2 mM EDTA
SureSelect Library Prep Kit	Agilent Technologies
SureSelect Human All Exome Kit v.4 and v.6	Agilent Technologies
SureSelectXT Kit	Agilent Technologies

2.2 Human Subjects

2.2.1 Ethics statement

The study was performed according to the principles of the Helsinki Declaration. All cases were recruited as part of the FAP study (Functional Annotation of Psoriasis susceptibility alleles, approved by the London - Chelsea Research Ethics Committee, reference 14/LO/2169, 20th January 2015) or the PLUM study (Pustular psoriasis: eLucidating Underlying Mechanisms, approved by the London - London Bridge Research Ethics Committee (reference 16/LO/2190, 30th January 2017). All participants granted their written informed consent.

2.2.2 Recruitment to the study

Patients were ascertained at St John's Institute of Dermatology and Royal Free Hospital (London, UK), Leicester Royal Infirmary (Leicester, UK), University Hospital of North Durham (Durham, UK) and Hospital Sultanah Aminah (Johor Bahru, Malaysia). All cases were physically examined and diagnosed by trained dermatologists. Patient demographic and clinical details were recorded in a standardised Case Report Form (Appendix I). Healthy controls were recruited among the personnel of St John's Institute of Dermatology.

2.2.3 Gene discovery study cohort

Family 8GPP included nine affected individuals suffering from GPP, PsV and or psoriatic arthritis. Demographics and clinical details are summarised in Table 2.1. A family pedigree is provided in Chapter 3 (Figure 3.1).

The psoriasis cohort consisted of 375 unrelated individuals, including 140 GPP, 105 PPP, 9 ACH and 121 PsV patients. Details of the patient groups that were included in exome sequencing experiments, follow-up studies and mutation screens are reported in the relevant sections of Chapter 3 (Table 3.6) and 4 (Table 4.2).

Table 2.1 Demographics and clinical characteristics of family 8GPP

Patient ID	Sex	Age of onset	GPP	PsV	PsA
8GPP1	F	32	Y	Y	Y
8GPP2	F	19	Y	N	Y
8PsV1	M	unknown	N	Y	N
8PsV2	M	unknown	N	Y	N
8PsV3	F	33	N	Y	Y
8PsV4	M	39	N	Y	N
8PsV5	M	25	N	Y	Y
8PsV6	M	23	N	Y	N
8PsV7	F	unknown	N	Y	N

GPP, generalised pustular psoriasis; PsV, psoriasis vulgaris; PsA, psoriatic arthritis
F, female; M, male; Y, yes; N, no

2.2.4 RNA-sequencing study cohort

2.2.4.1 Generalised Pustular Psoriasis cases

Eight unrelated GPP patients (1 male and 7 females, average age: 51) were ascertained for neutrophil RNA-sequencing. For the validation studies, fresh blood was obtained from 17 GPP individuals (2 males and 15 females, average age: 56.5), 7 of whom had also been included in the RNA-sequencing experiment (Table 2.2).

2.2.4.2 Plaque psoriasis cases

Seventeen unrelated PsV individuals (13 males and 4 females, average age: 45.2) were recruited for the validation of RNA-sequencing results. The main inclusion criterion was a diagnosis of moderate-to-severe psoriasis vulgaris (Psoriasis Area Severity Index >10) (Table 2.3).

2.2.4.3 Disease controls

Thirteen individuals with acral pustular psoriasis (APP) (3 males and 10 females, average age: 54.3) and nine with cryopyrin associated periodic syndrome (CAPS) (3 males and 6 females, average age: 44.6) were recruited for the validation of RNA-sequencing results (Table 2.4) in order to investigate whether the signature found in the GPP RNA-seq was also observed in other dermatological conditions.

2.2.4.4 Healthy controls

Eleven healthy controls (1 male and 10 females, average age: 50) were recruited for neutrophil RNA-sequencing. For the validation studies, fresh blood samples were obtained from 26 control individuals (3 males and 23 females, average age: 46.4), 10 of whom had been included in the RNA-sequencing cohort (Table 2.5).

2.2.5 DNA isolation and plating

DNA was isolated from 2 ml of saliva (using an Oragene DNA kit) or 5 ml of blood (salting out method[235]) by technical staff at St John's Institute of Dermatology. Sample

concentrations were quantified with a NanoDrop ND-1000 Spectrophotometer. DNAs were diluted to 25 ng/µl, aliquoted in 96-well plates and stored at -20°C.

Table 2.2 Demographics and clinical characteristics of GPP patients recruited for the RNAseq and validation studies

Patient ID	Ethnicity	Sex	Age of onset	Concurrent PsV	Systemic Inflammation[1]	Treatment	IL36RN status	Age at recruitment	Analysis group
GYFAP0011	European	F	42	Y	Y	none	S113L/-	50	RNA-seq and validation
GYFAP0014	European	F	36	N	Y	infliximab	wild-type	50	RNA-seq and validation
GYFAP0016	European	M	5	N	Y	MTX	S113L/S113L	48	RNA-seq
GYFAP0029	European	F	7	N	Y	infliximab and MTX	R48W/S113L	48	RNA-seq and validation
GYFAP0032	European	F	82	N	Y	acitretin	wild-type	89	RNA-seq and validation
GYFAP0089	European	F	29	N	Y	MTX	wild-type	40	RNA-seq and validation
GYFAP0096	European	F	19	Y	Y	adalimumab	wild-type	71	RNA-seq and validation
GYPLM0001	European	F	17	N	Y	topicals	wild-type	30	RNA-seq and validation
GYFAP0041	Indian	F	31	Y	unknown	ustekinumab and MTX	wild-type	48	Validation
GYFAP0100	European	F	35	Y	unknown	adalimumab and MTX	wild-type	43	Validation
GYFAP0157	European	F	78	Y	unknown	ciclosporin	wild-type	78	Validation
GYFAP0159	European	M	60	Y	Y	ciclosporin	wild-type	65	Validation

GYFAP0163	European	F	76	Y	unknown	topicals	wild-type	76	Validation
GYPLM0002	European	F	73	N	unknown	prednisolone	wild-type	75	Validation
GYPLM0003	Asian/Indian	F	29	Y	unknown	adalimumab and ciclosporin	wild-type	31	Validation
GYPLM0004	Indian	F	41	Y	unknown	topicals	wild-type	44	Validation
GYPLM0006	Asian	F	21	Y	unknown	certolizumab and MTX	wild-type	44	Validation
GYPLM0013	European	M	74	Y	unknown	topicals	wild-type	76	Validation

[1]Systemic upset was defined as the concurrence of two of the following: fever > 38°C, neutrophil count > $15x10^9$/L, CRP> 100mg/L
MTX, Methotrexate; F, female; M, male; Y, yes; N, no

Table 2.3 Demographics and clinical characteristics of PsV patients recruited for the validation studies.

Patient ID	Ethnicity	Sex	Treatment	PASI	Age at recruitment
P338	Indian	M	topicals	23.2	31
P341	European	M	topicals	10.4	37
GYFAP0172	Unknown	M	ixekizumab	19.9	55
GYFAP0180	European	F	topicals	14	48
GYPLM0044	European	F	MTX	12.4	58
GYPLM0045	European	M	ustekinumab	12.6	40
GYPLM0052	European	M	topicals	14.2	43
GYPLM0053	Asian/Indian	M	ustekinumab	10	54
GYPLM0054	African	M	PUVA	19	46
GYPLM0055	European	M	ustekinumab	12.5	38
GYPLM0057	African	F	topicals	30	37
GYPLM0058	European	M	topicals	27	63
GYPLM0059	European	F	etanercept	11.4	49
GYPLM0060	European	M	secukinumab and MTX	19	50
GYPLM0062	Asian	M	infliximab and MTX	22.2	23
GYPLM0063	European	M	apremilast	35	53
GYPLM0064	European	M	ustekinumab and MTX	12.2	48

F, female; M, male; Y, yes; N, no; PASI, Psoriasis Area Severity Index

Table 2.4 Demographics and clinical characteristics of disease controls recruited for the validation studies.

Patient ID	Ethnicity	Sex	Disease	Treatment	Age at recruitment
GYFAP0012	European	F	PPP	secukinumab and MTX	55
GYFAP0017	European	F	ACH	infliximab and MTX	65
GYFAP0079	European	M	PPP	topicals	55
GYFAP0103	European	M	ACH	adalimumab	80
GYFAP0113	European	F	PPP	topicals	51
GYFAP0156	European	F	PPP	no treatment	41
GYFAP0160	European	F	PPP	no treatment	81
GYFAP0166	European	F	PPP	topicals	30
GYFAP0174	European	M	PPP	infliximab, MTX and topicals	42
GYPLM0012	European	F	ACH	adalimumab	54
GYPLM0019	European	F	PPP	acitretin	51
GYPLM0030	European	F	PPP	unknown	54
GYPLM0033	European	F	PPP	no treatment	47
RFPLM0001	European	F	CAPS	canakinumab	30
RFPLM0002	European	F	CAPS	canakinumab	57
RFPLM0003	European	M	CAPS	canakinumab	51
RFPLM0004	European	F	CAPS	canakinumab	48
RFPLM0005	European	F	CAPS	anakinra	34
RFPLM0006	European	M	CAPS	canakinumab	35
RFPLM0007	European	F	CAPS	anakinra	64
RFPLM0008	European	M	CAPS	canakinumab	35
RFPLM0009	European	F	CAPS	canakinumab	47

PPP, Palmoplantar Pustular Psoriasis; ACH, Acrodermatitis Continua of Hallopeau; CAPS, Cryopyrin Associated Periodic Syndrome; F, female; M, male

Table 2.5 Demographics of healthy control individuals recruited for the RNAseq and validation studies

Patient ID	Ethnicity	Sex	Age at recruitment	Analysis group
GYFAP0035	European	F	48	RNA-seq and validation
GYFAP0036	European	M	58	RNA-seq and validation
GYFAP0039	European	F	53	RNA-seq and validation
GYFAP0040	European	F	56	RNA-seq and validation
GYFAP0042	European	F	56	RNA-seq and validation
GYFAP0175	European	F	41	RNA-seq and validation
GYFAP0176	European	F	43	RNA-seq and validation
GYPLM0009	European	F	37	RNA-seq and validation
GYPLM0011	European	F	65	RNA-seq and validation
GYPLM0016	European	F	53	RNA-seq
GYPLM0031	European	F	44	RNA-seq and validation
GYFAP0038	Indian	F	49	Validation
GYPLM0010	European	F	37	Validation
GYPLM0014	European	F	37	Validation
GYPLM0015	European	M	38	Validation
GYPLM0017	European	F	49	Validation
GYPLM0018	Chinese	F	40	Validation
GYPLM0020	European	F	43	Validation
GYPLM0021	European	F	42	Validation
GYPLM0022	European	F	49	Validation
GYPLM0023	European	F	45	Validation
GYPLM0024	European	F	63	Validation
GYPLM0025	Asian/Indian	F	32	Validation
GYPLM0026	European	F	38	Validation
GYPLM0027	Chinese	M	41	Validation
GYPLM0028	Indian	M	52	Validation
GYPLM0029	European	F	37	Validation

F, female; M, male

2.3 Whole-exome sequencing

Whole-exome sequencing was performed by technical staff within the Genomics Core facility of Guy's and St Thomas' Hospital Biomedical Research Centre (BRC). Briefly, 3 µg of genomic DNA were diluted in 130 µl of 1X TE buffer and sheared into 150-200 bp fragments using an ultrasonicator (Covaris M220). Libraries were then prepared with the SureSelect Library Prep Kit. Agencourt AMPure XP beads were used to purify the DNA fragments, which were next repaired to produce blunt-ended 5'-phosphorylated ends and purified. Once 3'-dA overhangs were added and indexing-specific paired-end adapters were ligated, the fragments underwent a further purification with Agencourt AMPure XP beads. Next, the library was amplified using the Herculase II Fusion DNA Polymerase Kit as follows: 2 min at 98°C, (30 sec at 98°C, 30 sec at 65°C, 1 min at 72°C) x 5, 10 min at 72°C. Once the library was again purified, its quality and concentration were determined with a TapeStation 2200 (Agilent) and a Qubit 4 fluorometer (Thermo Fisher Scientific), respectively.

Whole-exome capture was performed using the Agilent SureSelect Human All Exome Kit v4 or v6, according to the manufacturer's instructions. Briefly, a 24-hour library hybridisation at 65°C was performed, followed by purification on a Dynal magnetic separator. The resulting products were amplified with the following cycling conditions: 2 min at 98°C, (30 sec at 98°C, 30 sec at 57°C, 1 min at 72°C) x 10, 10 min at 72°C. Once index tags were added, the quality and concentration of the preparation were determined with the Agilent 2100 Bioanalyzer High Sensitivity DNA assay. Lastly, the samples were pooled for multiplex sequencing and prepared for cluster amplification. Whole-exome sequencing was performed on an Illumina HiSeq1000 or HiSeq3000/4000.

2.4 Sanger sequencing and microsatellite genotyping

2.4.1 Primer design

PCR and real-time PCR primers were designed using Primer3Plus (http://primer3.ut.ee/) to amplify the appropriate exons and intron/exon junctions. The primer specificity was

ensured by aligning each oligonucleotide to the human genome sequence using BLAST (https://www.ncbi.nlm.nih.gov/tools/primer-blast/). Primers were purchased from Sigma Aldrich-Merck and reconstituted in nuclease-free water as 100 µM stock solutions. PCR were then carried out using 10 µM working dilutions.

2.4.2 Polymerase Chain Reaction

All PCR were performed in an Eppendorf Mastercycler Pro and were set up as 15 µl reactions containing 1X reaction buffer, 0.3 µM forward and reverse oligonucleotide primers, 0.2 mM dNTPs, 25 ng of DNA template and 0.625 U DreamTaq DNA polymerase. Cycling conditions were as follows: 5 min initial denaturation at 95°C; 30 replication cycles at 95°C for 30 sec, 62-64°C for 30 sec, 72 °C for 30 sec, followed by a final extension at 72 °C for 10 min. Primer annealing temperatures were optimized by means of gradient PCR and are reported in Appendix II.

2.4.3 Agarose gel electrophoresis

The results of the PCR reactions were visualised by agarose gel electrophoresis. Each PCR product (3 µl) was mixed with 1.5 µl of 5X loading dye, then loaded on a 2% agarose gel containing 0.5 mg/ml ethidium bromide. The amplicons were run at 200 volts alongside the 100bp or 1Kb molecular weight marker. After 25 min gels were visualised under UV light, using a “GelDoc-It310 Imaging System” trans-illuminator from UVP.

2.4.4 Sanger sequencing

To remove unincorporated dNTPs and oligonucleotides, 2 µl of each amplicon was purified using the Illustra ExoStart kit. Next, the sequencing reaction was set up by adding 1.75 µl of sequencing mastermix (1.25 µl 5X BigDye Terminator sequencing buffer, 0.25 µl of 10 µM primer and 0.25 µl of BigDye Terminator v 3.1) to the purified PCR products. The following cycling conditions were used: (96°C for 30 sec, 55°C for 15 sec, 60°C for 60 sec) x 35. The resulting products were purified by incubating them with 26 µl of precipitation solution (50 ml of 95% ethanol solution mixed with 2ml of 3M NaOAc, pH=4.6) for 10 min at room temperature. After 30 min centrifugation (Rotanta

460 R benchtop centrifuge, Hettich) at 3,000 rpm, the supernatants were removed by spinning inverted plates for 5 sec at 500 rpm. The pellets were then washed with 100 µl of 70% ethanol, followed by 10 min centrifugation at 3,000 rpm. Finally, the washing solution was removed as described above, the pellets were air-dried and 10 µl of HiDi Formamide were added to each sample. Following a 2 min denaturation at 90°C, the samples were run on a 3730xl ABI Sequencer (Applied Biosystems) and the results were analysed with the Sequencher software (v 4.9, Genecodes).

2.4.5 Microsatellite genotyping

The regions spanning the three microsatellites of interest (D6S273, AP1S3-TG and D2S2299) were amplified by PCR using primers labelled with 5'-FAM. The amplification products were then diluted 1:5, 1:50 or 1:100, based on the intensity of the band observed by agarose gel electrophoresis. Next, 1µl of diluted sample was mixed with 8.75 µl HiDi Formamide and 0.25 µl of GeneScan 500 TAMRA Size Standard. Samples were run on a 3730xl ABI Sequencer (Applied Biosystems) and results analysed with Peak scanner (v2.0, Thermo Fisher Scientific).

2.5 Transcript analysis

2.5.1 RNA extraction

RNA was extracted from freshly isolated neutrophils or frozen PBMCs, using a GeneJET RNA purification kit and pipettes that had been cleaned with RNaseZap RNase Decontamination Solution. The RNAs were eluted in 30 µl of nuclease-free water, quantified using a Qubit 4 fluorometer (Invitrogen) and stored at -80°C. Samples were prepared with the RNA TapeStation kit and RNA quality was measured using a TapeStation2200, according to the manufacturer's instructions.

2.5.2 cDNA synthesis

Between 100 and 200 ng of total RNA were reverse-transcribed in a final volume of 20 µl, using the Precision nanoScript2 Reverse Transcription kit according to the manufacturer's instructions. The reactions were incubated at 65°C for 5 min, placed on

ice for 5 min, then again heated at 42°C for 20 min and at 75°C for 10 min. Each cDNA sample was then diluted to 50 µl with nuclease-free water.

2.5.3 Real-time PCR

Gene expression was assessed by real-time PCR using the primers listed in Appendix II. *RPL13A* and *B2M* were analysed as endogenous controls, using oligonucleotide purchased from PrimerDesign. Reactions were set up in a final volume of 20 µl containing 70 nM of primers, 1X PrecisionPLUS qPCR Master Mix with ROX and SYBRgreen and 2 µl of diluted cDNA. All reactions were prepared in duplicate. Samples were analysed with a 7900HT Fast Real Time PCR System (Applied Biosystems) under the following cycling conditions: 95° for 2 minutes, (95° for 10 seconds, 60° for 60 seconds) x 40 cycles. Relative gene expression was quantified using the ΔΔCt method[236].

2.6 Cell isolation, culture and stimulation

2.6.1 Neutrophils

2.6.1.1 Neutrophil isolation

Neutrophils were isolated by negative selection, using the MACSxpress® Neutrophil Isolation Kit for human (Miltenyi) to process 4ml of whole blood. Erythrocyte contamination was removed with a Red Blood Cell lysis solution (Miltenyi). Cells were resuspended in Roswell Park Memorial Institute (RPMI 1640 medium) containing 1% Bovine Serum Albumin (BSA) and counted with a Marienfeld Superior haemocytometer.

2.6.1.2 Purity assessment by flow cytometry

Neutrophil purity was assessed on 8 independent samples.

Neutrophils were seeded in 5 ml round-bottom polystyrene tubes at a concentration of $1x10^6$ cells/100 µl. Cells were centrifuged at 300 x g for 10 min and the supernatants were discarded. For live cell detection, 5 µl of 7-AAD were used.

The pellets were resuspended in staining buffer and placed on ice. After 20 min, 5 µl of the appropriate antibody were added to the samples (Table 2.6). Following 20 min incubation in the dark at 4°C, the samples were washed with 200 µl of staining buffer and centrifuged at 300 × g for 10 min. Cells were then resuspended in 400 µl of staining buffer, passed through a 40 µm cell strainer (BD Falcon) and analysed on a BD FACSCanto II machine. The results were analysed using FlowJo v10 software (https://www.flowjo.com/).

2.6.1.3 Neutrophil culture and stimulation

Cells were cultured under aseptic conditions at 37°C and 5% CO_2 in a NUAire Air-Jacketed Automatic CO_2 (NU-5500) incubator.

Neutrophils isolated from the blood of healthy donors (4 females and 1 male, average age: 30) were seeded in 48-well plates at a density of $1x10^6$ cells per well, in 500 µl of RPMI medium supplemented with 1% BSA. Cells were stimulated with 50ng/ml IL36-α or 50ng/ml IL-1β (positive control), or vehicle (RPMI medium) for 2 hours. To investigate the possibility of a synergy between IL-36 and other IL-1 family cytokines, cells were treated with 25ng/ml IL-1β and 25ng/ml IL-6 for 4 hours followed by 50ng/ml IL36-α or vehicle for 2 hours. At the end of each stimulation, cells were harvested and centrifuged at 300 x g for 10 min. The response to treatment was then measured by real-time PCR, as described in section 2.5.3. Each experiment was performed three times in triplicate.

2.6.2 Peripheral blood mononuclear cells (PBMCs)

2.6.2.1 PBMC isolation

PBMCs were isolated from 20 ml of blood via Ficoll density gradient centrifugation (carried out in the absence of Red Blood Cells lysis). Cells were resuspended in RPMI/GlutaMAX medium supplemented with 10% FBS and 1% penicillin/streptomycin solution, then counted using a Marienfeld Superior haemocytometer.

2.6.2.2 PBMC culture and stimulation

Freshly isolated PBMCs obtained from healthy donors (see 2.6.1.3) were seeded in 48-well plates at a density of $1x10^6$ cells per well. Cells were incubated overnight in 500 µl of RPMI/GlutaMAX medium supplemented with 10% FBS and 1% penicillin/streptomycin. The next day, the PBMCs were stimulated for 6 hours with 50ng/ml IL36-α or vehicle followed by 6 hours with 1.6µg/ml of ODN-A CpG or vehicle. Alternatively, PBMCs were pre-incubated for 1 hour with 1 µM SB-203580 followed by 6 hours with 50ng/ml IL36-α or vehicle. Afterwards, cells were harvested and centrifuged at 3000 rpm for 7 min. The cell pellets were then stored at -80°C. The response to stimulation was measured by real-time PCR. Each experiment was carried out at least three times in triplicate.

2.6.3 Plasmacytoid dendritic cells (pDCs)

2.6.3.1 pDC isolation

Plasmacytoid dendritic cells were purified by negative selection, using the Plasmacytoid Dendritic Cell Isolation Kit II for human (Miltenyi) to process 400 µl of freshly isolated PBMCs. Cells were resuspended in RPMI/GlutaMAX medium supplemented with 10% FBS and 1% penicillin/streptomycin solution, then counted with a Marienfeld Superior haemocytometer.

2.6.3.2 pDC culture and stimulation

Freshly isolated pDCs obtained from healthy donors were seeded in 96-well plates at a density of $1x10^5$ cells per well. Cells were incubated overnight in 500 µl of RPMI/GlutaMAX medium supplemented with 10% FBS and 1% penicillin/streptomycin. The next day, pDCs were stimulated for 6 hours with 50ng/ml IL36-α or vehicle. After 3 hours, 1:1,000 of Brefeldin A (BioLegend) was added to IL36-α stimulated pDCs. At the end of the incubation, cells were harvested for flow cytometry analysis.

2.6.3.3 PLSCR1 intracellular staining for flow cytometry

Cells were washed with PBS, stained with the appropriate pDC antibodies (Table 2.7) and incubated for 20 min in the dark at 4°C. Following another PBS wash, 500 µl of the Perm/Fix solution were added for 30 min and cells were washed with PERM buffer (FIX & PERM™ Cell Permeabilization Kit). Next, cells were incubated for 20 min with 1.5 µl of anti-PLSCR1, washed with PBS and treated with 1 µl of anti-Rabbit IgG for a further 20 min in the dark at 4°C. After a final wash in PBS, cells were resuspended in PERM buffer and kept in the fridge overnight. The next day, data was acquired on a BD Fortessa LSR.

2.6.4 IL36R expression analysis

PBMCs and neutrophils were obtained from 4 GPP cases (3 females and 1 male, average age: 54) and 4 controls (3 females, and 1 male, average age: 36). Neutrophils were stimulated as described in section 2.6.1.3.

Cells were first incubated with 10 nM LIVE/DEAD™ Fixable Near-IR (APC-Cy7) for 15 min at 4°C. After a PBS wash, cells were mixed with Monocytes and Fc blocker (1:40) for 20 min. Following a further PBS wash, cells were incubated for 20 min at 4°C with three separate sets (panels) of antibodies (Table 2.6), in order to identify the different leukocyte populations present in the samples. Once washed, cells were incubated with the secondary antibody (2ng/µl, final volume of 100 µl) for 20 min at 4°C, washed again and resuspended in 300 µl of PBS. Data was analysed on a BD Fortessa LSR machine, after 10^5 events were acquired.

Table 2.6 Flow cytometry antibodies

Target	Dilution	Fluorochrome	Supplier	Application
CD16	1:20	Efluor450	ThermoFisher	Panel 1/3
	1:22	APC	Miltenyi Biotec	Neutr purity
CD56	1:33	Alexa Fluor 700	BioLegend	Panel 1
CD19	1:20	BV510	BioLegend	Panel 1
	1:22	FITC	BD	Neutr purity
CD20	1:33	PE-Cy7	Miltenyi Biotec	Panel 1
CD14	1:20	PE	BD	Panel 1/3
CD3	1:33	FITC	BioLegend	Panel 1
	1:22	FITC	Miltenyi Biotec	Neutr purity
CD127	1:20	PE-Cy7	BioLegend	Panel 2
HLA-DR	1:33	BV421	BioLegend	Panel 2
CD11c	1:20	BV650	BioLegend	Panel 2
CD123	1:30	BV711	BioLegend	Panel 2
Lineage marker[1]	1:10	PE	Beckman Coulter	Panel 2
CD15	1:33	FITC	BioLegend	Panel 3
	1:22	PE	Miltenyi Biotec	Neutr purity
IL36R	1:10	Streptavidin	BD	Panel 1/2/3
Streptavidin[2]	1:100	APC	BioLegend	Panel 1/2/3
CD45	1:22	VioBlue	Miltenyi Biotec	Neutr purity
CD24	1:22	APC Vio770	Miltenyi Biotec	Neutr purity
PLSCR1	1:50	Rabbit-IgG	Abcam	PLSCR1 intracell staining
Rabbit IgG[3]	1:100	Alexa Fluor 488	BioLegend	PLSCR1 intracell staining

[1]CD3/CD14/CD19/CD20/CD56; [2]Target of secondary biotinylated antibody used for IL36R detection; [3]Target of secondary antibody used for PLSCR1 detection

Panel 1: HLA-DR, CD11c, CD123, CD141, CD127, Lineage, L/D marker; Panel 2: CD3, CD16, CD20, CD56, CD19, CD14, L/D marker; Panel 3: CD14, CD16, CD15, L/D marker.

Table 2.7 Gating strategy for IL36R detection

Cell-type	Markers
B cells	CD3-,CD14-,CD16-,CD20+,CD19+
T cells	CD14-,CD16-,CD19-,CD20-,CD3+
Monocytes - Classical	CD20-,CD3-,CD14+,CD16-
Monocytes - Intermediate	CD20-,CD3-,CD14+,CD16+
Monocytes - Proinflammatory	CD20-,CD3-,CD14-,CD16+
pDCs	Lineage-, HLA-DR+,CD123+,CD11c-
mDCs	Lineage-, HLA-DR+,CD123-,CD11c+
ILCs	Lineage-, HLA-DR-,CD127+
Neutrophils	CD14-,CD16+,CD15+

2.7 Statistics and bioinformatics analyses

2.7.1 Publicly available databases

The data generated by the Blueprint Consortium (http://www.blueprint-epigenome.eu/) and the Fantom5 project (http://fantom.gsc.riken.jp/zenbu/) were queried to investigate cell-specific patterns of gene expression[237,238]. The Genotype-Tissue Expression (GTex) database (https://gtexportal.org/home/) was used to retrieve tissue-specific expression data, while the GWAS catalogue (https://www.ebi.ac.uk/gwas/) was utilized to search for the results of published genome-wide association studies[239,240].

The Ensembl Genome browser was used to obtain reference DNA and protein sequences, as well as orthologue and paralogue sequences for genes of interest (https://www.ensembl.org/index.html)[241]. Minor Allele Frequencies (MAFs) were obtained from the Exome Aggregation Consortium browser (ExAC, http://exac.broadinstitute.org/)[242].

A list of MPO deficiency alleles was obtained from OMIM[243]. Next, the Geneatlas[244] was used to run the PheWAS analysis on the identified variants.

2.7.2 Analysis of whole-exome sequence data

2.7.2.1 Data processing

Raw whole-exome sequence data was processed by personnel at the BRC Bioinformatics Core. Briefly, the paired-end reads were aligned to the hg19 reference genome with Novoalign (Novocraft Technologies), then duplicates and low-quality reads were removed with MarkDuplicates[245]. Changes covered by more than 4 reads were called with SAMtools and annotated using the ANNOVAR package[246].

2.7.2.2 Step-wise filtering of variant profiles

ANNOVAR annotated files were imported into Microsoft Excel for step-wise filtering. For family 8GPP, after removing unknown and synonymous variants, changes were retained if they were: i) heterozygous, ii) rare (global MAF ≤ 0.01) and iii) shared by the three affected relatives. A further filter based on allele frequencies observed in the East Asian population was applied to the resulting changes. The reads for the remaining variants were visually inspected with Integrative Genomics Viewer (IGV)[247], in order to exclude alignment artefacts. Finally, the effects of the changes were assessed in-silico (see section 2.7.2.3) and only the variants with deleterious potential were retained.

For the 19 unrelated GPP cases, variants were retained if they were: i) homozygous, ii) splicing, stop-gain, stop-loss and frameshift changes iii) rare (global MAF ≤ 0.01) and iv) rare in an in-house sequencing dataset (MAF ≤ 0.05). Finally, the effects of the changes were assessed in-silico with CADD (see section 2.7.2.3) and only the variants with deleterious potential were retained.

2.7.2.3 Evolutionary conservation and pathogenicity predictions

Clustal Omega[248] was used to align orthologue sequences obtained from Ensembl Genome browser.

The pathogenic potential of missense changes was determined using PROVEAN[249], SIFT[250], Polyphen-2[251], Mutation Taster[252] and the Combined Annotation Dependent Depletion webserver (CADD)[253]. MaxEntScan[254] and Spliceman[255] were used to analyse splicing variants.

The mutational load tolerated by *PRR13* has been measured using the Residual Variation Intolerance score and the Gene Damage Index score[256,257].

2.7.3 Analysis of RNA-sequencing data

2.7.3.1 Data processing

FastQC (http://www.bioinformatics.babraham.ac.uk/projects/fastqc) was used to assess the quality of the sequence data and all reads with a Phred score lower than 30 were removed from the analysis. The remaining reads were trimmed to remove adapters and high-repeat k-mers, while overrepresented sequences were eliminated using FASTX-Toolkit (http://hannonlab.cshl.edu/fastx_toolkit/). Once the reads were mapped and aligned to the hg38 human genome with TopHat[258] and Bowtie2[259], they were counted with HTseq[260] and SAMtools[245].

2.7.3.2 In-silico assessment of neutrophil purity

The genes identified by RNA-sequencing analysis were over 15,000 in both patient and control datasets, in line with published reports[261,262]. These were compared to those expressed in the lymphocytes, monocytes, eosinophils and neutrophils sequenced by the Blueprint Consortium. To account for the lower number of genes present in the Blueprint dataset (n=7,217 neutrophil expressed genes), those with a median expression <0.1 transcript per million (TPM) were discarded. The analysis was carried out using the dplyr package in RStudio v.0.8.0.1[263].

2.7.3.3 Differential expression analysis

Differential expression analysis of the full RNA-sequencing cohort (8 cases vs. 11 controls) was performed with DESeq2 (R package, v 1.16.1)[264], using sex as a covariate. Fold changes (FC) were calculated with a zero-centered normal prior and P values were derived with the Wald test and a Benjamini–Hochberg[265] correction for multiple testing.

For the differential expression analysis of the case carrying the *MPO* splicing variant and the 11 healthy controls, fold changes were calculated by dividing the gene expression levels (measured as RPKM, reads per kilobase per million) observed in the patient by the mean RPKM of the controls. Z-scores were calculated and P values were computed from the z-scores using the "NORM.S.DIST" function available on Microsoft Excel and

corrected for multiple testing (padj, adjusted p value) by multiplying the P value for the total number of tests (one for each gene). Genes with padj <0.05 and FC >1.5 were considered differentially expressed.

2.7.3.4 Analysis of blood transcription modules

Marika Catapano adapted a published script[266] to identify blood transcription modules that were enriched among genes up-regulated in GPP. Briefly, the genetable_to_activityscores function was applied to select the blood modules that were active in the neutrophil dataset. The enrichment_test function was then applied to our list of differentially expressed genes (DEGs), taking into account the module activity score and the FC of the genes mapping to each module. Finally, enrichment P values were computed and corrected for multiple testing, using a False Discovery Rate (FDR) <0.05 as a significance threshold.

2.7.3.5 Pathway and upstream regulator enrichment analysis

Genes with a FC >1.5 and an FDR <0.05 were used as input for Ingenuity Pathway Analysis (IPA, Qiagen). Briefly, each DEG was assigned a weight (reflecting the magnitude of its up-regulation) and mapped against reference pathways. Enrichment P values were then calculated with a Fisher's exact test, taking into account the weight of the DEGs and the size of the pathway. Finally, the Benjamini-Hochberg method was used to correct P values for multiple testing. FDR values <0.05 were considered statistically significant.

The "Upstream Analysis" function in IPA was used to perform the upstream regulator enrichment analysis. The dataset was examined as a subgraph with unknown a priori causal edges in the master network. To identify the regulators, each gene was scored based on the downstream targets identified, which were defined by an enrichment P value. An activation score built on co-expression values was then assigned to each network and the enrichment in the dataset calculated. STAT1- and IRF7-centered networks were visualised with the igraph v1.0.1 R Package.

2.7.3.6 Interferon score

The interferon score (IS)[267] was computed using five interferon stimulated genes (ISGs: *PLSCR1, OASL, IFI6, IFIT3* and *IFITM3*) that had been previously used to establish interferon signatures[268]. They were most up-regulated in a GPP whole-blood dataset produced by the Capon lab. A calibrator was used to normalise the expression of each gene and the IS was calculated as the median expression of the 5 ISGs.

2.7.4 Statistical tests

Experimental data are shown as means +/- standard deviation (SD) or standard error of the mean (SEM). Differences in interferon score between cases and controls were analysed with an unpaired t-test or one-way ANOVA followed by Dunn's post-test[269], as appropriate. As the assumption of equal variance between samples may not have been met, cytokine stimulations were assessed with non-parametric methods, using the Wilcoxon signed-rank test (when comparing 2 groups) or Friedman test (when comparing 3 groups). The P value of the enrichment for *MPO* variants in GPP and PPP patients was calculated using the Chi-square test with Yates correction. All statistical tests were implemented with GraphPad Prism v7.05 and P values <0.05 were considered statistically significant.

3 IDENTIFICATION OF A NEW PSORIASIS GENE ASSOCIATED WITH NEUTROPHIL COUNT VARIATION

3.1 Genetic analysis of three related patients

The aim of this project was to uncover novel genetic determinants of psoriasis through the analysis of PsV pedigrees and GPP cases that are not accounted for by known disease genes.

An extended pedigree of Chinese-Malay origin was ascertained through a collaboration with Dr Siew-Eng Choon from the Sultanah Aminah Hospital in Johor Bahru, Malaysia (Figure 3.1, Table 2.1). While several family members suffered from PsV, two were affected by GPP, suggesting that neutrophil activation was an important component of the phenotype segregating in this pedigree.

None of the affected individuals carried mutations in *IL36RN, AP1S3*, or *CARD14*. Whole-exome sequencing (WES) was therefore undertaken in three patients (8GPP1, 8GPP2 and 8PsV3; Figure 3.1) with a view to identifying a new disease gene. The analysis identified between 25,782 and 26,467 variants per affected individual. The average sequence coverage was 117x, with 94% of the target exome covered at a depth of at least 20x (Table 3.1).

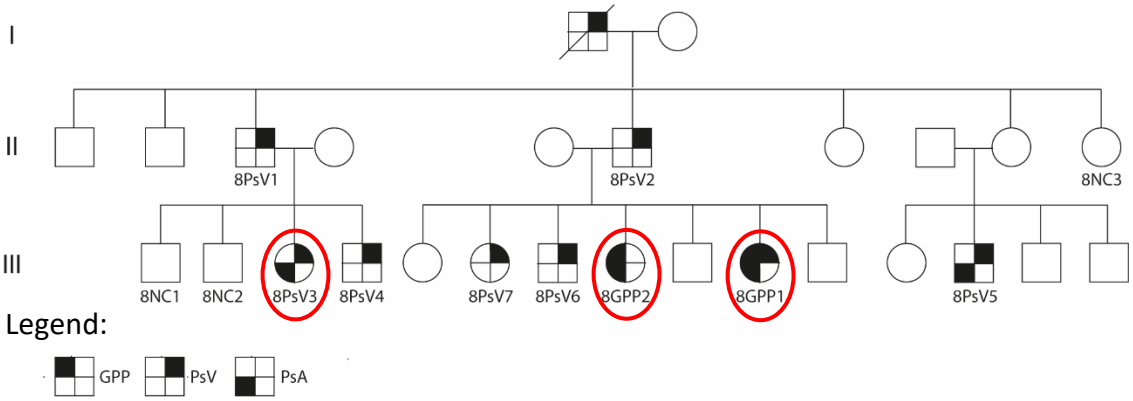

Figure 3.1 Pedigree of family 8GPP

8GPP1, 8GPP2 and 8PsV3 (circled in red) were selected for whole-exome sequencing. DNA was available for all the individuals labelled in the figure, but the samples for 8PsV7, 8NC1, 8NC2 and 8NC3 were only collected towards the end of the study. Shading of the top left, top right and bottom left quadrants identifies patients suffering from GPP, PsV and PsA, respectively. Some individuals presented with more than one disease subtypes, therefore multiple areas are shaded in black.

NC, normal control

Table 3.1 Whole-exome sequencing summary statistics

	8GPP1	**8GPP2**	**8PsV3**
Variants detected	25,861	25,782	26,467
Mean Coverage	100.96x	109.78x	140.04x
CCDS bases with coverage >10x	97.11%	97.28%	98.92%
CCDS bases with coverage >20x	94.26%	94.84%	98.20%

CCDS, consensus coding sequence

Based on the pedigree structure, an autosomal dominant mode of inheritance was assumed. Therefore, the WES data was filtered to remove synonymous and unknown variants and retain only variants that were heterozygous, rare (global Minor Allele Frequency (MAF) ≤ 0.01) and shared by the three affected relatives. A further filter based on allele frequencies observed in the East Asian population was then applied, using the data produced by the Exome Aggregation Consortium (ExAC)[242]. Finally, the deleterious potential of the remaining variants was assessed using five pathogenicity prediction algorithms. This process uncovered nine damaging variants that were followed-up as candidate mutations (Table 3.2, Appendix III).

Table 3.2 Rare non-synonymous variants shared among the three cases that were exome sequenced

Gene	Variant	MAF among East Asians	Pathogenicity prediction					Consensus
			Mutation Taster	Provean	SIFT	PolyPhen2	CADD[1]	
GLI3	R989W	NA	disease causing	deleterious	damaging	probably damaging	29.2	DAMAGING
ITGB6	G593R	0.002	disease causing	deleterious	damaging	possibly damaging	26.8	DAMAGING
MAN2B2	W967X	0.0002	disease causing	/	/	/	41.0	DAMAGING
PITPNM3	P339R	0.005	disease causing	deleterious	tolerated	probably damaging	26.3	DAMAGING
PRR13	K131T	0.0007	disease causing	deleterious	damaging	probably damaging	16.9	DAMAGING
PTCH1	Y494C	NA	disease causing	neutral	tolerated	probably damaging	23.5	DAMAGING
SDK1	A871T	0.005	disease causing	deleterious	damaging	probably damaging	26.2	DAMAGING
SVIL	R747W	0.01	disease causing	deleterious	damaging	benign	24.2	DAMAGING
TMEM184A	T375M	0.01	disease causing	deleterious	damaging	possibly damaging	23.7	DAMAGING

[1]CADD scores above 15 are considered pathogenic. MAF, minor allele frequency; NA, not available; pathogenicity prediction tools are described in the Methods section of this thesis.

3.2 Screening of candidate genes in additional family members

To determine which of the nine variants could be responsible for the inflammatory skin phenotype seen in family 8GPP, the affected individuals who had not been exome sequenced were screened by Sanger sequencing. Surprisingly, none of the 9 changes was found in all affected relatives (Table 3.3). A closer inspection of the data also revealed that 8PsV6 did not share any of the 10 variants with his two sisters (8GPP1 and 8GPP2; Table 3.3), which suggested that his paternity was questionable.

To further investigate this possibility, 8PsV6 and his first-degree relatives were genotyped for 3 microsatellite markers (D6S273, AP1S3-TG, D2S2299). Four additional unrelated individuals whose DNA had arrived in the same shipment as 8PsV6 were also examined, to investigate the possibility of a sample swap.

While the D6S273 and AP1S3-TG genotypes were compatible with paternity, the analysis of D2S2299 showed that 8PsV6 carried a 290 bp allele which was not present in the paternal or maternal genome. Conversely, the genotype of unrelated patient 135GPP1 was compatible with that of 8PsV6's parents (Figure 3.2). These results suggested that the two DNA samples had been swapped.

Table 3.3 Summary of candidate variant screening in all 8GPP family members.

Gene	Variant	8GPP1	8GPP2	8PsV1	8PsV2	8PsV3	8PsV4	8PsV5	8PsV6
GLI3	R989W	Y	Y	Y	Y	Y	Y	N	N
ITGB6	G593R	Y	Y	Y	Y	Y	Y	Y	N
MAN2B2	W967X	Y	Y	Y	Y	Y	Y	N	N
PITPNM3	P339R	Y	Y	Y	Y	Y	N	Y	N
PRR13	K131T	Y	Y	Y	Y	Y	Y	Y	N
PTCH1	Y494/645C	Y	Y	Y	Y	Y	N	Y	N
SDK1	A871T	Y	Y	Y	Y	Y	N	N	N
SVIL	R747W	Y	Y	Y	Y	Y	N	N	N
TMEM184A	T375M	Y	Y	Y	Y	Y	N	N	N

Y, Yes; N, No

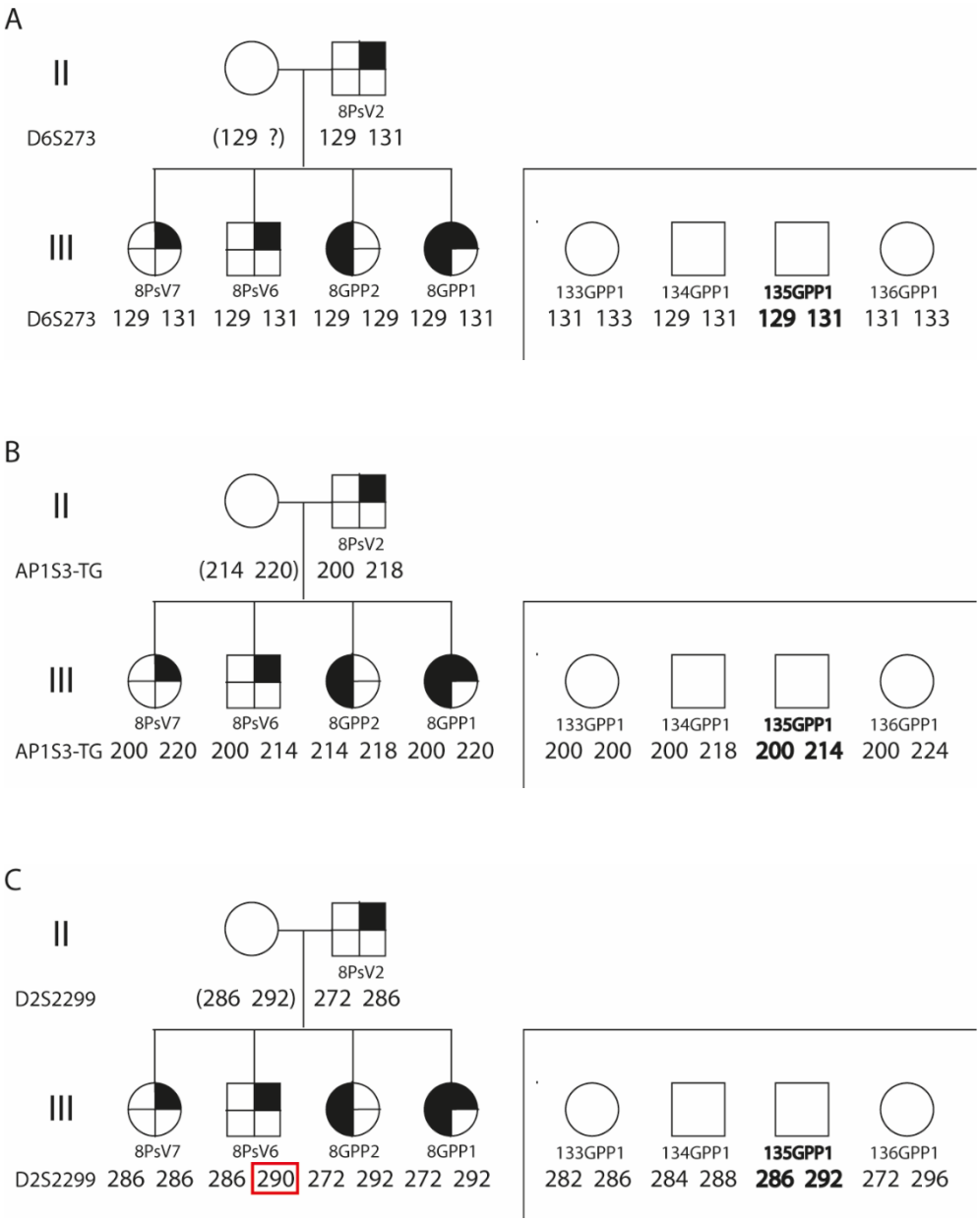

Figure 3.2 Microsatellite genotyping identifies a sample swap

Three microsatellites were typed in 8PsV6, his first-degree relatives (left) and in four unrelated GPP individuals who had been recruited in the same centre (right). Genotypes are defined by the molecular weight of PCR products (A-B) The genotypes of markers D6S273 and AP1S3-TG are compatible with the notion that 8PsV6 is a member of family 8GPP. (C) Genotyping of marker D2S2299 revealed that 8PsV6 harboured a 290 bp allele (red square) that he could not have inherited from either parent. Conversely the genotype of 135GPP1 (highlighted in bold) was compatible with that of 8PsV6's parents. Genotypes in brackets were inferred.

3.3 Identification of *PRR13* as a candidate gene

To confirm that the two DNA samples had been swapped, the nine candidate mutations were screened by Sanger sequencing in the four unrelated patients that had been included in the microsatellite genotyping experiment. This showed that 135GPP1 shared 5 changes with the affected individuals from family 8GPP, validating the notion of a swap with 8PsV6 (Table 3.4).

Once the data was re-analysed on the basis of this information, one variant shared by all affected relatives was identified (Table 3.4). This was a Lysine to Threonine substitution affecting a highly conserved residue in *PRR13* (K131T) (Figure 3.3). Of note, the screening of further family members who had by then become available (8PsV7, 8NC1 8NC2 and 8NC3) revealed that the variant was present in the newly recruited case and absent from two of the three clinically assessed unaffected relatives (Table 3.5 and Figure 3.4). Of note, the unaffected carrier 8NC2 was 48 years old at the time of the analysis, so we cannot exclude the possibility that he might develop psoriasis later in life. Thus, the K131T substitution in *PRR13* is the most likely disease allele segregating in family 8GPP.

Table 3.4 Screening of candidate variants in family 8GPP and in 4 unrelated individuals recruited from the same centre. 135GPP1 is suggested to replace the 8PsV6 sample.

Gene	Variant	8GPP1	8GPP2	8PsV1	8PsV2	8PsV3	8PsV4	8PsV5	135GPP1	8PsV6	133GPP1	134GPP1	136GPP1
GLI3	R989W	Y	Y	Y	Y	Y	Y	N	Y	N	N	N	N
ITGB6	G593R	Y	Y	Y	Y	Y	Y	Y	N	N	N	N	N
MAN2B2	W967X	Y	Y	Y	Y	Y	Y	N	Y	N	N	N	N
PITPNM3	P339R	Y	Y	Y	Y	Y	N	Y	Y	N	N	N	N
PRR13	K131T	Y	Y	Y	Y	Y	Y	Y	Y	N	N	N	N
PTCH1	Y494/645C	Y	Y	Y	Y	Y	N	Y	N	N	N	N	N
SDK1	A871T	Y	Y	Y	Y	Y	N	N	N	N	N	N	N
SVIL	R747W	Y	Y	Y	Y	Y	N	N	Y	N	N	N	N

Y, Yes; N, No

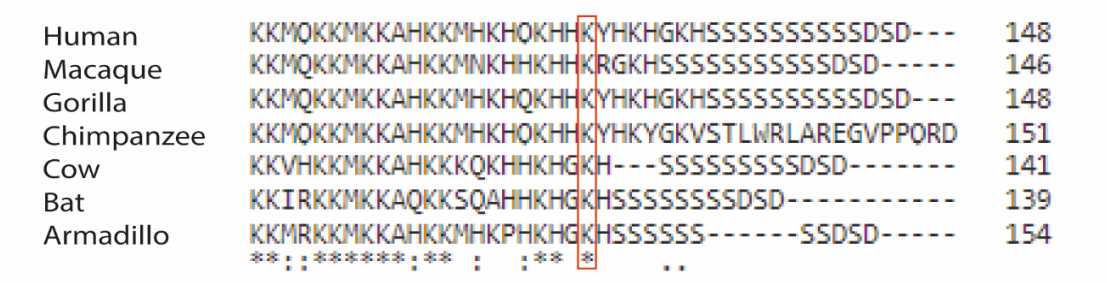

Figure 3.3 Evolutionary conservation of the Lys131 amino acid residue

Protein sequence alignment showing the evolutionary conservation of the Lys131 residue. Asterisks (*) indicate positions with a conserved residue; colons (:) indicate conservation between groups of amino acids with very similar properties; periods (.) indicate conservation between groups of residues with moderately similar properties.

Table 3.5 Screening of K131T change in the entire 8GPP family, including the additional available samples.

Gene	Variant	8GPP1	8GPP2	8PsV1	8PsV2	8PsV3	8PsV4	8PsV5	135GPP1/ 8PsV6	8PsV7	8NC1	8NC2	8NC3
PRR13	K131T	Y	Y	Y	Y	Y	Y	Y	Y	Y	N	Y	N

Y, Yes; N, No

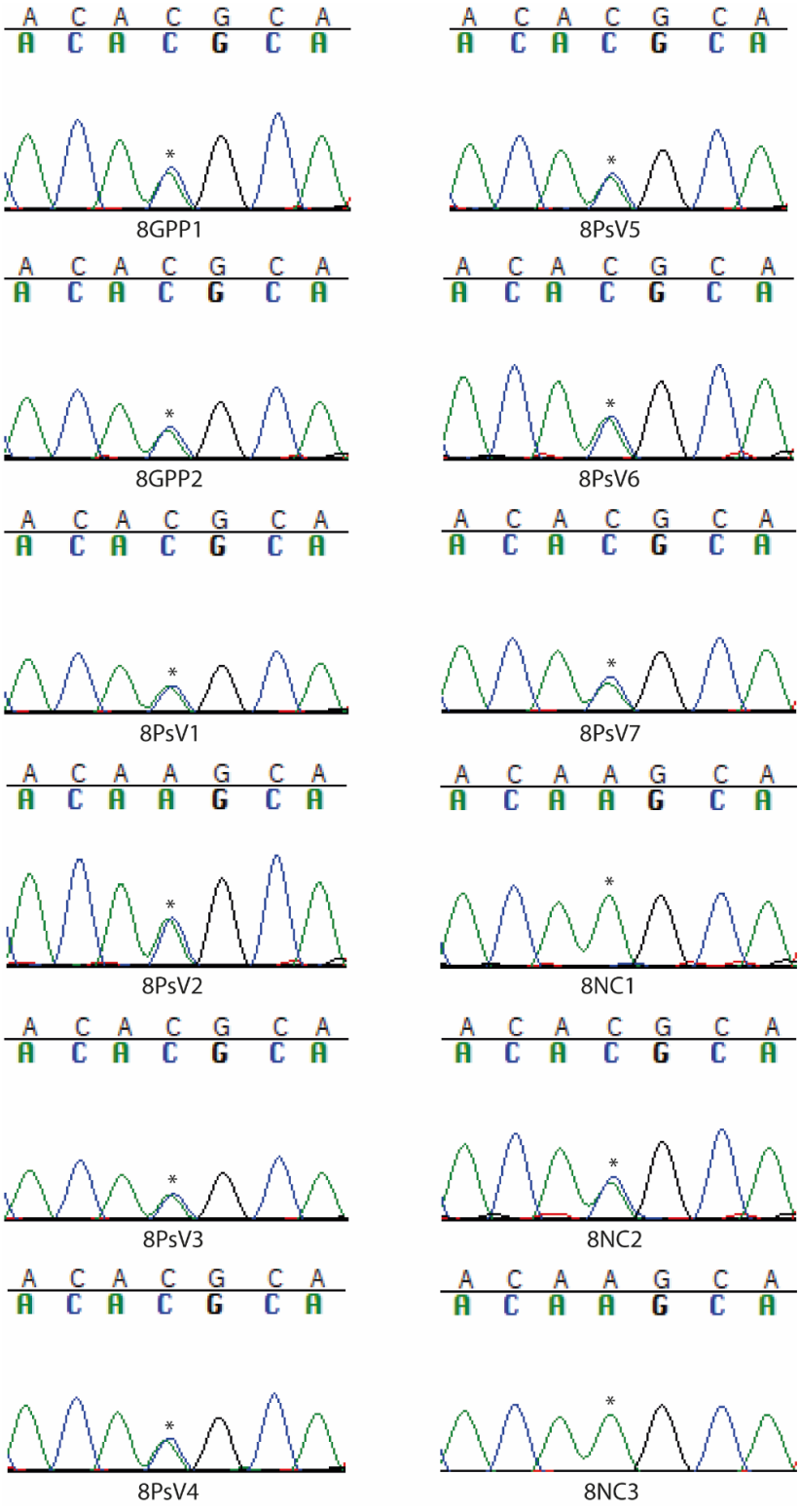

Figure 3.4 Screening of the K131T *PRR13* variant in family 8GPP

Sequence chromatograms of the heterozygous K131T substitution. Asterisks indicate the nucleotide change.

3.4 Screening of *PRR13* in an extended patient cohort

To further investigate *PRR13* as a candidate disease gene, the K131T substitution was screened in a dataset selected to match the characteristics of family 8GPP. This included 107 unrelated subjects affected by GPP and in 121 PsV cases available in house (Table 3.6). A subset of the above samples (32 GPP and 16PsV cases) was also sequenced for the entire *PRR13* coding region. The analysis did not identify any further individuals harbouring K131T or any other *PRR13* deleterious allele.

Next, whole-genome sequence data generated by the 100,000 Genomes Project[270] for 11 unrelated GPP cases was queried. This revealed a deleterious *PRR13* variant (P16S) in a British European child suffering from early onset GPP (Table 3.7, Figure 3.5). Thus, deleterious *PRR13* alleles are observed in GPP individuals of varying ethnicity.

Table 3.6 Summary of the patient cohort screened for the *PRR13* genetic analysis

Disease	Cases (target sequence)	Family history of PsV	Concomitant PsA	Ethnicity
GPP	75 (K131T only)	9	4	Asian 75
GPP	32 (whole coding region)	18	23	Asian 32
PsV	105 (K131T only)	53	3	Asian 53
				European 52
PsV	16 (whole coding region)	13	3	Asian 16

Table 3.7 Rare non-synonymous *PRR13* variant identified in a British patient

Gene	Variant	MAF among Europeans	Pathogenicity prediction					Consensus
			Mutation Taster	Provean	SIFT	PolyPhen2	CADD[1]	
PRR13	P16S	0.000034	polymorphism	deleterious	damaging	probably damaging	21	DAMAGING

[1]CADD scores above 15 are considered pathogenic. MAF, minor allele frequency; pathogenicity prediction tools are described in the Methods section of this thesis.

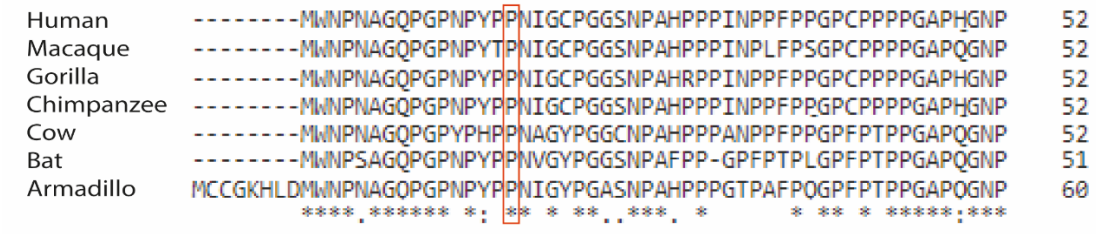

Figure 3.5 Evolutionary conservation of the Pro16 amino acid residue

Protein sequence alignment showing the evolutionary conservation of the Pro16 residue. Asterisks (*) indicate positions with a conserved residue; colons (:) indicate conservation between groups of amino acids with very similar properties; periods (.) indicate conservation between groups of residues with moderately similar properties.

3.5 *PRR13* is highly expressed in neutrophils

PRR13 encodes Proline Rich 13, a poorly understood protein that is also known as TXR1 (Taxane-Resistance protein 1). To further explore its role in psoriasis, a number of publicly available resources were mined.

The RNA-seq data generated by the Genotype-Tissue Expression (GTex) consortium[239] showed that *PRR13* is expressed in a variety of tissues, including skin (median read count: 72 Transcripts Per Million (TPM)). Transcript levels, however, were highest in whole-blood (median: 337.5 TPM) (Figure 3.6). Further investigation of cell-specific data produced by the Blueprint and Fantom5 projects[237,238] revealed that *PRR13* expression was especially abundant in neutrophils and eosinophils (Table 3.8).

To obtain further insights into gene function, the GWAS catalogue, a curated collection of all published genome-wide association studies[240] was queried for associations driven by *PRR13* alleles. This revealed that an intronic *PRR13* variant (rs550235164) is associated with neutrophil count variation ($P=5 \times 10^{-23}$)[271].

Taken together, these observations indicate that *PRR13* is likely to play an important role in neutrophil biology.

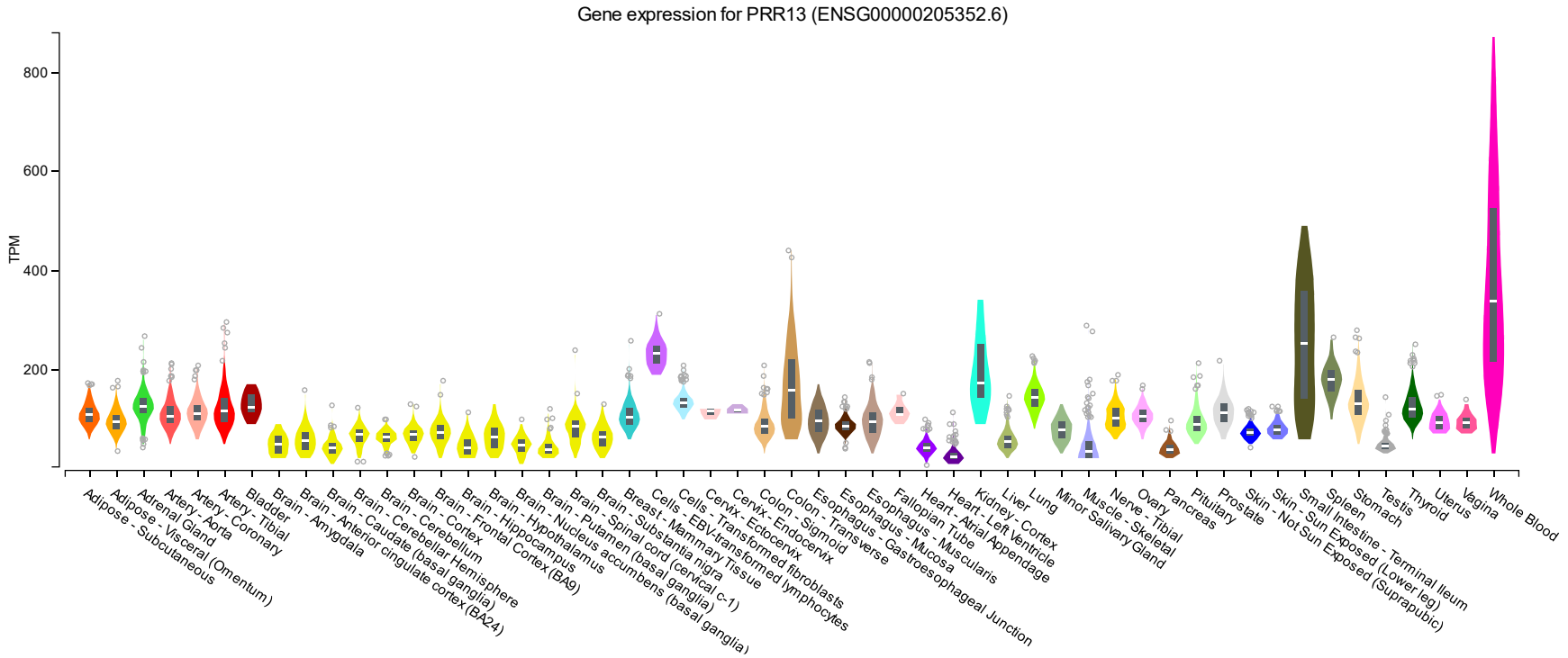

Figure 3.6 *PRR13* expression in human tissue

PRR13 is highly expressed in whole blood (337.5 TPM) (Adapted from https://gtexportal.org/home/gene/PRR13)

Table 3.8 *PRR13* expression in white blood cells

Blueprint	
Cell type	**TPM[1]**
mature eosinophil	98
segmented neutrophil of bone marrow	88
mature neutrophil	82
conventional dendritic cell	74
neutrophilic metamyelocyte	66
inflammatory macrophage	55
macrophage	50
regulatory T cell	29
CD4-positive, alpha-beta T cell	28
CD8-positive, alpha-beta T cell	23
FANTOM5	
Cell type	**Read counts[2]**
neutrophils	756
eosinophils	507
macrophage - monocyte derived	117
CD8+ T cells	115
CD4+ T cells	93
DC - monocytes immature derived	80

[1]TPM, Transcripts Per Million; [2]FANTOM 5 uses 5'-end cap analysis gene expression (CAGE) reads

3.6 Discussion

The aim of this study was to identify new genetic determinants of plaque and pustular psoriasis, through the analysis of a unique pedigree of Chinese-Malay origin. Whole-exome sequencing of three affected relatives and follow-up of nine putative disease loci highlighted *PRR13* as the most likely candidate gene. In keeping with this observation, the analysis of WGS data generated by the 100,000 Genomes Project[270] revealed a deleterious *PRR13* allele in a British European child affected by GPP. The Capon lab is now seeking to access electronic health records for the proband and their parents, in order to establish whether there is a history of plaque or pustular psoriasis within the family.

Difficulties in identifying a candidate variant shared by all affected relatives were initially encountered. Due to the elevated cost of whole-exome sequencing more family members, the paternity test was successfully performed using microsatellite analysis. However, it is important to consider that only 1 of the 3 markers used was informative, and that the genotype of 8PsV6 could still be accounted for by de-novo slippage of the D2S2299 290 repeat. Therefore, the use of further markers could have helped strengthen our thesis that the two DNA samples had been swapped.

It is also worth noticing that while the filtering strategy applied to the WES data allowed me to uncover *PRR13* as the most likely candidate gene, the identification of additional shared variants could have been hindered by the exclusion of synonymous changes, as recent evidence suggests that they may contribute to disease pathogenesis by affecting RNA conformation and splicing[272,273].

PRR13 encodes a 148 aa protein which spans 44 Proline residues and terminates with a stretch of 10 Serines. Its function is poorly understood, as the protein does not encompass known functional domains and has no paralogues. The amino acid sequence is conserved across placental mammals, but no orthologues exist in other species. Of note, limited variation is presented within the *PRR13* sequence, so that the gene is classified as likely-to-be-disease-causing, based on its Residual Variation Intolerance

score and Gene Damage Index score[256,257] (two parameters measuring the mutational load tolerated by human genes).

In the absence of any information on PRR13 structure and functional motifs, it is difficult to speculate on the effects of the K131T and P16S mutations. Thus, the over-expression of wild-type and mutagenized constructs will be needed, in order to determine whether disease alleles disrupt the stability or sub-cellular localization of the protein.

PRR13 has been implicated in resistance to chemotherapeutics, as cells that overexpress the gene are protected from the lethal effects of taxane and oxaliplatin[274,275]. In keeping with these observations, PRR13 up-regulation has been associated with decreased survival in ovarian cancer patients receiving platinum-taxane therapy, with similar findings reported for gastric cancer suffers treated with oxaliplatin[276,277].

It has been suggested that the above effects reflect a role of *PRR13* in the negative regulation of thrombospondin 1 (*TSP1*), which in turn would cause a reduction in apoptotic cell clearance[278,279]. Of note, TSP1 has also been implicated in the clearance of apoptotic neutrophils from the circulation. In fact, TSP1 blockade inhibits macrophage-mediated neutrophil phagocytosis[209,210].

A recent paper also proposed that *PRR13* overexpression could confer resistance to oxaliplatin by potentiating autophagy[279]. The latter plays a crucial role in innate immunity by ensuring the degradation of inflammatory mediators and infectious agents, as well as regulating cytokine secretion downstream of pattern recognition receptors[280]. For instance, our group and others have shown that mutations in *AP1S3* and changes in *SQSTM1* expression lead to autophagy dysregulation and associate with psoriasis[118,281,282]. Of note, autophagy is also essential to neutrophil homeostasis, as it is required for degranulation, NET formation and innate immune effector functions[283,284].

TSP1 is also a potent angiogenic inhibitor which antagonises vascular endothelial growth factor (VEGF) through a variety of mechanisms, such as the inhibition of MMP9 activation[285–287]. While the anti-angiogenic function of TSP1 has clear relevance to

tumour biology, it also suggests a link with psoriasis, which is characterised by new vessel formation and increased expression of VEGF[61,288,289].

Therefore, the information that is available in the literature suggest that the *PRR13* variants detected in this study may be gain-of-function alleles, which may promote angiogenesis and disrupt neutrophil clearance through constitutive TSP1 inhibition.

Unfortunately, the difficulty of shipping intact fresh blood from Malaysia and the short life-span of neutrophils have prevented me from investigating this disease model in patient cells. While this is one of the main limitation of the current study, the Capon lab is poised to contact the centre which recruited the British patient carrying a *PRR13* P16S variant. Owing to the geographical proximity of this hospital (Cambridge, UK), it should be possible to obtain fresh patient neutrophils for immune phenotyping and autophagy stimulation assays.

In conclusion, the evidence provided in this chapter show that *PRR13* is a likely candidate gene for GPP and an important player in the regulation of neutrophil immune homeostasis.

4 MYELOPEROXIDASE MUTATIONS ARE ASSOCIATED WITH PUSTULAR PSORIASIS

4.1 Stepwise filtering of whole-exome sequence profiles

As described in the previous chapter, the aim of the genetic studies described in this thesis was to identify additional candidate genes for pustular psoriasis. While both familial and sporadic disease cases have so far been identified[108,109,115], the focus of this chapter was on the latter. Therefore, the whole-exome profiles of 19 unrelated GPP cases were interrogated.

The 19 exomes contained ~500,000 variants, with an average of 25,000 changes per patient. To account for the lack of parent-to-offspring transmission and for the severity of the phenotype, the data was analysed by assuming autosomal recessive inheritance and only retaining rare homozygous loss-of-function variants (splicing, stop-gain, stop-loss and frameshift changes with a global Minor Allele Frequency (MAF) ≤ 0.01)). Any alleles found at high frequency (MAF ≥ 0.05) in an in-house sequencing dataset were also filtered out, as they were likely to represent sequencing artefacts. While this analysis identified 37 changes, only six had deleterious potential (CADD ≥ 15) (Table 4.1, Appendix IV), none of which was shared between any of the cases. Among the pathogenic changes, a homozygous splicing variant in *MPO* (2031-2A>C) was selected for follow-up, due to the fundamental role of the gene in neutrophil microbial killing. The change was found in a female of European origin, who also carried a heterozygous missense variant in *AP1S3*. Of note, the possibility of epistasis involving *AP1S3* alleles has been previously suggested by our group[118].

Table 4.1 Rare homozygous loss-of-function variants identified in 19 unrelated GPP cases

Patient ID	Gene	Variant	Mutation type	Global MAF (ExAC)	Pathogenicity prediction: CADD[1]	Gene function
41GPP2	*ARAP1*	4070+5G>T	Splicing	0.0005	22.8	Modulates actin cytoskeleton remodelling by regulating ADP-ribosylation factor (ARF) and Ras homologous (RHO) family members; might regulate cell-specific trafficking of TRAIL receptor thus affecting apoptosis
8GPP2	*CCSER2*	1868+5T>A	splicing	0.0003	15.8	Might play a role in microtubule bundling
38GPP1	*DMBT1*	C1504T	Stop-gain	0.00002	35.0	Might play a role in the interaction of tumour cells and the immune system
17GPP1	*EIF4G1*	698-3C>T	splicing	0.0016	16.5	Component of the EIF4F protein complex that facilitates recruitment of mRNA to the ribosome
GYFAP0029	*FAM83A*	C871T	Stop-gain	0.0018	36.0	Functions in the epidermal growth factor receptor (EGFR) signalling pathway
GYFAP0014	*MPO*	2031-2A>C	splicing	0.0043	32.0	Major component of neutrophil azurophilic granules; produces hypohalous acids central to the microbicidal activity of neutrophils

[1]CADD scores above 15 are considered pathogenic. MAF, minor allele frequency

4.2 The *MPO* 2031-2A>C variant is associated with pustular psoriasis

To further investigate *MPO* as a candidate disease gene, its coding region was screened by Sanger sequencing in 14 additional unrelated subjects affected by GPP. This did not identify any further individuals harbouring 2031-2A>C or any other deleterious allele.

The analysis was then extended to include 105 patients affected by palmoplantar pustulosis (PPP) and 9 with Acrodermatitis Continua of Hallopeau (ACH), for whom WES data was available. This revealed another individual carrying the homozygous splicing variant.

In both the GPP and PPP patient, the presence of the 2031-2A>C substitution was confirmed by Sanger sequencing (Figure 4.1). The clinical and phenotypic characteristics of the two cases are summarised in Table 4.2.

Of note, the 2031-2A>C allele was observed in homozygosity in only one of the 33,217 healthy European individuals sequenced by the ExAC project[290]. Thus, the association with pustular psoriasis is statistically significant ($P=4.6x10^{-5}$) (Table 4.3).

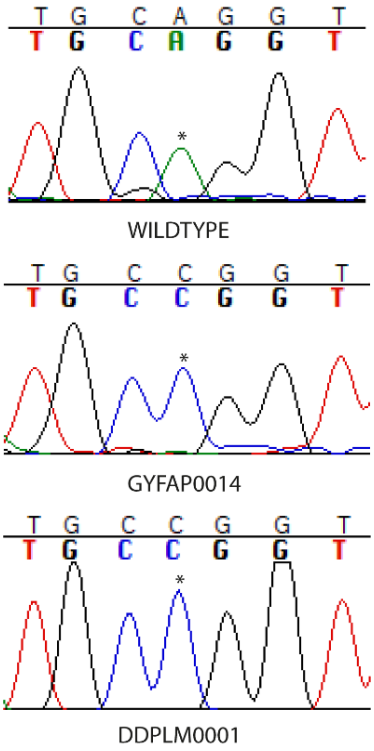

Figure 4.1 Sequence chromatograms of the homozygous 2031-2A>C variant.

Asterisks indicate the nucleotide change in individuals GYFAP0014 (affected by GPP) and DDPLM0001 (affected by PPP) compared to wildtype.

Table 4.2 Disease presentation in the two cases carrying the 2031-2A>C variant in *MPO*

Patient	Sex	Age of onset	Clinical presentation	Neutrophil count (%WBC)[1]
GYFAP0014	F	36	First GPP episode during pregnancy and subsequent severe flare when taken off infliximab.	8.5 x 10^9/L (60.3%)
DDPLM0001	F	24	PPP in right heel, ACH in left hand with nail loss, crusting around lips (occasional pustules on lips), fissured tongue, PsV in lower limbs, PsA; poorly controlled on acitretin	7.4 x 10^9/L (75.5%)

WBC: White blood cell counts; [1]Reference neutrophil values 1.5-7 x 10^9/L

Table 4.3 Association test for the 2031-2A>C *MPO* variant in the European population

CC homozygous individuals (frequency)		**P value[3]**
Cases[1]	Controls[2]	
2/131 (1.5%)	1/33,217 (0.003%)	4.6×10^{-5}

[1]19 GPP, 103 PPP and 9 ACH individuals of European descent;
[2] Control data from ExAC; [3]One-tailed Fisher exact test.

4.3 Literature review strengthens the link between *MPO* variants and pustular skin phenotypes

The *MPO* variant observed in the two pustular psoriasis cases had been previously described as a myeloperoxidase deficiency allele[291]. To further investigate the significance of this observation, the hypothesis that MPO deficiency is associated with neutrophilic skin inflammation was investigated through a systematic literature review (Figure 4.2).

Twenty-three case reports were identified and carefully inspected. This uncovered two cases of myeloperoxidase deficiency presenting with generalised pustular psoriasis[292,293]. Two further articles reported MPO deficiency associated with disseminated pustular candidiasis[294] and pyoderma gangrenosum (PG, a severe neutrophilic dermatosis)[295]. Given the rarity of the above conditions (1-9:1,000,000 for GPP and 1-3.3 in 330,000 for PG[296,297]), these observations strengthen the link between loss of *MPO* and neutrophilic skin inflammation (Table 4.4).

Key words: ((MPO or Myeloperoxidase) and (skin or dermatol* or cutaneous) and (deficien* or mut* or variant* or allele* or KO or knockout* or knockdown* or GWAS or genome wide association stud* or genome wide linkage))

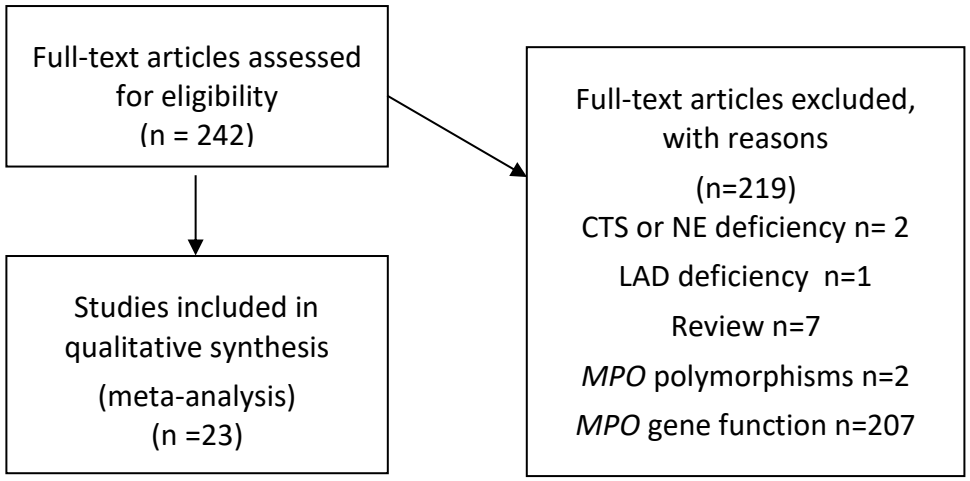

Figure 4.2 Flow diagram of the literature review

Out of 242 articles identified, 219 were excluded as they were reviews or did not describe patients with MPO deficiency. The 23 remaining papers were retained and analysed.

CTS, cathepsin; NE, neutrophil elastase or ELANE; LAD, leucocyte adhesion deficiency

Table 4.4 Articles reporting MPO deficiency and pustular skin phenotypes.

Reference	Disease presentation
Stendahl and Lindgren *Scand. J. Haematol.* 16, 144–153 (1976).	46-year-old man with MPO deficiency. Reported a deceased identical twin who suffered from mild pustular psoriasis. Patient's illness started as psoriasis vulgaris. Then he developed a GPP flare accompanied by high fever.
De Argila et al. *Dermatology* 193, 270 (1996)	61-year-old woman with MPO deficiency. She suffered for 2 years from episodes of annular pustular psoriasis. Lesions tended to spread and form enlarged rings over the trunk and limbs. Flares were accompanied by chills and joint inflammation.
Disdier et al. *JAAD* 24, 654 (1991)	81-year-old woman with MPO deficiency. She injured her leg and developed a high fever, as well as a necrotic, bullous eruption suggestive of pyoderma gangrenosum.
Nguyen and Katner *Clin. Infect. Dis.* 24, 258-260 (1997)	20-year-old male with MPO deficiency. He was admitted to hospital after a motorcycle accident and developed a high fever as well as a generalized pustular eruption. Cultures of skin specimens were positive for Candida albicans.

4.4 *MPO* disease variants are associated with increased neutrophil count

To obtain further insights into the phenotypic effects of the 2031-2A>C mutation, I interrogated the data generated by UK Biobank, which includes SNP genotypes for 500,000 individuals ascertained from the general population[244,298]. Here, I queried the results of phenome-wide association scans (PheWAS) carried on the dataset[244,299], in order to determine whether the mutation was associated with any of the traits that had been observed in the study participants. This hypothesis-free approach revealed that the phenotypes that are most strongly associated with 2031-2A>C (rs35897051) relate to white blood cell homeostasis. In fact, the variant causes a decrease in monocyte numbers and an increase in basophil and neutrophil counts (Table 4.5). Of note, the largest effect size (beta) was observed for the association with neutrophil percentage.

To validate this observation, I investigated the effects of other alleles that had previously been associated with myeloperoxidase deficiency[291,300–302]. I found that all the variants for which genotype data was available in UK Biobank (4 in total) were strongly associated with increased neutrophil percentage (Table 4.6). These findings are in keeping with the high neutrophil count observed in the two individuals with the 2031-2A>C mutation (Table 4.2).

Table 4.5 PheWAS analysis of 2031-2A>C

Trait	P value	Beta	Imputation score
Monocyte percentage	5.3×10^{-38}	-0.31	0.92
Monocyte count	3.9×10^{-21}	-0.02	0.92
Basophil count	4.6×10^{-11}	0.003	0.92
Basophil percentage	1.1×10^{-9}	0.03	0.92
Neutrophil percentage	5.1×10^{-6}	0.45	0.92
Neutrophil count	3.2×10^{-5}	0.07	0.92

Beta represents the effect size; Imputation scores measure the reliability of the inferred genotype

Table 4.6 Summary of the association between MPO deficiency alleles and neutrophil percentage

Variant[1]	MAF	P value	Beta
p.Ala332Val (rs28730837)	0.016	4.5×10^{-22}	0.57677
p.Met251Thr (rs56378716)	3.9×10^{-28}	0.013	0.74621
p.Tyr173Cys (rs78950939)	0.0012	0.008	0.57164
p.Arg569Trp (rs119468010)	0.0036	3.6×10^{-12}	0.5261

[1]All variants were directly genotyped, therefore no imputation score is reported. MAF, minor allele frequency; Beta represents the effect size

4.5 *MPO* variants are associated with the up-regulation of genes that modulate apoptosis

To understand how *MPO* alleles might affect granulocyte counts, gene expression levels measured in GYFAP0014 (the GPP patient carrying the 2031-2A>C variant) were compared to those of 11 healthy controls, using neutrophil RNA sequencing data generated for a related study (see chapter 5). This analysis identified 95 upregulated genes (fold change ≥ 1.5) at a False Discovery Rate (FDR) <0.05 (Figure 4.3, Appendix V). Of note, most of these transcripts (85/95) were not over-expressed in 7 unrelated GPP cases examined in parallel, which suggests that their increased expression is a specific consequence of MPO deficiency rather than a secondary effect of inflammation. Of note, while the number of differentially expressed genes did not allow me to perform a pathway enrichment analysis, two of the five most up-regulated loci (*PBK* and *GUCYA2*) encode proteins (PDZ binding kinase and soluble guanylate cyclase alpha-2 subunit) that can inhibit apoptosis[303,304]. Thus, RNA sequencing of patient cells suggests that MPO deficiency may disrupt the transcriptional networks that regulate neutrophil survival and apoptosis, two key mechanisms for the control of neutrophil numbers.

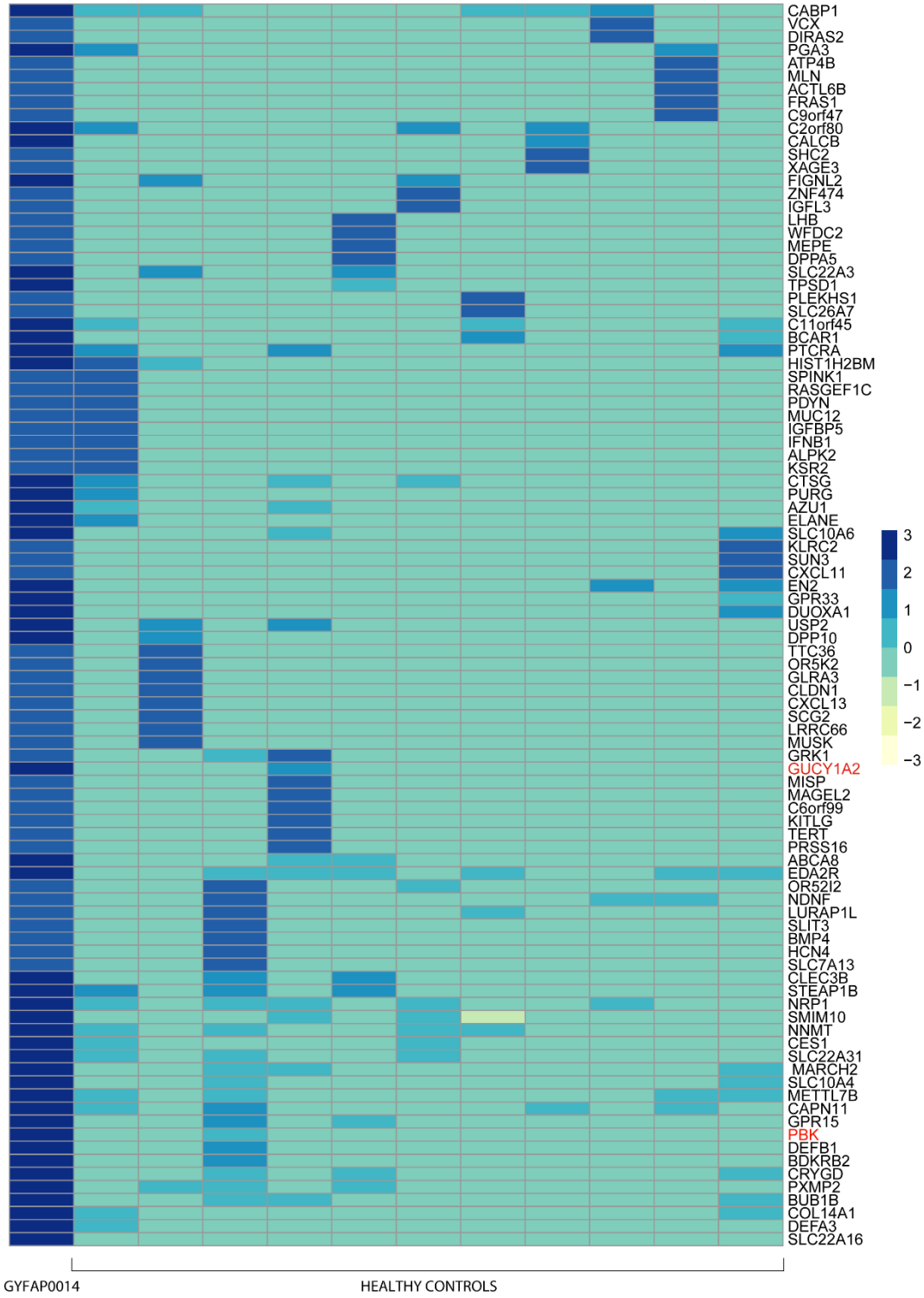

Figure 4.3 Differential gene expression in GYFAP0014 neutrophils

Heatmap showing the 80 genes with the most significant over-expression in GYFAP0014 compared to healthy controls. *PBK* and *GUCYA2* (two highly upregulated genes that can inhibit apoptosis) are highlighted in red.

4.6 Discussion

The aim of this study was to identify new genetic determinants of pustular psoriasis through the analysis of whole-exome sequencing data. This had been previously generated by the group for several affected individuals who lacked a molecular diagnosis.

While mono- and bi-allelic variants have both been reported[108,109,115], my filtering strategy focused on the latter, as the severity of the disease suggested the involvement of recessive loss-of-function alleles. On this occasion, compound heterozygous variants were not considered, owing to the difficulty of distinguishing *cis* and *trans* inheritance in the absence of parental genotypes. Should those become available in the future, the variant analysis could be usefully revisited.

The current filtering approach highlighted a pathogenic *MPO* splicing change as the most promising variant. The same substitution was later uncovered in an unrelated patient of European origin, who was affected by PPP and ACH. A literature review and PheWAS analysis further suggested that the 2031-2A>C mutation affects neutrophil survival.

While the genetic analysis did not uncover any shared genes between the 19 GPP cases, this was not completely unexpected due to the heterogeneity of the disease. In addition, the patient selection was only based on their GPP diagnosis and the absence of psoriasis family history. In the future, the application of tighter inclusion criteria (e.g. early age of onset or acute disease presentation) might lead to the ascertainment of a more homogeneous sample where shared genetic defects may be observed.

MPO encodes a 745 aa protein, which is synthesised during neutrophil myeloid differentiation and constitutes the major component of azurophilic granules. The protein was first isolated in 1941 from the purulent fluid of patients with tuberculous empyema[305]. It was initially named verdoperoxidase, due to its intense green colour. The term myeloperoxidase was adopted later, once it became apparent that the protein is only expressed in myeloid cells[225].

In 1970, Klebanoff demonstrated that MPO promotes oxygen-dependent killing during phagocytosis[306,307]. Several studies have since shown that MPO catalyses the production of hypohalous acid (HOCl) from hydrogen peroxide and Cl^-, thus creating a toxic environment within phagolysosomes (Figure 4.4)[148,308,309]. Of note, MPO-mediated damage is not restricted to phagosomes, as HOCl and its by-products can harm host tissues as well. Thus, excessive MPO activity has been implicated in the pathogenesis of several inflammatory disorders, including Alzheimer Disease, multiple sclerosis, atherosclerosis and certain tumors[310]. Conversely, reduced MPO function can affect responses to pathogens[311], with consequences ranging from very mild immune deficiency to the recurrence of life-threatening infections[312].

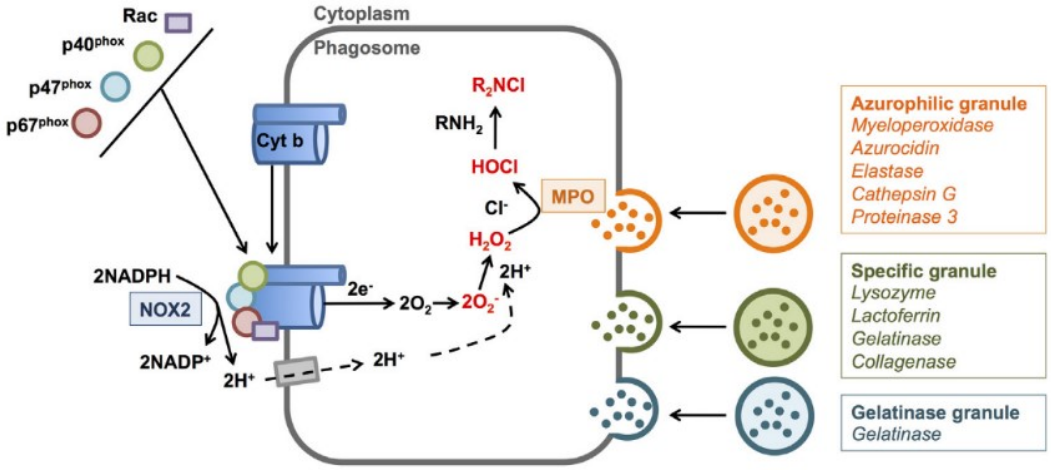

Figure 4.4 Reactive oxygen species production within the neutrophil phagosome

Neutrophil priming triggers the mobilisation of cytoplasmic phagocyte oxidase (phox) proteins, Ras-related C3 botulinum toxin substrate (Rac) and membrane-expressed cytochrome b558 (Cyt b), leading to the assembly of the NADPH oxidase (NOX2) at the phagosomal membrane. NADPH-dependent oxygen reduction by NOX2 produces O_2. This in turn dismutates into H_2O_2. PMN priming also stimulates the fusion of neutrophil granules with the phagosome. This leads to the release of myeloperoxidase (MPO), which produces secondary HOCl from reactions with H_2O_2. From Glennon-Alty et al. 2018[313].

The 2031-2A>C homozygous change was first identified in 2004 and was shown to cause activation of a cryptic 3' splice site situated 109bp upstream of the authentic 3' splice site of intron 11. This insertion results in a frameshift, leading to a premature stop codon and synthesis of an abnormal MPO precursor lacking enzymatic activity[291].

In this chapter I provide evidence for an association between MPO deficiency and neutrophil count variation. Firstly, elevated neutrophil numbers were observed in the two cases carrying the 2031-2A>C change. Secondly, the PheWAS showed a consistent association between MPO deficiency alleles and increased neutrophil percentage in white blood cells. Of note, the PheWAS results were further confirmed when mining the GWAS catalogue, a curated collection of all published genome-wide association studies[240]. This showed that common non-coding *MPO* SNPs were also associated with neutrophil count variation[271].

Finally, the transcriptomic analysis suggested a link between MPO deficiency and apoptosis, which is consistent with the effect on PMN counts. Unfortunately, constraints on the amount of blood that could be obtained from affected individuals prevented me from directly investigating the regulation of cell death in MPO deficient neutrophils. At the same time, the function of the genes that are upregulated in patient cells strongly suggests that a disruption of apoptosis would have been observed in such experiments.

In conclusion, the evidence provided in this chapter shows that deleterious *MPO* variants are linked to pustular skin phenotypes and that they could predispose to the disease by increasing neutrophil numbers through an effect on apoptosis.

5 IDENTIFICATION OF A TYPE-I-IFN TRANSCRIPTIONAL SIGNATURE IN THE NEUTROPHILS OF GPP AND PsV PATIENTS

5.1 RNA-sequencing of a pure neutrophil population

The aim of this part of the study was to investigate the transcriptional networks that drive neutrophil activation in GPP. To achieve this purpose, RNA-sequencing was carried out in neutrophils obtained from affected individuals and healthy donors.

Eight unrelated GPP cases were identified among the patients attending the psoriasis clinic at St. John's Institute of Dermatology, while 11 age and sex-matched healthy controls were recruited among the Institute personnel. Untouched neutrophils were isolated from whole-blood and cell purity was measured by flow cytometry in 8 representative samples. Overall, neutrophils accounted for 97% of the isolated cells, while the contamination from monocytes, lymphocytes and eosinophils was negligible (Figure 5.1).

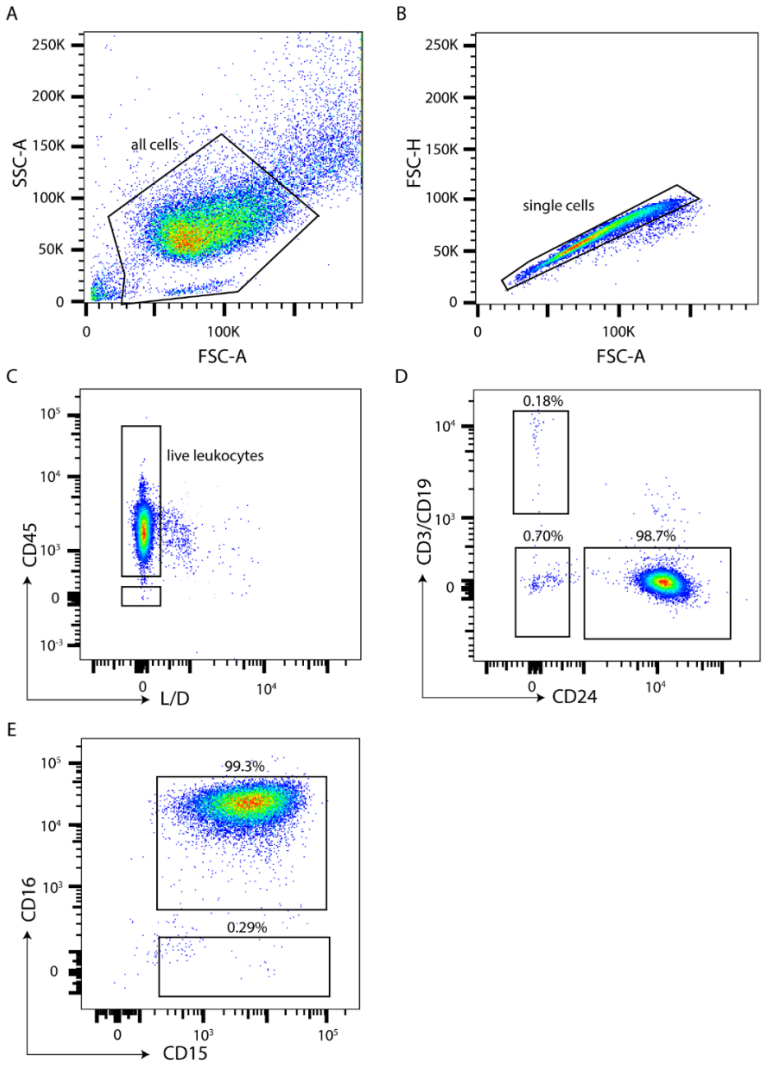

Figure 5.1 Purity of the neutrophil population used for RNA-sequencing

Representative flow cytometry plots showing that neutrophils represent >97% of live cells, whereas contaminating eosinophils, lymphocytes and monocytes account for around 1% of the sample. (A) Cells are selected based on their size and granularity, while debris and dead cells (bottom left) and doublets (top right) are excluded. (B) Single cells are selected and more doublets excluded. (C) Live leukocytes (gated as $CD45^+$ and live/dead marker $(L/D)^-$) are selected. (D) Lymphocytes (gated as $CD3/19^+$) and monocytes (gated as $CD24^-$ and $CD3/19^-$) contamination is quantified. Granulocytes (gated as $CD24^+$) are selected. (E) Neutrophils (gated as $CD16^+$ $CD15^+$ cells) and eosinophils (gated as $CD16^-$ $CD15^+$ cells) are quantified.

Next, neutrophil RNA was extracted, and its quality was assessed on a TapeStation 2200. As this uncovered an extensive DNA contamination (Figure 5.2), the samples were subject to DNase treatment (Figure 5.3). New TapeStation measurements showed that the DNase treatment had been successful and had not affected the integrity of the RNA (average RNA Integrity Number equivalent (RIN^{e}): 8.2). The samples were therefore sent to the NGS Facility at St. James's University Hospital in Leeds for library preparation and RNA sequencing.

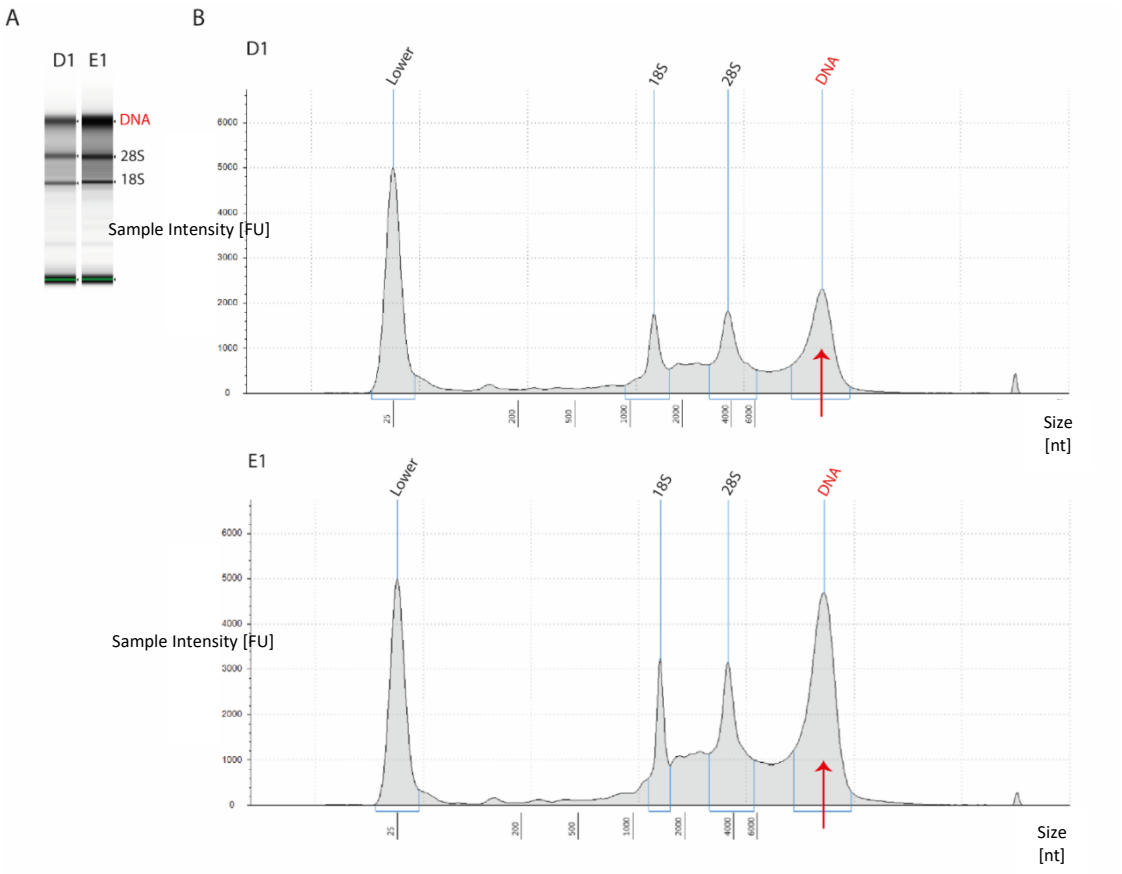

Figure 5.2 Quality of neutrophil RNA prior to DNase treatment

Two representative TapeStation measurements (samples D1 and E1). Both gel electrophoresis (A) and electropherograms (B) show that the RNAs were heavily contaminated by DNA.

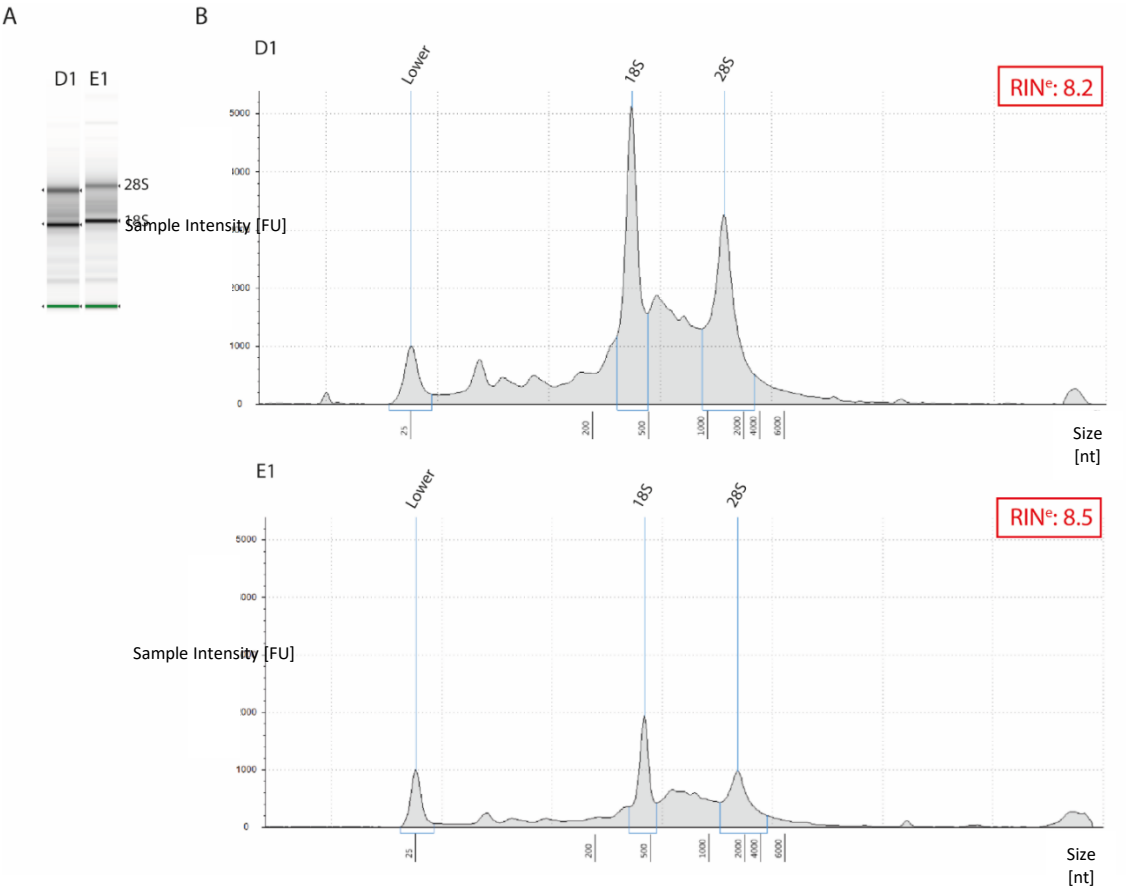

Figure 5.3 Quality of neutrophil RNA after DNase treatment

Two representative TapeStation measurements (samples D1 and E1). Both gel electrophoresis (A) and electropherograms (B) show that the DNA has been degraded by the DNase treatment, while the RNA integrity was not affected, as shown by the presence of the 18S and 28S ribosomal RNA subunits. RNA integrity number equivalent (RIN^E) is given for the two samples.

The analysis of the RNA-sequencing detected an average of 40 million reads per sample. After these were aligned to the reference genome and counted, a further purity check was carried out by comparing gene expression levels to those observed in the healthy neutrophils sequenced by the Blueprint Consortium (a large European collaboration that aims to better understand immune gene activation in health and disease)[237]. This analysis showed that all the genes that are transcribed in the Blueprint neutrophils (n=3,133) are also found in our samples, with very low expression levels observed for a further 252 genes originating from monocytes, eosinophils and lymphocytes (<0.3 transcript per million (TPM) on average) (Figure 5.4). These results further validated the high purity of our neutrophil samples.

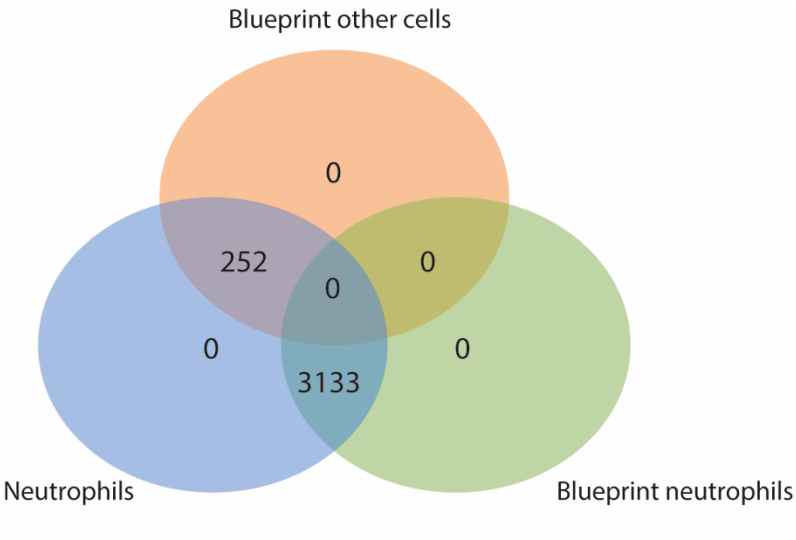

Figure 5.4 *In-silico* purity of the neutrophil population used for RNA-sequencing

Venn diagram showing that all neutrophil genes detected by the Blueprint consortium (green circle) were present in our neutrophil population (blue). Only 252 genes found in our dataset originated from other cell types (orange), but those were expressed at very low levels (average TPM <0.3).

5.2 Type-I-IFN related pathways are enriched among the genes that are up-regulated in GPP neutrophils

To identify any outliers or subgroups of samples which might be present in the dataset, Principal Component Analysis (PCA) was performed on the normalised read counts. The PCA revealed that the healthy controls tend to cluster together, apart from the males, while the patients are a more heterogeneous group (Figure 5.5).

Next, gene expression levels were compared in the 8 GPP cases versus the 11 healthy controls. This analysis identified 231 differentially expressed genes (DEGs, Appendix VI), of which 200 were up-regulated (fold change≥1.5) and 31 were down-regulated (fold change≤0.70) at a False Discovery Rate (FDR) <0.05 (Figure 5.6).

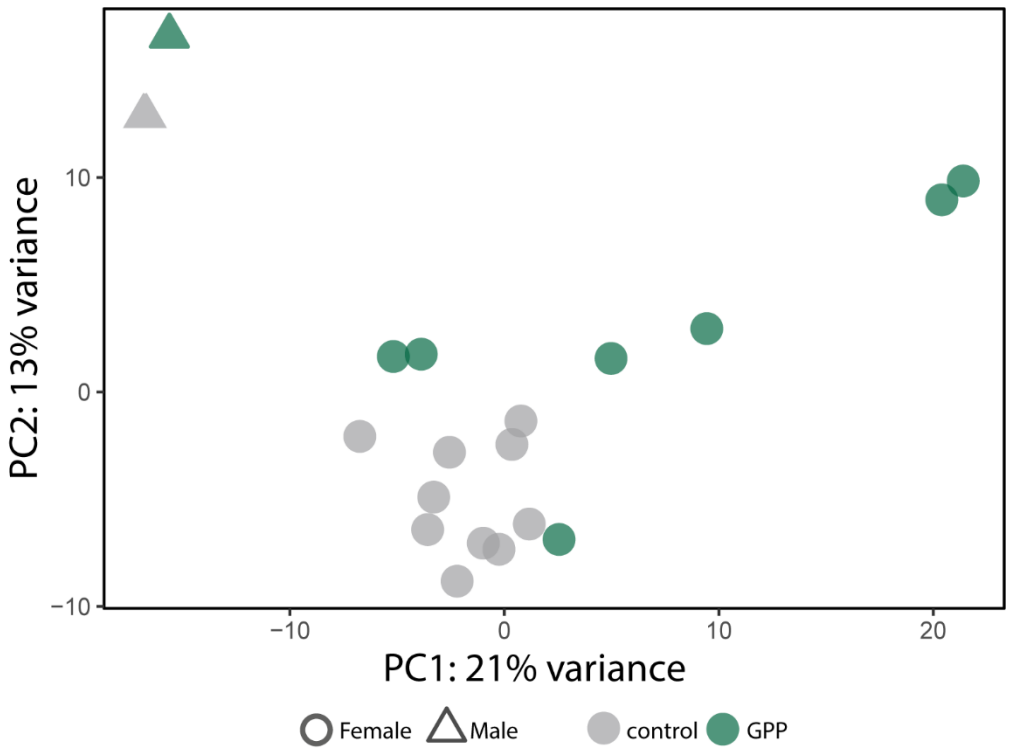

Figure 5.5 Principal Component Analysis (PCA) of neutrophil RNA-sequencing data

The plot shows the distribution of neutrophil samples along the first two principal components. While the female controls seem to cluster together, the cases are more spread out and diverse. Neutrophils from the 2 males in the dataset (one affected and one unaffected) cluster separately.

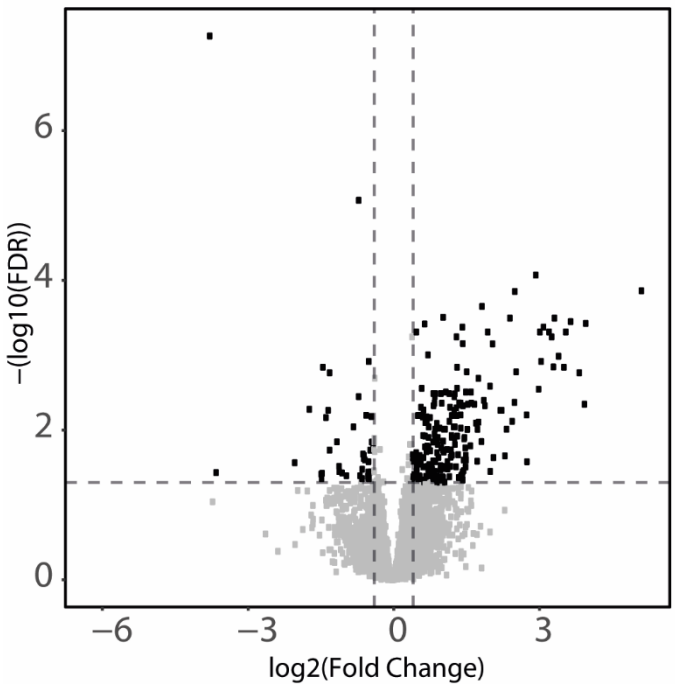

Figure 5.6 Differential gene expression in GPP neutrophils vs. healthy controls

Volcano plot showing the genes that are differentially expressed in GPP patients (black dots). The horizontal and vertical dashed lines represent the threshold for significance (FDR <0.05) and fold change (FC>1.5; FC<0.7), respectively.

The up-regulated genes (Appendix VI) were then mapped to the co-expression modules defined by Li et al.[266], which describe well characterised features of immune function. This revealed a significant over-representation of modules related to innate immune activation. Among these, *type-I interferon response* was the most significantly enriched module (10 out of 12 genes found among the DEGs; FDR<10^{-12}), followed by *innate antiviral response* (9 out of 12 genes among the DEGs; FDR<10^{-10}) and *antiviral interferon signature* (11 out of 22 genes among the DEGs; FDR<10^{-10}) (Figure 5.7).

These results were further confirmed by Ingenuity Pathway Analysis (IPA), which identified 4 enriched pathways associated with IFN responses. These included *IFN signalling* (FDR<10^{-12}), *Activation of IRF by Cytosolic Pattern Recognition Receptors* (FDR<10^{-6}) and *Role of JAK1, JAK2 and TYK2 in Interferon Signalling* (FDR<10^{-2}) (Figure 5.8). Furthermore, an IPA upstream regulator analysis highlighted IRF7 and STAT1 (two known mediators of IFN signal transduction), as the most likely drivers of gene up-regulation (FDR<10^{-30} for both) (Figure 5.9).

Taken together, the results of these analyses demonstrate that type-I-IFN responses are abnormally active in GPP neutrophils.

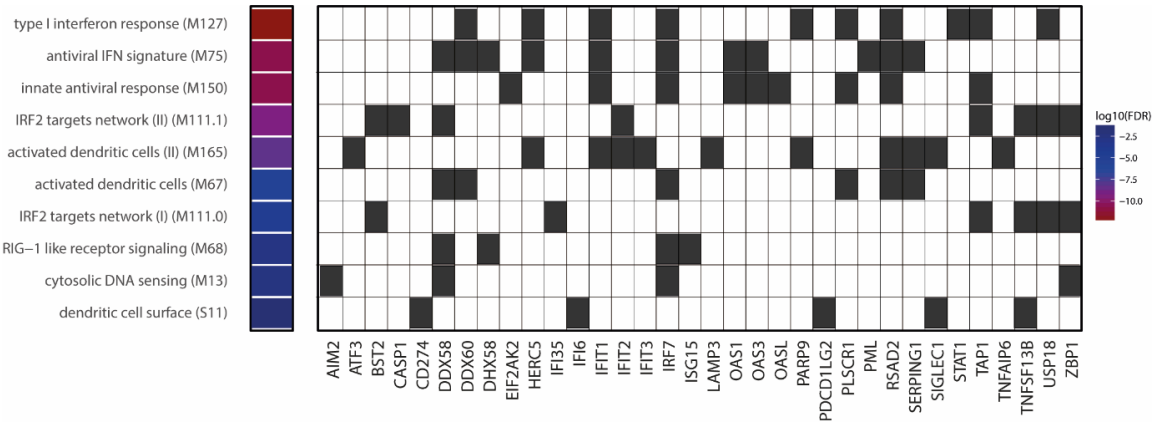

Figure 5.7 Genes up-regulated in GPP neutrophils map to type-I-IFN related expression modules

Diagram showing the most significantly enriched transcriptional modules among the genes that are up-regulated in GPP. The heat map on the left reports the log10(FDR) associated with each module, while the genes belonging to each different module are shown on the grid as grey cells. The analysis has been carried out using the co-expression modules defined by Li et al. [266].

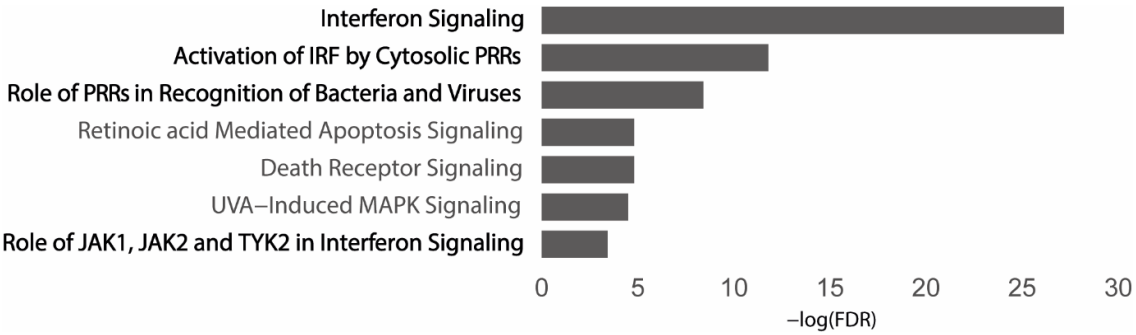

Figure 5.8 Results of Ingenuity pathway enrichment analysis

Bar plot illustrating the most significantly enriched pathways detected among the genes that are up-regulated in GPP. IFN-related pathways are highlighted in bold font.

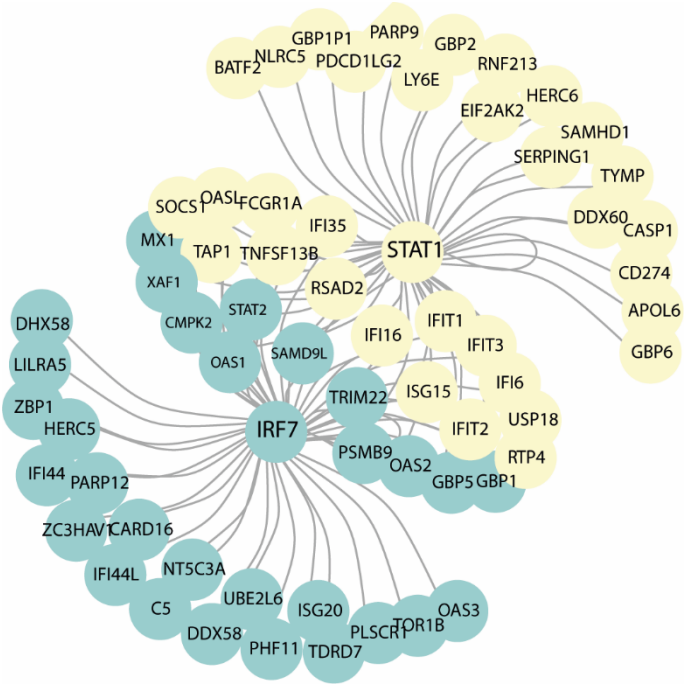

Figure 5.9 Key results of Ingenuity upstream regulator enrichment analysis

Upstream regulatory network showing that IRF7 and STAT1 drive the up-regulation of numerous genes that are over-expressed in GPP neutrophils.

5.3 The up-regulation of type-I-IFN signature genes can be detected in extended GPP and PsV datasets

To further explore the relevance of these findings, a type-I-IFN score[267] was defined by calculating the median expression of five IFN-stimulated genes (ISGs; *IFI6, IFIT3, IFITM3, OASL* and *PLSCR1*) selected as discussed in section 2.7.3.6. As expected, the score was higher in GPP cases compared to controls (P=0.01) (Figure 5.10). The expression of the same genes was then measured in an expanded dataset, which was characterized by means of real-time PCR.

Freshly isolated neutrophils were obtained from 17 GPP cases, including 7 subjects from the RNA-sequencing cohort and 10 newly ascertained patients. To determine whether the up-regulation of type-I-IFN genes was also relevant to the pathogenesis of common psoriasis vulgaris, 16 individuals with moderate-to-severe PsV (Psoriasis Area Severity Index >10) were also recruited. Finally, 3 control groups were included in the analysis: 9 patients affected by Cryopirin Associated Periodic Syndrome (CAPS, an IL-1-driven neutrophilic disease), 13 cases with Acral Pustular Psoriasis (APP, a localised form of the disease that solely affects hands and feet) and 26 healthy volunteers (10 of whom had been included in the RNA-sequencing cohort).

Real-time PCR of the 5 ISGs showed that the IFN score was significantly higher in the GPP and PsV cohorts compared to unaffected individuals (P=0.0046 and P=0.0021, respectively). Conversely, the scores of CAPS and APP patients were similar to those of the healthy controls (Figure 5.11). Thus, the type-I-IFN signature can be reproducibly and specifically detected in patients suffering from severe forms of psoriasis.

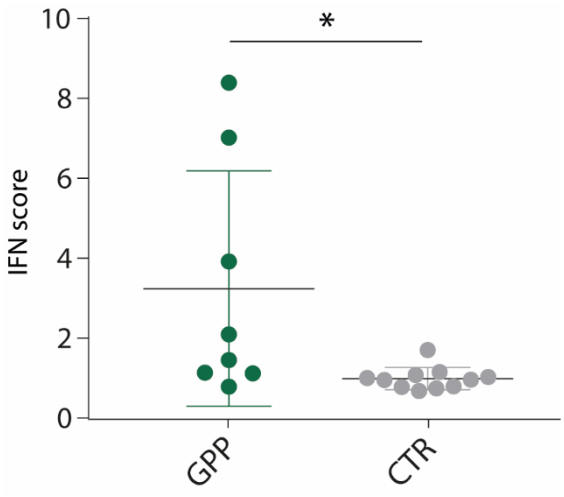

Figure 5.10 Analysis of RNA-seq data shows elevated IFN scores in GPP patients

Dot plots showing an elevated IFN score in the neutrophils of GPP patients, compared to healthy controls. The data are presented as mean +/- standard deviation; *P<0.05 (unpaired t-test).

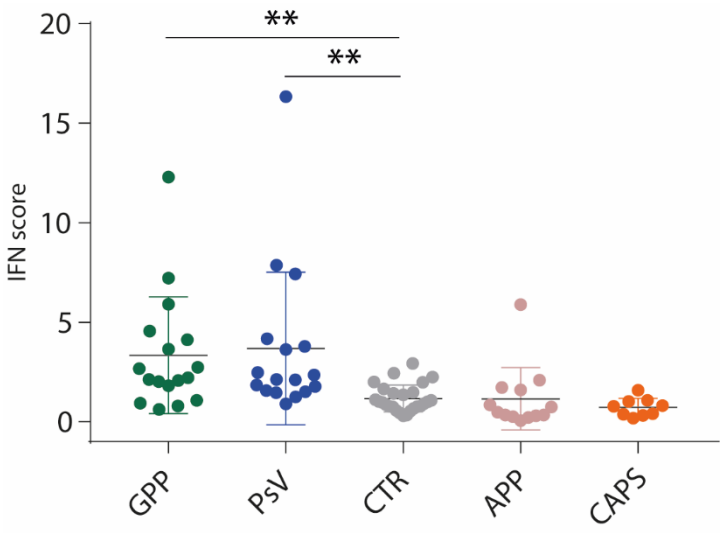

Figure 5.11 Real-time PCR of the 5 ISGs shows that elevated IFN scores can be detected extended GPP and PsV datasets

Dot plot showing an elevated IFN score in the neutrophils of GPP and PsV patients, compared to healthy individuals (CTR). CAPS and APP cases were analysed as negative controls. The data are presented as mean +/- standard deviation; **P<0.01 (one-way ANOVA followed by Dunn's post-test).

5.4 Neutrophils do not respond to IL-36 stimulation nor express the IL-36 Receptor

Given the well-established role of IL-36 signalling in psoriasis[123,127,314], we hypothesised that the up-regulation of type-I-IFN responses observed in patient neutrophils may be the consequence of abnormal IL-36 activity.

To explore this possibility and determine whether neutrophils can respond to direct IL-36 stimulation, freshly isolated cells obtained from three healthy donors were stimulated for 2 hours with the cytokine. Of note, as Mahil et al. showed a substantial overlap between the genes upregulated by IL-36α, β and γ[127], IL-36α was used in all subsequent experiments as a representative cytokine. The response to treatment was then determined by measuring the mRNA expression of *IL8,* a known IL-36 target gene[108,109].

While *IL8* levels increased after a control IL-1β stimulation, IL-36 did not elicit any response. Moreover, since IL-36R expression can be enhanced by the synergistic effects of IL-6 and IL-1β[315], attempts were also made to stimulate neutrophils in such conditions. However, no difference in *IL8* induction could be detected between cells treated with IL-6, IL-1β and IL-36 vs. those treated with IL-6 and IL-1β alone (Figure 5.12).

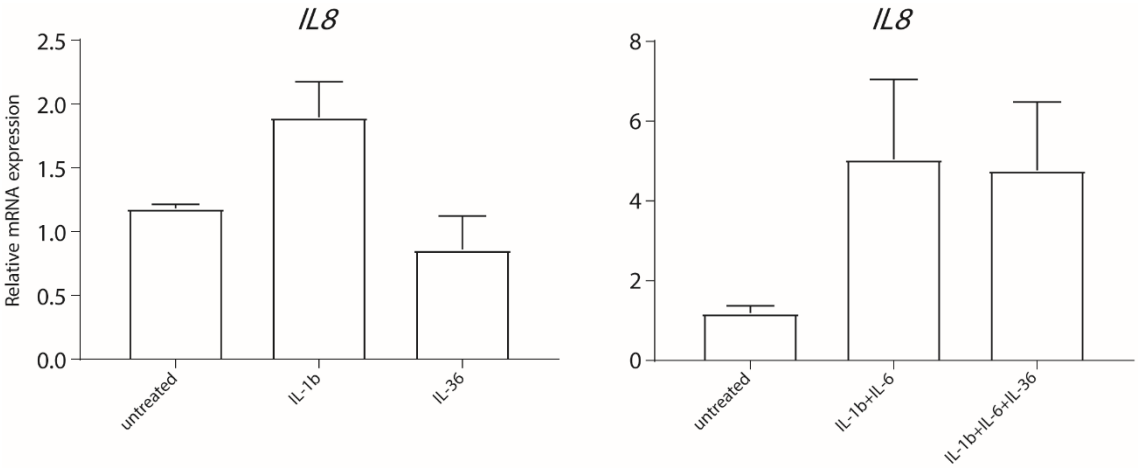

Figure 5.12 Healthy donor neutrophils don't respond to direct IL-36 stimulation

Following treatment of neutrophils with IL-36, IL-1β or vehicle (untreated), *IL8* mRNA expression was measured by real-time PCR and normalised to *RPL13A* levels. Data represents the mean +/- SD of results obtained in three independent donors, each stimulated in duplicate (left). Following treatment of neutrophils with IL-1β and IL-6 in the presence or absence of IL-36, *IL8* mRNA expression was measured by real-time PCR and normalised to *RPL13A* levels. Data represents the mean +/- SD of results obtained in two independent donors, each stimulated in duplicate (right).

To further validate these observations and confirm that neutrophils do not respond to IL-36 stimulation, the surface expression of the IL-36 Receptor (IL-36R) was investigated. Neutrophils obtained from healthy individuals (n=3) and GPP patients (n=3) were analysed by flow cytometry. In keeping with the stimulation results and published findings[316], IL-36R surface expression was scarcely detectable in the neutrophils of GPP cases or healthy controls (Figure 5.13). Neutrophils, therefore, cannot respond to IL-36 cytokines, indicating that the type-I-IFN signature seen in these cells is likely to reflect an IL-36-mediated activation of other cell populations.

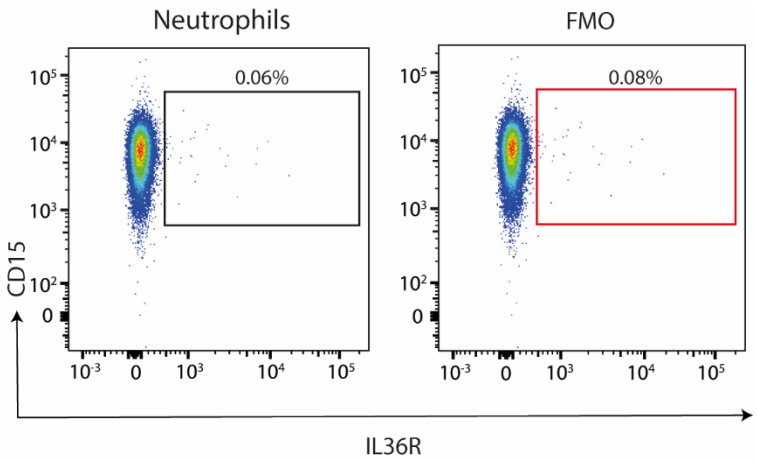

Figure 5.13 Neutrophils do not express IL-36R

Representative flow cytometry analysis of IL36R surface expression (left) and fluorescence minus one (FMO) control (right) in neutrophils (gated as $CD14^-$, $CD15^+$, $CD16^+$ cells).

5.5 IL-36R is robustly expressed in plasmacytoid dendritic cells

To determine which cell types respond to IL-36, the surface expression of the IL-36 Receptor (IL-36R) was systematically measured in innate immune cells. These experiments were carried out in collaboration with my colleague Marika Catapano.

Peripheral blood mononuclear cells (PBMCs) obtained from healthy individuals (n=3) and GPP patients (n=3) were analysed by flow cytometry. Myeloid and plasmacytoid dendritic cells (mDCs and pDCs) showed robust IL-36R surface expression, with the highest receptor levels observed in the pDCs of GPP patients (Figure 5.14). Importantly, pDCs are the main producers of type-I-IFN (especially IFN-α) in the immune system[195,317,318]. Thus, the flow cytometry results suggest that IL-36 may influence IFN-α production by pDCs, which in turn would drive the activation of type-I-IFN genes in neutrophils.

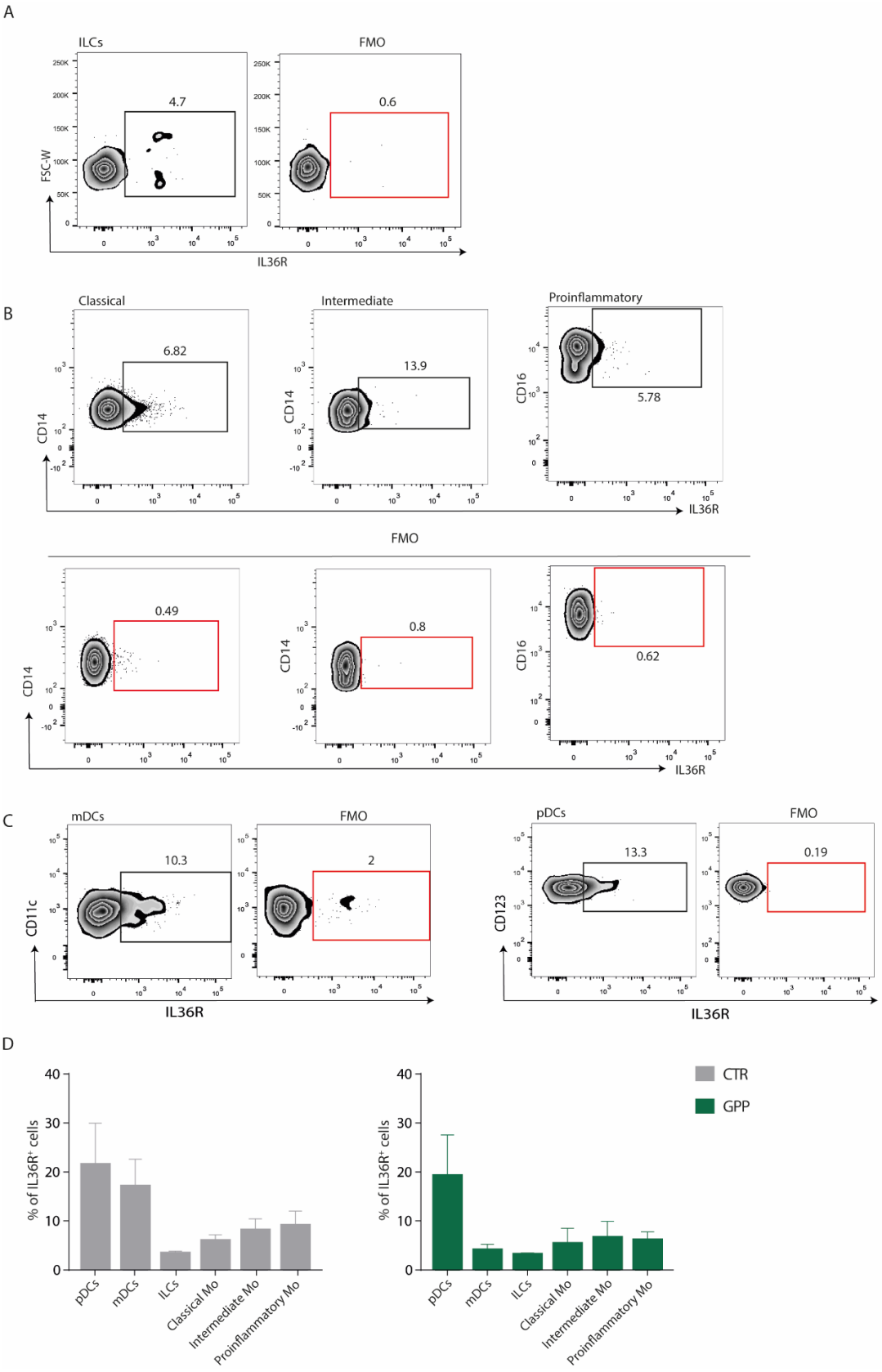
A
ILCs
FMO
4.7
0.6
FSC-W
IL36R
B
Classical
Intermediate
Proinflammatory
6.82
13.9
5.78
CD14
CD16
IL36R
FMO
0.49
0.8
0.62
C
mDCs
FMO
pDCs
FMO
10.3
2
13.3
0.19
CD11c
CD123
IL36R
D
% of IL36R+ cells
CTR
GPP
pDCs
mDCs
ILCs
Classical Mo
Intermediate Mo
Proinflammatory Mo

Figure 5.14 The IL-36 receptor is robustly expressed in dendritic cells

(A-C) Representative flow cytometry plots of IL36R+ cells in six leukocyte populations. Fluorescence minus one (FMO) controls are shown for each population. The following cell types were analysed: (A) innate lymphoid cells (lineage^{-} (CD3^{-}, CD4^{-}, CD19^{-}, CD20^{-}, CD56^{-}), CD127^{+}); (B) monocytes (CD3^{-}, CD20^{-}, CD19^{-}, CD56^{-}) separated into classical (CD16^{-}, CD14^{high}), intermediate (CD16^{+}, CD14^{+}) and pro-inflammatory (CD16^{high}, CD14^{-}) populations; (C) pDCs (lineage^{-}, HLADR^{+}, CD123^{+}, CD11c^{-}) and mDCs (lineage^{-}, HLADR^{+}, CD123^{-}, CD11c^{+}). (D) Histograms illustrating the percentage of IL36R+ cells in six leukocyte populations. Data are shown as mean +/- SEM. No significant differences were observed between GPP cases and healthy donors. CTR: healthy controls; ILCs: Innate Lymphoid Cells; Mo: Monocytes.

5.6 IL-36 potentiates IFN-α production by up-regulating the expression of PLSCR1

Building on the flow cytometry results, the hypothesis that IL-36 potentiates type-I-IFN production in pDCs was investigated. The following experiments were carried out in collaboration with Marika Catapano.

PBMCs obtained from healthy donors (n=3) were pre-treated with IL-36α or vehicle and stimulated with CpG-containing DNA (CpG), a Toll-like receptor (TLR)-9 ligand which drives IFN-α production by pDCs[319]. Type-I-IFN activation was then assessed by measuring the expression of the five ISGs by real-time PCR. The experiment demonstrated that IL-36 potentiates the response to CpG, as the expression of the IFN signature genes was higher in cells treated with IL-36α and CpG, compared to those treated with CpG only (Figure 5.15).

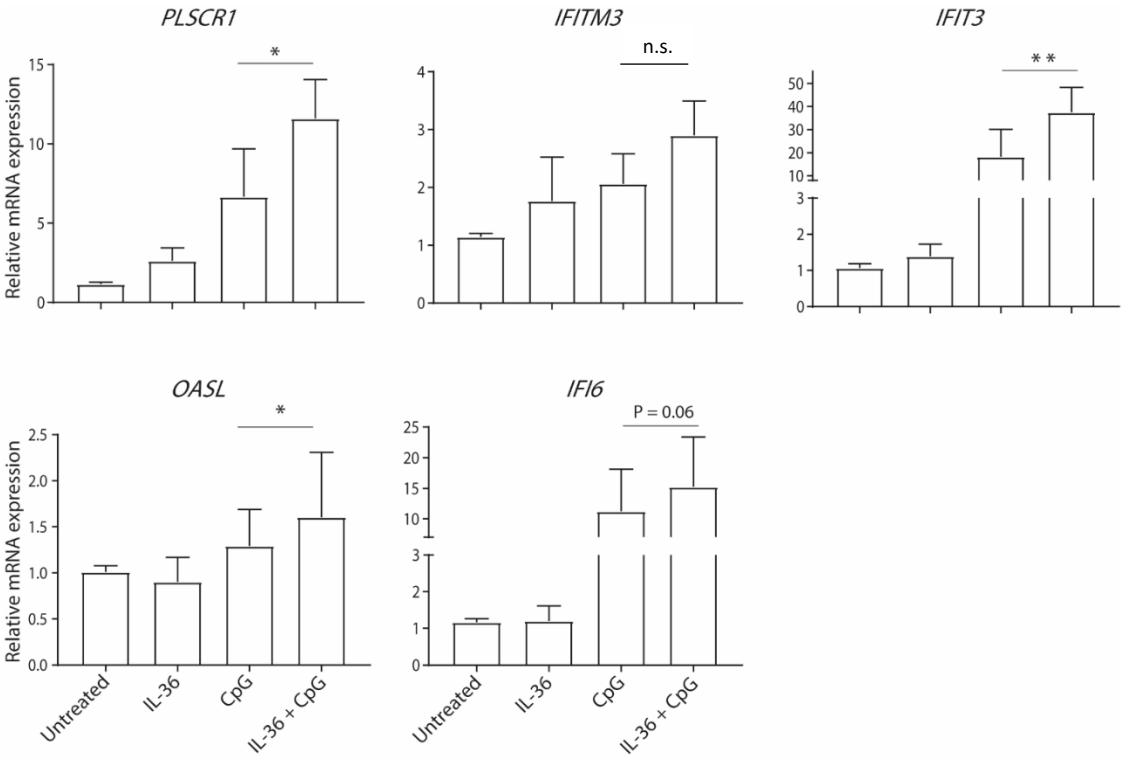

Figure 5.15 IL-36 up-regulates expression of ISGs downstream of TLR-9

After pre-treatment with IL-36α or vehicle (6h), PBMCs from healthy donors were stimulated with CpG for 6h. ISGs expression was then measured by real-time PCR and normalised to *B2M* levels. Data is shown as the mean +/- SEM of results obtained in three independent donors, each stimulated in triplicate. *P<0.05; **P<0.01 (Friedman's test, with Dunn's post-test); n.s., not significant.

To further explore the relevance of these findings, the mechanisms whereby IL-36 potentiates TLR9- dependent IFN responses were investigated. Of note, the results of PBMC stimulations showed that IL-36α can up-regulate *PLSCR1* expression even in the absence of CpG (Figure 5.15). This is of interest, given that *PLSCR1* encodes a phospholipid scramblase mediating TLR-9 translocation to the endosomal compartment[320]. The effect of IL-36 on *PLSCR1* was therefore investigated in more detail.

Fresh PBMCs were obtained from 5 additional healthy donors and treated with IL-36α. The results validated the previous experiments and confirmed that IL-36 up-regulates PLSCR1 expression (P=0.03) (Figure 5.16). Moreover, flow cytometry analysis of IL-36 treated pDCs demonstrated a significant increase in PLSCR1 protein levels (Figure 5.17), proving a direct effect of the cytokine on these cells.

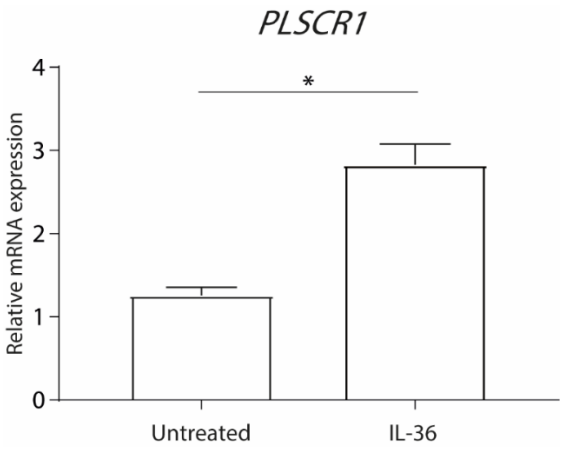

Figure 5.16 IL-36 upregulates *PLSCR1* expression in PBMCs

After treating PBMCs from additional healthy donors with IL-36α or vehicle, *PLSCR1* expression was measured by real-time PCR and normalised to *B2M* levels. Data is shown as the mean +/- SEM of results obtained in five independent donors, each stimulated in triplicate. *P<0.05 (Wilcoxon signed-rank test).

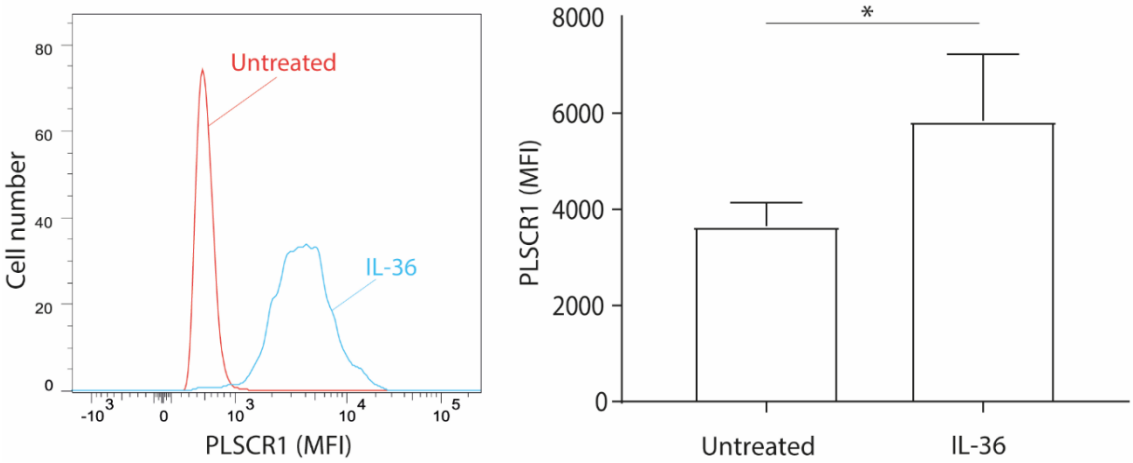

Figure 5.17 IL-36 upregulates PLSCR1 protein expression in pDCs

After treating pDCs with IL-36αα or vehicle, PLSCR1 mean fluorescence intensity (MFI) was measured by flow-cytometry. The panel on the left shows a representative histogram, while the plot on the right illustrates the results (mean +/- SEM) obtained in 3 independent healthy donors. *P<0.05 (Wilcoxon signed-rank test).

Finally, the mechanism whereby IL-36 up-regulates *PLSCR1* was explored. Given that *PLSCR1* is an IFN-stimulated gene, an involvement of STAT1 was hypothesised. This was supported by the identification of a STAT1 binding site within the gene promoter. Since IL-36 can signal through mitogen-activated protein kinase (MAPK), and a cross-talk between STAT1 and MAPK has been previously demonstrated[314,321], the latter pathway was selected for further investigation. PBMCs were pre-incubated with a MAPK inhibitor (SB-203580) and then stimulated with IL-36α. Real-time PCR demonstrated that the effect of IL-36α on *PLSCR1* expression was abolished in cells that had been pre-treated with SB-203580, indicating that the up-regulation of PLSCR1 is MAPK-dependent (Figure 5.18).

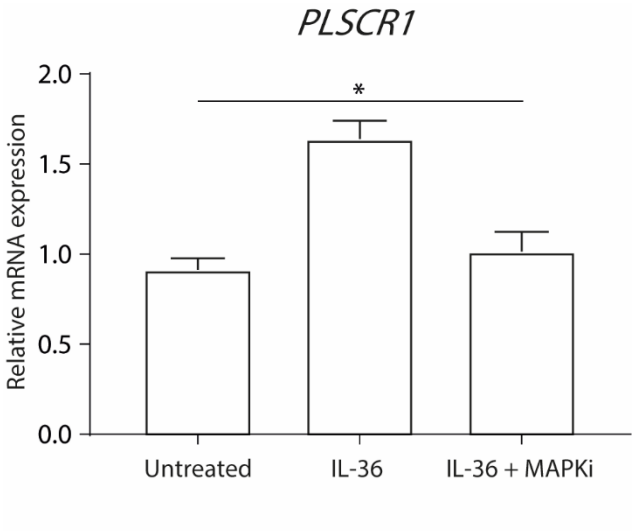

Figure 5.18 MAPK inhibition abolishes the effects of IL-36 on *PLSCR1* expression

After pre-treating PBMCs with SB203580 (MAPKi) or vehicle, the cells where stimulated with IL-36α. *PLSCR1* expression was then measured by real-time PCR and normalised to *B2M* levels. Data are shown as the mean +/- SEM of results obtained in four independent donors, each stimulated in triplicate. *P<0.05 (Friedman's test with Dunn's post-test).

5.7 Discussion

While the GPP transcriptome has been investigated at the skin level[123,127,322], circulating neutrophils have received little attention, despite their pathogenic role in systemic inflammation. The final part of my study aimed to fill this research gap and elucidate the transcriptional networks that cause neutrophil activation in GPP.

Difficulties in isolating neutrophils from fresh blood were initially encountered. A literature review of purification protocols was then undertaken and identified two main methodologies: density gradient and magnetic separation[323–325]. After testing both approaches, the latter was chosen for its reproducibility and yield of highly pure cells. Of note, Calzetti et al. recently showed that neutrophil isolated with our method of choice contain very low numbers of slan^{+}CD16^{+} cells that may, under some conditions express IFN regulated genes[323]. Unfortunately, by the time this finding was published it was not possible for me to adapt my isolation technique. However, the possibility of a slan^{+}CD16^{+} contamination should be kept in mind and considered as a possible limitation to my study.

The protocol for RNA isolation also required some optimization. In fact, the contamination of RNA samples with genomic DNA caused a 2-month delay in the project. However, once the appropriate DNase treatment was applied, the DNA could be removed without compromising RNA integrity. RNA sequencing then produced high quality results, as confirmed by the read QC (average mapped reads: 96%) and the comparison with the data generated by the Blueprint Consortium[237].

The differential-expression analysis and follow-up studies revealed a distinctive type-I-IFN signature in the neutrophils of patients affected by GPP and severe PsV. This did not correlate with patient ethnicity or disease treatment. Of note, an increase in type-I-IFN activity has been previously associated with several inflammatory conditions such as systemic lupus erythematosus (SLE), Aicardi-Goutieres syndrome (AGS) and Chronic atypical neutrophilic dermatosis with lipodystrophy and elevated temperature (CANDLE)[326,327]. These diseases, which are now classified as Type-I-Interferonopathies,

present with severe skin lesions and prominent systemic upset, caused by abnormal IFN levels. Of note, neutrophils play a key role in the development of Type-I-Interferonopathies, particularly at the skin level, where extensive neutrophil infiltration is observed[328]. Therefore, the phenotypic similarities between GPP, PsV and IFN-driven diseases further substantiate our results.

Given that IL-36 is a key disease driver in GPP and has also been implicated in the pathogenesis of PsV[123,127,314,329–333], we hypothesised that the up-regulation of type-I IFN genes was a consequence of abnormal IL-36 activity. However, flow-cytometry experiments and *ex-vivo* stimulations demonstrated that blood neutrophils do not respond to the cytokine due to a lack of IL-36R surface expression. While these findings confirmed previous results by Foster et al.[316], the recently published discovery of a synergistic effect of IL-6 and IL-1β on IL-36 responses could not be replicated[315]. A possible explanation for this discrepancy could be that our experiments were based on shorter neutrophil stimulations. Indeed, the extended incubations described in Wang et al. (>24h in total) were, in our hands, detrimental to neutrophil viability.

Further flow cytometry experiments demonstrated for the first time that IL-36R is strongly expressed in pDCs, the main producers of IFN-α in the immune system[195,317,318]. This suggests that circulating IL-36 could affect IFN-α production by pDCs, which in turn would promote the activation of type-I-IFN genes in patient neutrophils. In keeping with this hypothesis, real-time PCR and flow-cytometry experiments demonstrated that IL-36 acts directly on pDCs, where it up-regulates the expression of PLSCR1. This gene encodes phospholipid scramblase 1, a protein that interacts with TLR-9 and mediates its trafficking to the endosomal compartment [320,334,335]. Importantly, siRNA knockdown of *PLSCR1* inhibits type-I-IFN production in human pDCs. It is therefore reasonable to hypothesise that PLSCR1 up-regulation would have an opposite effect. This would set in motion a feed-forward loop, where PLSCR1 enhances IFN-α production, which subsequently induces further *PLSCR1* transcription (Figure 5.19). Interestingly, PLSCR1 is also up-regulated in SLE, which suggests that this

protein might have a pathogenic role in other type-I IFN mediated diseases, beyond psoriasis[336].

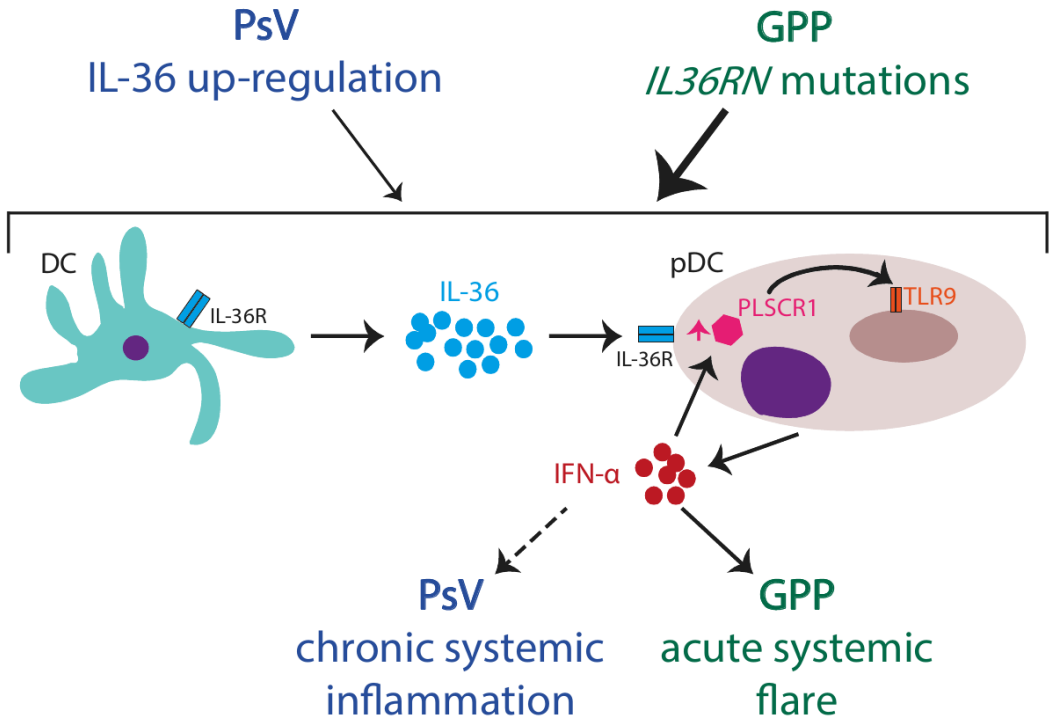

Figure 5.19 Proposed pathogenic model

IL-36 produced by mDCs up-regulates PLSCR1 in pDCs, enhancing IFN-α release via TLR-9. In turn, IFN-α induces further *PLSCR1* transcription, thus promoting a positive inflammatory feedback loop.

It is important to notice that the 8 GPP cases selected for RNA-sequencing had been previously genotyped. While three patients carried variants in *IL36RN*, this did not correlate with the uncovered type-I IFN signature and therefore broadens the scope of our finding, suggesting the presence of an underlying disease mechanism regardless of the patient mutation status. Moreover, while our PCA results showed that the two males cluster separately from the rest of the samples, a trend that has so far never been reported, this has been kept into consideration when computing the differential expression analysis, as sex was used as a covariate.

It is possible that IL-36 could influence type-I-IFN production through the up-regulation of other genes. Of note, real-time PCR experiments showed that IL-36 does not directly affect the expression of *TLR9* nor does it up-regulate IFN signalling mediators such as *IRF1*, *IRF3* or *IRF7* (data not shown). However, the effect of IL-36 on other innate regulators cannot be excluded and will have to be investigated in a more systematic fashion. In fact, the RNA-sequencing of IL-36 stimulated PBMCs is currently underway in the Capon lab and is expected to elucidate the effects of the cytokine on other type-I IFN related genes.

In conclusion, the computational analyses presented in this chapter identified a prominent type-I-IFN signature in the neutrophils of patients affected by GPP and severe PsV. Follow-up studies showed that the activation of type-I-IFN responses was driven by increased IL-36/IFN-α signalling in pDCs.

Since GPP and PsV both present with severe extra-cutaneous manifestations, it could be hypothesised that IL-36-driven type-I-IFN activity contributes to systemic disease symptoms. In PsV, for example, chronic IL-36 and type-I IFN up-regulation may be involved in the onset of atherosclerosis and psoriatic arthritis, two disease co-morbidities that have been linked to abnormal type-I IFN activity[9,10,97,337,338].

Of note, type-I-IFN blockers such as Anifrolumab are already being trialled for the treatment of SLE and other type-I interferonopathies[339–345]. Although the IFN-a blocker

Sifalimumab did not show therapeutic efficiency in PsV, other agents could potentially be beneficial in this disease and in GPP[346–348].

6 FINAL DISCUSSION

While the treatment of psoriasis has hugely benefited from our improved understanding of disease pathogenesis, the management of severe clinical variants (most notably pustular psoriasis and recalcitrant PsV) remains problematic, as these conditions are only partially understood at the immunological level[91]. The role of neutrophils, in particular, has received little attention, since most studies have focused on keratinocytes, dendritic cells and T lymphocyte sub-populations[1]. In this context, the objective of my PhD was to apply genetic and transcriptomic approaches to the study of neutrophil activation in psoriasis. The results reported in chapters 3, 4 and 5 highlight the potential of these strategies, but also their limitations.

6.1 Genetic studies

Although neutrophil accumulation in the stratum corneum and stratum spinosum is seen in all psoriasis subtypes, this phenomenon is particularly prominent in pustular forms of the disease, where systemic neutrophilia can also be observed. In fact, one of the main effects of *IL36RN* disease alleles is the up-regulation of IL-8, a powerful neutrophil chemo-attractant. On the basis of these observations, we proposed that pustular psoriasis would represent an ideal model for the study of neutrophil activation in psoriasis. We further hypothesised that the identification of new disease genes would uncover further regulators of neutrophil functions.

In keeping with our initial proposition, this study identified disease alleles in two genes, (*PRR13* and *MPO*) that appear to contribute to pustular psoriasis by disrupting neutrophil homeostasis and survival. While this success underscores the biological insights that can be obtained through the genetic analysis of rare and severe phenotypes, there might be limited scope for further discoveries.

To find additional genetic determinants of pustular psoriasis, the Capon group has recently exome sequenced 100 unrelated PPP individuals (briefly described in chapter 4). The analysis of this dataset, however, has shown that the disease is extremely heterogeneous, with no single gene accounting for a substantial fraction of affected

individuals. Further work by our lab also demonstrated key clinical and genetic differences between individuals affected by PPP and GPP[103]. Thus, it appears that locus and phenotypic heterogeneity within and across pustular psoriasis subtypes can greatly hinder the discovery of novel genetic determinants of the disease.

Given the rarity of pustular psoriasis, this problem can only be overcome by ascertaining larger patient cohorts through multi-centre collaborations. This will boost the power of exome sequencing studies and increase the prospect of ascertaining familial cases. To facilitate this process, our group has contributed to the set-up of the European Rare and Severe Psoriasis Expert Network (ERASPEN), which aims to standardise diagnostic criteria as well as protocols for patient recruitment and phenotyping[349]. The work of ERASPEN members has already enabled the ascertainment and characterisation of an extended clinical resource[103], so that plans are now in place to extend the reach of the Consortium beyond Europe.

The use of immune phenotyping techniques, which should also be standardised across recruiting centres, could aid to define patient subsets that are more homogeneous and amenable to genetic analysis. Here, the 2031-2A>C *MPO* mutation was uncovered in 2 subjects who presented with elevated neutrophil counts, despite receiving systemic treatment. In the future, the screening of affected individuals based on specific cell and protein markers could help select the most appropriate candidates for sequencing studies.

Finally, the use of public repositories can be of great help when patient numbers are limited. For example, freely accessible databases such as ClinVar[350] and GeneMatcher[351] enable clinicians and researchers to report putative mutations and early genotype-phenotype correlations, thus aiding in the identification of novel disease genes. Here, the hypothesis that *PRR13* mutations are a likely cause of GPP was only substantiated once the 100,000 Genomes Project[270] was queried. Then, data reported by the Genotype-Tissue Expression (GTex) consortium[239], the Blueprint[237] and Fantom5 projects[238] as well as the GWAS catalogue[240] helped to frame the hypothesis that the gene plays an important role in neutrophil biology. Similarly, data from the UK

Biobank[244,298] and the GWAS catalogue demonstrated an association between *MPO* mutations and neutrophil count variation.

Of note, the genomes of 50,000 UK Biobank participants are currently being sequenced, with plans to extend this analysis to the entire cohort. Thus, the wealth of publicly available genetic data is only set to increase in the coming years.

6.2 Transcriptomic approaches

As a supplement to the gene discovery approaches, this study used transcription profiling of patient cells to obtain further insights into the pathogenic role of neutrophils.

By undertaking RNA-sequencing in GPP patients and healthy controls, we demonstrated that type-I-IFN responses are abnormally active in the PMNs of affected individuals. Importantly, this finding was validated in a severe PsV cohort, demonstrating the validity of investigating pustular psoriasis as a broadly relevant model of recalcitrant disease. Mechanistic *ex-vivo* experiments then showed that the up-regulation of type-I-IFN signalling is mediated by an IL-36/TLR-9 axis that is active in pDCs. A manuscript describing these findings has been recently accepted for publication by the *Journal of Investigative Dermatology* (see "Publication arising from this thesis").

The above results might also be relevant to the pathogenesis of other inflammatory disorders characterised by IL-36 over-expression. Diseases presenting with joint inflammation are an interesting example. In fact, Boutet et al. found that IL-36 is up-regulated in approximately 20% of individuals suffering from rheumatoid arthritis (RA)[352], while Wright et al. detected a type-I interferon signature in RA patient neutrophils[353]. The IL-36/TLR9/IFN-α axis could also contribute to the pathogenesis of PsA, as high levels of IL-36α and low levels of IL-36Ra are found in inflamed synovium[354]. Finally, individuals affected by SLE (a well-established Interferonopathy) show markedly increased serum IL-36 levels and significantly decreased IL-36Ra production, compared to healthy controls[355]. Taken together, these observations suggest that the IL-36/type-I IFN axis may also be an important driver of joint diseases. The group is therefore

establishing collaborations with academic rheumatologists to facilitate the recruitment of relevant patient resources and pursue this new research avenue.

While the focus on a single cell type (whole-blood untouched neutrophils) removed important confounders from the differential expression analysis, it is important to bear in mind that PMNs are not a homogeneous population. In fact, neutrophils undergo important phenotypic changes during their life cycle[356]. These include an increase in CXCR4 and a decrease in L selectin (CD62L) and CD47 surface expression, as well as a reduction in the size and number of granules (see Figure 1.6 and Figure 1.7)[142]. At the transcriptional level, these changes affect several signalling pathways (cell activation, adhesion, migration, microbial detection and apoptosis), which are differently activated between aging and freshly released neutrophils[357]. Thus, the samples used in my experiments likely included both fresh and aged PMNs. Of note, inflammatory mediators (e.g. cytokines and microbial products) increase the numbers and lifespan of circulating neutrophils. Hence, GPP samples might have contained higher percentages of fresh and activated neutrophils, compared to healthy controls.

The presence of neutrophils migrating towards different tissues also contributes to the heterogeneity of PMNs. In this context, our observation that type-I-IFN activation was detectable in systemic (GPP and severe PsV) but not in localised forms of psoriasis (PPP and ACH), suggests that the neutrophils driving the IFN signature might not be those that are poised to extravasate to the skin.

While the IFN scores were elevated in the GPP and PsV cohorts, there was heterogeneity within both groups. In fact, most patients could be classified as IFN-high or IFN-low, an observation which could affect treatment choice and response, as discussed in section 6.3.

Finally, the diversity of circulating PMN is compounded by the presence of a distinct subset, known as low-density neutrophils (LDNs)[358]. Unlike other PMNs, these are found in the low-density fraction of blood samples that have been subject to density gradient centrifugation[359].

LDNs express surface markers that are specific to mature neutrophils ($CD15^{high}/CD14^{low}/CD10^{+}/CD16^{+}$)[360], but show a distinctive transcriptional profile. For example, the LDNs of SLE patients express higher levels of serine proteases and bactericidal proteins compared to their healthy counterparts[361], but the same does not apply to normal-density SLE neutrophils[362]. In addition, SLE LDNs have an increased tendency to form NETs [362].

Here, magnetic separation rather than density gradient centrifugation was used to isolate PMNs from whole blood. We can therefore assume that both normal and low-density neutrophil populations were present in the samples used for RNA-sequencing. Of note, the numbers of circulating LDNs have been shown to correlate with the severity of skin and vascular inflammation in psoriasis[363]. Moreover, LDNs have been shown to have enhanced capacity to synthetize IFN. Thus, it is tempting to speculate that LDNs may be driving, or at least significantly contributing to the type-I-IFN signature observed in severe psoriasis.

Given the numerous sources of heterogeneity within the PMN compartment, the results of this study should be followed-up with methods that afford better resolution of the underlying sub-populations. These could include multi-dimensional immune phenotyping by time of flight cytometry (CyTOF) and single cell RNA-sequencing. Such approaches would help to dissect the specific neutrophil populations that contribute to the systemic and cutaneous manifestations of psoriasis, assisting in patient diagnosis, and in the identification of markers of treatment response.

6.3 Future directions

In recent years, genome- and transcriptome-wide approaches have been increasingly applied to the study of drug responses and treatment resistance. In this context, Wright et al. showed that higher expression of IFN-signalling genes correlates with a positive outcome of TNF inhibitor therapy in RA[353]. These authors subsequently identified a set of 23 genes that could be used as biomarkers of response to TNF blockers[364]. Given that the TNF inhibitor adalimumab (which is now also available as a low-cost biosimilar) is

still a mainstay of psoriasis treatment, these observations warrant further analyses of IL-36 serum levels and type-I IFN genes in consecutive patient series. Such studies would have the potential to uncover novel predictors of drug response in psoriasis.

All the experiments described in this thesis have been complicated to some extent by the difficulty of working with neutrophils. This was particularly apparent in the follow-up of gene identification findings, where the short life of PMNs prevented me from executing experiments to recapitulate the effects of disease alleles. Since neutrophils can only be kept in culture for very short periods of time, they cannot be manipulated with RNAi or CRISPR-based methods that are routinely used in other cell types[365–367]. As a results, researchers have been investigating the biology of PMNs by generating knockouts in animal models and cell lines, such as HL-60 and PLB-985[368–374]. Both approaches, however, have their limitations. There are well documented differences between murine and human immune responses[375], and immortalised cell lines do not fully reproduce the features of their primary counterparts. HL-60 cells, for example, are unable to mount an effective intracellular respiratory burst and lack LL-37/hCAP-18 protein expression[367,376–378].

In this context, individuals harbouring loss of function mutations in neutrophil-related genes can be considered as very informative "human knockouts". While logistic issues (e.g. the difficulty of shipping fresh blood from overseas) have limited the analysis of patient neutrophils in this study, the group is trying to overcome these difficulties by identifying further, UK-based individuals bearing disease alleles. Protocols for the *ex-vivo* assessment of neutrophil proliferation and apoptosis are also being optimised. This work will allow the lab to thoroughly characterise rare *MPO* and *PRR13* knockouts, with the potential to investigate the role of these genes in neutrophil biology and, ultimately, human health.

ONLINE RESOURCES

Blueprint Consortium	http://www.blueprint-epigenome.eu/
CADD	https://cadd.gs.washington.edu/
Ensembl	http://www.ensembl.org/index.html
ExAC	http://exac.broadinstitute.org/
Fantom5	http://fantom.gsc.riken.jp/zenbu/
FastQC	http://www.bioinformatics.babraham.ac.uk/projects/fastqc
Geneatlas	http://geneatlas.roslin.ed.ac.uk/
GTex	https://gtexportal.org/home/
GWAS catalogue	https://www.ebi.ac.uk/gwas/
MutationTaster	http://www.mutationtaster.org/
PolyPhen-2	http://genetics.bwh.harvard.edu/pph2/bgi.shtml
Primer3	http://primer3.ut.ee
Primer-BLAST	https://www.ncbi.nlm.nih.gov/tools/primer-blast/
PROVEAN + SIFT	http://provean.jcvi.org/genome_submit_2.php?species=human

BIBLIOGRAPHY

1. Nestle et al. Psoriasis. *N. Engl. J. Med.* 361, 496–509 (2009).

2. Parisi et al. Global Epidemiology of Psoriasis: A Systematic Review of Incidence and Prevalence. *J. Invest. Dermatol.* 133, 377–385 (2013).

3. Capon. The genetic basis of psoriasis. *Int. J. Mol. Sci.* 18, 1–9 (2007).

4. Boehncke et al. Psoriasis. *Lancet* 386, 983–994 (2015).

5. Raychaudhuri et al. Diagnosis and classification of psoriasis. *Autoimmun. Rev.* 13, 490–495 (2014).

6. Griffiths et al. A classification of psoriasis vulgaris according to phenotype. *Br. J. Dermatol.* 156, 258–262 (2007).

7. Murphy et al. The histopathologic spectrum of psoriasis. *Clin. Dermatol.* 25, 524–528 (2007).

8. Schmitt et al. The psoriasis area and severity index is the adequate criterion to define severity in chronic plaque-type psoriasis. *Dermatology* 210, 194–199 (2005).

9. Davidovici et al. Psoriasis and Systemic Inflammatory Diseases: Potential Mechanistic Links between Skin Disease and Co-Morbid Conditions. *J. Invest. Dermatol.* 130, 1785–1796 (2010).

10. Fang et al. Association between Psoriasis and Subclinical Atherosclerosis: A Meta-Analysis. *Medicine (Baltimore).* 95, e3576 (2016).

11. Kaushik et al. Psoriasis: Which therapy for which patient: Psoriasis comorbidities and preferred systemic agents. *J. Am. Acad. Dermatol.* 80, 27–40 (2019).

12. Mease et al. Prevalence of rheumatologist-diagnosed psoriatic arthritis in patients with psoriasis in European/North American dermatology clinics. *J. Am.*

Acad. Dermatol. 69, 729–735 (2013).

13. Coates et al. Psoriatic arthritis: State of the art review. *Clin. Med. (Northfield. Il).* 17, 65–70 (2017).

14. Ritchlin et al. Psoriatic Arthritis. *N. Engl. J. Med.* 376, 957–970 (2017).

15. Gelfand et al. Determinants of quality of life in patients with psoriasis: A study from the US population. *J. Am. Acad. Dermatol.* 51, 704–708 (2004).

16. Mahil et al. Genetics of Psoriasis. *Dermatol. Clin.* 33, 1–11 (2015).

17. Lønnberg et al. Heritability of psoriasis in a large twin sample. *Br. J. Dermatol.* 169, 412–416 (2013).

18. Elder et al. The Genetics of Psoriasis. *Arch. Dermatol.* 130, 216–224 (1994).

19. Capon et al. An update on the genetics of psoriasis. *Dermatol. Clin.* 22, 339–347 (2004).

20. Capon et al. Searching for the major histocompatibility complex psoriasis susceptibility gene. *J. Invest. Dermatol.* 118, 745–751 (2002).

21. Nair et al. Evidence for two psoriasis susceptibility loci (HLA and 17q) and two novel candidate regions (16q and 20p) by genome-wide scan. *Hum. Mol. Genet.* 6, 1349–1356 (1997).

22. Trembath et al. Identification of a major susceptibility locus on chromosome 6p and evidence for further disease loci revealed by a two stage genome-wide search in psoriasis. *Hum. Mol. Genet.* 6, 813–820 (1997).

23. Veal et al. Family-Based Analysis Using a Dense Single-Nucleotide Polymorphism–Based Map Defines Genetic Variation at PSORS1, the Major Psoriasis-Susceptibility Locus. *Am. J. Hum. Genet.* 71, 554–564 (2002).

24. Nair et al. Genome-wide scan reveals association of psoriasis with IL-23 and NF-

κB pathways. *Nat. Genet.* 41, 199–204 (2009).

25. Genetic Analysis of Psoriasis Consortium & the Wellcome Trust Case Control Consortium 2 et al. A genome-wide association study identifies new psoriasis susceptibility loci and an interaction between HLA-C and ERAP1. *Nat. Genet.* 42, 985–990 (2010).

26. Nair et al. Sequence and haplotype analysis supports HLA-C as the psoriasis susceptibility 1 gene. *Am. J. Hum. Genet.* 78, 827–851 (2006).

27. Jordan et al. PSORS2 Is Due to Mutations in CARD14. *Am. J. Hum. Genet.* 90, 784–795 (2012).

28. Jordan et al. Rare and common variants in CARD14, encoding an epidermal regulator of NF-kappaB, in psoriasis. *Am. J. Hum. Genet.* 90, 796–808 (2012).

29. Berki et al. Activating CARD14 mutations are associated with generalized pustular psoriasis but rarely account for familial recurrence in psoriasis vulgaris. *J. Invest. Dermatol.* 135, 2964–2970 (2015).

30. Capon et al. Searching for psoriasis susceptibility genes in Italy: Genome scan and evidence for a new locus on chromosome 1. *J. Invest. Dermatol.* 112, 32–35 (1999).

31. Oh et al. The Molecular Revolution in Cutaneous Biology: EDC and Locus Control. *J. Invest. Dermatol.* 137, e101–e104 (2017).

32. De Cid et al. Deletion of the late cornified envelope LCE3B and LCE3C genes as a susceptibility factor for psoriasis. *Nat. Genet.* 41, 211–215 (2009).

33. Riveira-Munoz et al. Meta-analysis confirms the LCE3C-LCE3B deletion as a risk factor for psoriasis in several ethnic groups and finds interaction with HLA-Cw6. *J. Invest. Dermatol.* 131, 1105–1109 (2011).

34. Stuart et al. Association of β-defensin copy number and psoriasis in three cohorts

of European origin. *J Invest Dermatol* 132, 2407–2413 (2012).

35. Capon et al. Identification of ZNF313/RNF114 as a novel psoriasis susceptibility gene. *Hum. Mol. Genet.* 17, 1938–1945 (2008).

36. Cargill et al. A Large-Scale Genetic Association Study Confirms IL12B and Leads to the Identification of IL23R as Psoriasis-Risk Genes. *Am. J. Hum. Genet.* 80, 273–290 (2007).

37. Ellinghaus et al. Genome-wide asociation study identifies a psoriasis susceptibility locus at TRAF3IP2. *Nat. Genet.* 42, 991–995 (2010).

38. Tsoi et al. Identification of 15 new psoriasis susceptibility loci highlights the role of innate immunity. *Nat. Genet.* 44, 1341–1348 (2012).

39. Tsoi et al. Enhanced meta-analysis and replication studies identify five new psoriasis susceptibility loci. *Nat. Commun.* 6:7001, doi: 10.1038/ncomms8001 (2015).

40. Zuo et al. Whole-exome SNP array identifies 15 new susceptibility loci for psoriasis. *Nat. Commun.* 6:6793, doi: 10.1038/ncomms7793 (2015).

41. Farh et al. Genetic and epigenetic fine mapping of causal autoimmune disease variants. *Nature* 518, 337–43 (2015).

42. Tsoi et al. Large scale meta-analysis characterizes genetic architecture for common psoriasis associated variants. *Nat. Commun.* 8:15382, doi: 10.1038/ncomms15382 (2017).

43. Tennessen et al. Evolution and Functional Impact of Rare Coding Variation from Deep Sequencing of Human Exomes. *Science* 337, 64–69 (2012).

44. Coventry et al. Deep resequencing reveals excess rare recent variants consistent with explosive population growth. *Nat. Commun.* 1:131, doi: 10.1038/ncomms1130 (2010).

45. Manolio et al. Finding the missing heritability of complex diseases. *Nature* 461, 747–753 (2009).

46. Lande et al. Plasmacytoid dendritic cells sense self-DNA coupled with antimicrobial peptide. *Nature* 449, 564–569 (2007).

47. Ganguly et al. Self-RNA-antimicrobial peptide complexes activate human dendritic cells through TLR7 and TLR8. *J. Exp. Med.* 206, 1983–1994 (2009).

48. Zaba et al. Psoriasis is characterized by accumulation of immunostimulatory and Th1/Th17 cell-polarizing myeloid dendritic cells. *J. Invest. Dermatol.* 129, 79–88 (2009).

49. Nestle et al. Plasmacytoid predendritic cells initiate psoriasis through interferon-α production. *J. Exp. Med.* 202, 135–143 (2005).

50. Lande et al. Neutrophils Activate Plasmacytoid Dendritic Cells by Releasing Self-DNA Peptide Complexes in Systemic Lupus Erythematosus. *Sci. Transl. Med.* 3, 73ra19 (2011).

51. Chiricozzi et al. Integrative responses to IL-17 and TNF-α in human keratinocytes account for key inflammatory pathogenic circuits in psoriasis. *J. Invest. Dermatol.* 131, 677–687 (2011).

52. Harper et al. Th17 cytokines stimulate CCL20 expression in keratinocytes in vitro and in vivo: Implications for psoriasis pathogenesis. *J. Invest. Dermatol.* 129, 2175–2183 (2009).

53. Res et al. Overrepresentation of IL-17A and IL-22 Producing CD8 T Cells in Lesional Skin Suggests Their Involvement in the pathogenesis of psoriasis. *PLoS One* 5, e14108 (2010).

54. Hawkes et al. Psoriasis pathogenesis and the development of novel targeted immune therapies. *J. Allergy Clin. Immunol.* 140, 645–653 (2017).

55. Hawkes et al. Discovery of the IL-23/IL-17 Signaling Pathway and the Treatment of Psoriasis. *J. Immunol.* 201, 1605–1613 (2018).

56. Elias et al. Epidermal vascular endothelial growth factor production is required for permeability barrier homeostasis, dermal angiogenesis, and the development of epidermal hyperplasia: Implications for the pathogenesis of psoriasis. *Am. J. Pathol.* 173, 689–699 (2008).

57. Mabuchi et al. Binding Affinity and Interaction of LL-37 with HLA-C*06:02 in Psoriasis. *J. Invest. Dermatol.* 136, 1901–1903 (2016).

58. Lande et al. The antimicrobial peptide LL37 is a T-cell autoantigen in psoriasis. *Nat. Commun.* 5:5621, doi: 10.1038/ncomms6621 (2014).

59. Cheung et al. Psoriatic T cells recognize neolipid antigens generated by mast cell phospholipase delivered by exosomes and presented by CD1a. *J. Exp. Med.* 213, 2399–2412 (2016).

60. Bergboer et al. Genetics of psoriasis: Evidence for epistatic interaction between skin barrier abnormalities and immune deviation. *J. Invest. Dermatol.* 132, 2320–2331 (2012).

61. Mahil et al. Update on psoriasis immunopathogenesis and targeted immunotherapy. *Semin. Immunopathol.* 38, 11–27 (2016).

62. Menter et al. Guidelines of care for the management of psoriasis and psoriatic arthritis: Section 6. Guidelines of care for the treatment of psoriasis and psoriatic arthritis: Case-based presentations and evidence-based conclusions. *J. Am. Acad. Dermatol.* 65, 137–174 (2011).

63. Tartar et al. Update on the Immunological Mechanism of Action Behind Phototherapy. *J Drugs Dermatol* 13, 564–568 (2014).

64. Weinstein et al. Cytotoxic and Immunologic Effects of Methotrexate in Psoriasis. *J. Invest. Dermatol.* 95, 49–52 (1990).

65. Czarnecka-Operacz et al. The possibilities and principles of methotrexate treatment of psoriasis - The updated knowledge. *Postep Derm Alergol* 31, 392–400 (2014).

66. Elango et al. Impact of methotrexate on oxidative stress and apoptosis markers in psoriatic patients. *Clin. Exp. Med.* 14, 431–437 (2014).

67. Golbari et al. Current Guidelines for Psoriasis Treatment: A Work in Progress. *Cutis* 101, 10–12 (2018).

68. Zaba et al. Amelioration of epidermal hyperplasia by TNF inhibition is associated with reduced Th17 responses. *J. Exp. Med.* 204, 3183–3194 (2007).

69. Zaba et al. Effective treatment of psoriasis with etanercept is linked to suppression of IL-17 signaling, not immediate response TNF genes. *J. Allergy Clin. Immunol.* 124, 1022–1030 (2009).

70. Bongartz et al. Anti-TNF antibody therapy in rheumatoid arthritis and the risk of serious infections and malignancies. *J. Am. Med. Assoc.* 295, 2275–2285 (2006).

71. Mahil et al. Demyelination during tumour necrosis factor antagonist therapy for psoriasis: A case report and review of the literature. *J. Dermatolog. Treat.* 24, 38–49 (2013).

72. Leonardi et al. Effi cacy and safety of ustekinumab , a human interleukin-12 / 23 monoclonal antibody , in patients with psoriasis : 76-week results from a randomised , double-blind , placebo-controlled trial (PHOENIX 1). *Lancet* 371, 1665–1674 (2008).

73. Langley et al. Efficacy and safety of ustekinumab, a human interleukin-12/23 monoclonal antibody, in patients with psoriasis: 52-week results from a randomised, double-blind, placebo-controlled trial (PHOENIX 2). *Lancet* 371, 1675–1684 (2008).

74. Griffiths et al. Comparison of Ustekinumab and Etanercept for Moderate-to-

Severe Psoriasis. *N. Engl. J. Med.* 362, 118–128 (2010).

75. Burden et al. The British Association of Dermatologists' Biologic Interventions Register (BADBIR): Design, methodology and objectives. *Br. J. Dermatol.* 166, 545–554 (2012).

76. Blauvelt et al. Secukinumab is superior to ustekinumab in clearing skin of subjects with moderate-to-severe plaque psoriasis up to 1 year: Results from the CLEAR study. *J. Am. Acad. Dermatol.* 76, 60–69 (2017).

77. Langley et al. Secukinumab in Plaque Psoriasis — Results of Two Phase 3 Trials. *N. Engl. J. Med.* 371, 326–338 (2014).

78. Griffiths et al. Comparison of ixekizumab with etanercept or placebo in moderate-to-severe psoriasis (UNCOVER-2 and UNCOVER-3): Results from two phase 3 randomised trials. *Lancet* 386, 541–551 (2015).

79. Lebwohl et al. Phase 3 Studies Comparing Brodalumab with Ustekinumab in Psoriasis. *N. Engl. J. Med.* 373, 1318–28 (2015).

80. Papp et al. Brodalumab, an Anti–Interleukin-17–Receptor Antibody for Psoriasis. *N. Engl. J. Med.* 366, 1181–1189 (2012).

81. Reich et al. Evidence that a neutrophil-keratinocyte crosstalk is an early target of IL-17A inhibition in psoriasis. *Exp. Dermatol.* 24, 529–535 (2015).

82. Braun et al. Effect of secukinumab on clinical and radiographic outcomes in ankylosing spondylitis: 2-year results from the randomised phase III MEASURE 1 study. *Ann. Rheum. Dis.* 76, 1070–1077 (2017).

83. Papp et al. Tildrakizumab (MK-3222), an anti-interleukin-23p19 monoclonal antibody, improves psoriasis in a phase IIb randomized placebo-controlled trial. *Br. J. Dermatol.* 173, 930–939 (2015).

84. Gordon et al. A Phase 2 Trial of Guselkumab versus Adalimumab for Plaque

Psoriasis. *N. Engl. J. Med.* 373, 136–144 (2015).

85. Schafer. Apremilast mechanism of action and application to psoriasis and psoriatic arthritis. *Biochem. Pharmacol.* 83, 1583–1590 (2012).

86. Papp et al. Apremilast, an oral phosphodiesterase 4 (PDE4) inhibitor, in patients with moderate to severe plaque psoriasis: Results of a phase III, randomized, controlled trial (Efficacy and Safety Trial Evaluating the Effects of Apremilast in Psoriasis [ESTEEM] 1). *J. Am. Acad. Dermatol.* 73, 37–49 (2015).

87. Bachelez et al. Tofacitinib versus etanercept or placebo in moderate-to-severe chronic plaque psoriasis: A phase 3 randomised non-inferiority trial. *Lancet* 386, 552–561 (2015).

88. Papp et al. Tofacitinib, an oral Janus kinase inhibitor, for the treatment of chronic plaque psoriasis: Long-term efficacy and safety results from 2 randomized phase-III studies and 1 open-label long-term extension study. *J. Am. Acad. Dermatol.* 74, 841–850 (2016).

89. Punwani et al. Downmodulation of key inflammatory cell markers with a topical Janus kinase 1/2 inhibitor. *Br. J. Dermatol.* 173, 989–997 (2015).

90. Papp et al. Phase 2 trial of selective tyrosine kinase 2 inhibition in psoriasis. *N. Engl. J. Med.* 379, 1313–1321 (2018).

91. Strober et al. Comparative effectiveness of biologic agents for the treatment of psoriasis in a real-world setting: Results from a large, prospective, observational study (Psoriasis Longitudinal Assessment and Registry [PSOLAR]). *J. Am. Acad. Dermatol.* 74, 851–861 (2016).

92. Naldi et al. The clinical spectrum of psoriasis. *Clin. Dermatol.* 25, 510–518 (2007).

93. Bachelez. Pustular psoriasis and related pustular skin diseases. *Br. J. Dermatol.* 178, 614–618 (2018).

94. Augey et al. Generalized pustular psoriasis (Zumbusch): A French epidemiological survey. *Eur. J. Dermatology* 16, 669–673 (2006).

95. Ohkawara et al. Generalized pustular psoriasis in Japan: Two distinct groups formed by differences in symptoms and genetic background. *Acta Derm. Venereol.* 76, 68–71 (1996).

96. Li et al. Mutation analysis of the IL36RN gene in Chinese patients with generalized pustular psoriasis with/without psoriasis vulgaris. *J. Dermatol. Sci.* 76, 132–138 (2014).

97. Hoegler et al. Generalized pustular psoriasis: a review and update on treatment. *J. Eur. Acad. Dermatology Venereol.* 12, doi: 10.1111/jdv.14949 (2018).

98. Naik et al. Autoinflammatory pustular neutrophilic diseases. *Dermatol. Clin.* 31, 405–425 (2013).

99. Navarini et al. European consensus statement on phenotypes of pustular psoriasis. *J. Eur. Acad. Dermatology Venereol.* 31, 1792–1799 (2017).

100. Kubota et al. Epidemiology of psoriasis and palmoplantar pustulosis: a nationwide study using the Japanese national claims database. *BMJ* 5, e006450 (2015).

101. Hellgreen et al. Pustulosis palmaris et plantaris. Prevalence, clinical observations and prognosis. *Acta Derm. Venereol.* 284–288 (1971).

102. De Waal et al. Pustulosis palmoplantaris is a disease distinct from psoriasis. *J. Dermatolog. Treat.* 22, 102–105 (2011).

103. Twelves et al. Clinical and genetic differences between pustular psoriasis subtypes. *J. Allergy Clin. Immunol.* 143, 1021–1026 (2019).

104. Wolska et al. What do we know about palmoplantar pustulosis? *J. Eur. Acad. Dermatology Venereol.* 31, 38–44 (2017).

105. Benjegerdes et al. Pustular psoriasis: pathophysiology and current treatment perspectives. *Psoriasis Targets Ther.* 6, 131–144 (2016).

106. Puig et al. Treatment of acrodermatitis continua of Hallopeau with TNF-blocking agents: Case report and review. *Dermatology* 220, 154–158 (2010).

107. Asumalahti et al. Genetic Analysis of PSORS1 Distinguishes Guttate Psoriasis and Palmoplantar Pustulosis. *J. Invest. Dermatol.* 120, 627–632 (2003).

108. Onoufriadis et al. Mutations in IL36RN/IL1F5 are associated with the severe episodic inflammatory skin disease known as generalized pustular psoriasis. *Am. J. Hum. Genet.* 89, 432–437 (2011).

109. Marrakchi et al. Interleukin-36-receptor antagonist deficiency and generalized pustular psoriasis. *N. Engl. J. Med.* 365, 620–628 (2011).

110. Sims et al. The IL-1 family: regulators of immunity. *Nat. Rev. Immunol.* 10, 89–102 (2010).

111. Saha et al. Signal transduction and intracellular trafficking by the interleukin 36 receptor. *J. Biol. Chem.* 290, 23997–24006 (2015).

112. Tauber et al. IL36RN Mutations Affect Protein Expression and Function: A Basis for Genotype-Phenotype Correlation in Pustular Diseases. *J. Invest. Dermatol.* 136, 1811–1819 (2016).

113. Infevers IL36RN variants [Online], Available at: https://fmf.igh.cnrs.fr/ISSAID/infevers/search.php?n=13. Accessed on 07/05/2019.

114. Setta-Kaffetzi et al. Rare pathogenic variants in IL36RN underlie a spectrum of psoriasis-associated pustular phenotypes. *J. Invest. Dermatol.* 133, 1366–1369 (2013).

115. Hussain et al. IL36RN mutations define a severe autoinflammatory phenotype of

generalized pustular psoriasis. *J. Allergy Clin. Immunol.* 135, 1067–1069 (2014).

116. Setta-Kaffetzi et al. AP1S3 Mutations Are Associated with Pustular Psoriasis and Impaired Toll-like Receptor 3 Trafficking. *Am. J. Hum. Genet.* 94, 790–797 (2014).

117. Hirst et al. Distinct and overlapping roles for AP-1 and GGAs revealed by the 'knocksideways' system. *Curr. Biol.* 22, 1711–1716 (2012).

118. Mahil et al. AP1S3 Mutations Cause Skin Autoinflammation by Disrupting Keratinocyte Autophagy and Up-Regulating IL-36 Production. *J. Invest. Dermatol.* 136, 2251–2259 (2016).

119. Fuchs-Telem et al. Familial pityriasis rubra pilaris is caused by mutations in CARD14. *Am. J. Hum. Genet.* 91, 163–170 (2012).

120. Sugiura et al. CARD14 c.526G>C (p.Asp176His) Is a Significant Risk Factor for Generalized Pustular Psoriasis with Psoriasis Vulgaris in the Japanese Cohort. *J. Invest. Dermatol.* 134, 1755–1757 (2014).

121. Mössner et al. Palmoplantar Pustular Psoriasis Is Associated with Missense Variants in CARD14, but Not with Loss-of-Function Mutations in IL36RN in European Patients. *J. Invest. Dermatol.* 135, 2538–2541 (2015).

122. Lenz et al. Oncogenic CARD11 Mutations in Human Diffuse Large B Cell Lymphoma. *Science* 319, 1676–1679 (2008).

123. Johnston et al. IL-1 and IL-36 are dominant cytokines in generalized pustular psoriasis. *J. Allergy Clin. Immunol.* 140, 109–120 (2017).

124. Henry et al. Neutrophil-Derived Proteases Escalate Inflammation through Activation of IL-36 Family Cytokines. *Cell Rep.* 14, 708–722 (2016).

125. Macleod et al. Neutrophil Elastase-mediated proteolysis activates the anti-inflammatory cytokine IL-36 Receptor antagonist. *Sci. Rep.* 6:24880, doi: 10.1038/srep24880 (2016).

126. Ainscough et al. Cathepsin S is the major activator of the psoriasis-associated proinflammatory cytokine IL-36γ. *Proc. Natl. Acad. Sci.* 114, e2748–e2757 (2017).

127. Mahil et al. An analysis of IL-36 signature genes and individuals with IL1RL2 knockout mutations validates IL-36 as a psoriasis therapeutic target. *Sci. Transl. Med.* 9, eaan2514 (2017).

128. Robinson et al. Treatment of pustular psoriasis: From the medical board of the National Psoriasis Foundation. *J. Am. Acad. Dermatol.* 67, 279–288 (2012).

129. Imafuku et al. Efficacy and safety of secukinumab in patients with generalized pustular psoriasis: A 52-week analysis from phase III open-label multicenter Japanese study. *J. Dermatol.* 43, 1011–1017 (2016).

130. Yamasaki et al. Efficacy and safety of brodalumab in patients with generalized pustular psoriasis and psoriatic erythroderma: results from a 52-week, open-label study. *Br. J. Dermatol.* 176, 741–751 (2017).

131. Viguier et al. Successful Treatment of Generalized Pustular Psoriasis With the Interleukin-1-Receptor Antagonist Anakinra: Lack of Correlation With IL1RN Mutations. *Ann. Intern. Med.* 153, 66–67 (2010).

132. Huffmeier et al. Successful therapy with anakinra in a patient with generalized pustular psoriasis carrying IL36RN mutations. *Br. J. Dermatol.* 170, 202–204 (2014).

133. Tauber et al. Is it relevant to use an interleukin-1-inhibiting strategy for the treatment of patients with deficiency of interleukin-36 receptor antagonist? *Br. J. Dermatol.* 170, 1198–1199 (2014).

134. Di Costanzo et al. Acrodermatitis continua of Hallopeau (ACH): Two cases successfully treated with adalimumab. *J. Dermatolog. Treat.* 25, 489–494 (2014).

135. Bissonnette et al. Increased expression of IL-17A and limited involvement of IL-23 in patients with palmo-plantar (PP) pustular psoriasis or PP pustulosis; Results

from a randomised controlled trial. *J. Eur. Acad. Dermatology Venereol.* 28, 1298–1305 (2014).

136. Saunier et al. Acrodermatitis Continua of Hallopeau Treated Successfully with Ustekinumab and Acitretin after Failure of Tumour Necrosis Factor Blockade and Anakinra. *Dermatology* 230, 97–100 (2014).

137. Bachelez et al. Inhibition of the Interleukin-36 Pathway for the Treatment of Generalized Pustular Psoriasis. *N. Engl. J. Med.* 380, 981–983 (2019).

138. Khanskaya et al. A Phase 1 study of ANB019, an Anti-IL-36 Receptor Monoclonal Antibody, in Healthy Volunteers. *Proc. Conf.* (2018).

139. Sheshachalam et al. Granule protein processing and regulated secretion in neutrophils. *Front. Immunol.* 5, doi: 10.3389/fimmu.2014.00448 (2014).

140. Dancey et al. Neutrophil Kinetics in Man. *J. Clin. Endocrinol. Metab.* 58, 705–715 (1976).

141. Vietinghoff et al. Homeostatic regulation of blood neutrophil counts. *J Immunol* 181, 5183–5188 (2008).

142. Rosales. Neutrophil: A cell with many roles in inflammation or several cell types? *Front. Physiol.* 9, doi: 10.3389/fphys.2018.00113 (2018).

143. Bjerregaard et al. The in vivo profile of transcription factors during neutrophil differentiation in human bone marrow. *Blood* 101, 4322–4332 (2003).

144. Hock et al. Intrinsic Requirement for Zinc Finger Transcription Factor Gfi-1 in Neutrophil Differentiation. *Immunity* 18, 109–120 (2003).

145. Hager et al. Neutrophil granules in health and disease. *J. Intern. Med.* 268, 25–34 (2010).

146. Kolaczkowska et al. Neutrophil recruitment and function in health and

inflammation. *Nat. Rev. Immunol.* 13, 159–175 (2013).

147. Cowland. Granulopoiesis and granules of human neutrophils. *Immunol. Rev.* 273, 11–28 (2016).

148. Amulic et al. Neutrophil Function: From Mechanisms to Disease. *Annu. Rev. Immunol.* 30, 459–489 (2012).

149. Mócsai. Diverse novel functions of neutrophils in immunity, inflammation, and beyond. *J. Exp. Med.* 210, 1283–1299 (2013).

150. Thomas et al. Pattern recognition receptor function in neutrophils. *Trends Immunol.* 34, 317–328 (2013).

151. Wright et al. Neutrophil function in inflammation and inflammatory diseases. *Rheumatology* 49, 1618–1631 (2010).

152. Brogden. Antimicrobial peptides: Pore formers or metabolic inhibitors in bacteria? *Nat. Rev. Microbiol.* 3, 238–250 (2005).

153. Lee et al. Transmembrane Pores Formed by Human Antimicrobial Peptide LL-37. *Biophysj* 100, 1688–1696 (2011).

154. Faurschou et al. Neutrophil granules and secretory vesicles in inflammation. *Microbes Infect.* 5, 1317–1327 (2003).

155. Soehnlein et al. Neutrophils launch monocyte extravasation by release of granule proteins. *Thromb. Haemost.* 102, 198–205 (2009).

156. Lew et al. Quantitative Analysis of the Cytosolic Free Calcium Dependency of Exocytosis from Three Subcellular Compartments in Intact Human Neutrophils. *J. Cell Biol.* 102, 2197–2204 (1986).

157. Borregaard et al. Ca2+-dependent translocation of cytosolic proteins to isolated granule subpopulations and plasma membrane from human neutrophils. *Fed.*

Eur. Biochem. Soc. 304, 195–197 (1992).

158. Faurschou et al. Defensin-rich granules of human neutrophils: Characterization of secretory properties. *Biochim. Biophys. Acta - Mol. Cell Res.* 1591, 29–35 (2002).

159. Sengeløv et al. Control of exocytosis in early neutrophil activation. *J. Immunol.* 150, 1535–1543 (1993).

160. Borregaard. Neutrophils, from Marrow to Microbes. *Immunity* 33, 657–670 (2010).

161. Delclaux et al. Role of Gelatinase B and Elastase in Human Polymorphonuclear Neutrophil Migration across Basement Membrane. *Am. J. Respir. Cell Mol. Biol.* 14, 288–295 (1996).

162. Kobayashi et al. Towards a comprehensive understanding of the role of neutrophils in innate immunty: a systems biology-level approach. *Wiley Imterdiscip Rev Syst Biol Med* 1, 309–333 (2009).

163. Arnold et al. A Review of Chronic Granulomatous Disease. *Adv. Ther.* 34, 2543–2557 (2017).

164. Lee et al. Phagocytosis by neutrophils. *Microbes Infect.* 5, 1299–1306 (2003).

165. Kruger et al. Neutrophils: Between Host Defence, Immune Modulation, and Tissue Injury. *PLoS Pathog.* 11, e1004651 (2015).

166. Fuchs et al. Novel cell death program leads to neutrophil extracellular traps. *J. Cell Biol.* 176, 231–241 (2007).

167. Brinkmann et al. Neutrophil Extracellular Traps Kill Bacteria. *Science* 303, 1532–1535 (2004).

168. Papayannopoulos et al. NETs: a new strategy for using old weapons. *Trends Immunol.* 30, 513–521 (2009).

169. Mantovani et al. Neutrophils in the activation and regulation of innate and adaptive immunity. *Nat. Publ. Gr.* 11, 519–531 (2011).

170. Nathan. Neutrophils and immunity: Challenges and opportunities. *Nat. Rev. Immunol.* 6, 173–182 (2006).

171. Sica et al. IL-1 transcriptionally activates the neutrophil chemotactic factor/IL-8 gene in endothelial cells. *Immunology* 69, 548–53 (1990).

172. Scapini et al. The neutrophil as a cellular source of chemokines. *Immunol. Rev.* 177, 195–203 (2000).

173. Meyer-Hoffert et al. Neutrophil serine proteases: Mediators of innate immune responses. *Curr. Opin. Hematol.* 18, 19–24 (2011).

174. De Yang et al. LL-37, the neutrophil granule- and epithelial cell-derived cathelicidin, utilizes formyl peptide receptor-like 1 (FPRL1) as a receptor to chemoattract human peripheral blood neutrophils, monocytes, and T cells. *J. Exp. Med.* 192, 1069–1074 (2000).

175. Chertov et al. Identification of Human Neutrophil-derived Cathepsin G and Azurocidin/CAP37 as Chemoattractants for Mononuclear Cells and Neutrophils. *J. Exp. Med.* 186, 739–747 (1997).

176. Akahoshi et al. Production of macrophage inflammatory protein 3α (MIP-3α) (CCL20) and MIP-31β (CCL19) by human peripheral blood neutrophils in response to microbial pathogens. *Infect. Immun.* 71, 524–526 (2003).

177. Yoshimura et al. IFN- -Mediated Survival Enables Human Neutrophils to Produce MCP-1/CCL2 in Response to Activation by TLR Ligands. *J. Immunol.* 179, 1942–1949 (2007).

178. Bennouna et al. Microbial Antigen Triggers Rapid Mobilization of TNF- to the Surface of Mouse Neutrophils Transforming Them into Inducers of High-Level Dendritic Cell TNF- Production. *J. Immunol.* 174, 4845–4851 (2005).

179. van Gisbergen et al. Neutrophils mediate immune modulation of dendritic cells through glycosylation-dependent interactions between Mac-1 and DC-SIGN. *J. Exp. Med.* 201, 1281–1292 (2005).

180. Megiovanni et al. Polymorphonuclear neutrophils deliver activation signals and antigenic molecules to dendritic cells: a new link between leukocytes upstream of T lymphocytes. *J. Leukoc. Biol.* 79, 977–988 (2006).

181. Balázs et al. Blood Dendritic Cells Interact with Splenic Marginal Zone B Cells to Initiate T-Independent Immune Responses. *Immunity* 17, 341–352 (2002).

182. Scapini et al. G-CSF–stimulated Neutrophils Are a Prominent Source of Functional BLyS. *J. Exp. Med.* 197, 297–302 (2003).

183. Schwaller et al. Neutrophil-derived APRIL concentrated in tumor lesions by proteoglycans correlates with human B-cell lymphoma aggressiveness. *Blood J.* 109, 331–339 (2007).

184. Puga et al. B cell-helper neutrophils stimulate the diversification and production of immunoglobulin in the marginal zone of the spleen. *Nat. Immunol.* 13, 170–180 (2012).

185. Pelletier et al. Evidence for a cross-talk between human neutrophils and Th17 cells. *Blood* 115, 335–343 (2010).

186. Himmel et al. Human CD4+FOXP3+ regulatory T cells produce CXCL8 and recruit neutrophils. *Eur. J. Immunol.* 41, 306–312 (2011).

187. Beauvillain et al. Neutrophils efficiently cross-prime naive T cells in vivo. *Blood* 110, 2965–2974 (2007).

188. Spörri et al. A novel role for neutrophils as critical activators of NK cells. *J. Immunol.* 181, 7121–7130 (2008).

189. Costantini et al. The defensive alliance between neutrophils and NK cells as a

novel arm of innate immunity. *J. Leukoc. Biol.* 89, 221–233 (2011).

190. Ordoñez-Rueda et al. A hypomorphic mutation in the Gfi1 transcriptional repressor results in a novel form of neutropenia. *Eur. J. Immunol.* 42, 2395–2408 (2012).

191. Jaeger et al. Neutrophil depletion impairs natural killer cell maturation, function, and homeostasis. *J. Exp. Med.* 209, 565–580 (2012).

192. Pelletier et al. Modulation of human neutrophil survival and antigen expression by activated CD4 + and CD8 + T cells. *J. Leukoc. Biol.* 88, 1163–1170 (2010).

193. Davey et al. Human neutrophil clearance of bacterial pathogens triggers anti-microbial γδ T cell responses in early infection. *PLoS Pathog.* 7, e1002040 (2011).

194. Sakamoto. Type I and type II interferons delay human neutrophil apoptosis via activation of STAT3 and up-regulation of cellular inhibitor of apoptosis 2. *J. Leukoc. Biol.* 78, 301–309 (2005).

195. Trinchieri. Type I interferon : friend or foe? *J. Exp. Med.* 207, 2053–2063 (2010).

196. Krishnamoorthy et al. Resolvin D1 binds human phagocytes with evidence for proresolving receptors. *Proc. Natl. Acad. Sci.* 107, 1660–1665 (2010).

197. Schwab et al. Resolvin E1 and protectin D1 activate inflammation-resolution programmes. *Nature* 447, 869–874 (2007).

198. Arita et al. Resolvin E1 selectively interacts with leukotriene B4 receptor BLT1 and ChemR23 to regulate inflammation. *J. Immunol.* 178, 3912–3917 (2007).

199. Filep et al. Anti-inflammatory actions of lipoxin A(4) stable analogs are demonstrable in human whole blood: modulation of leukocyte adhesion molecules and inhibition of neutrophil-endothelial interactions. *Blood* 94, 4132–4142 (1999).

200. Jozsef et al. Lipoxin A4 and aspirin-triggered 15-epi-lipoxin A4 inhibit peroxynitrite formation, NF- B and AP-1 activation, and IL-8 gene expression in human leukocytes. *Proc. Natl. Acad. Sci.* 99, 13266–13271 (2002).

201. Godson et al. Cutting Edge: Lipoxins Rapidly Stimulate Nonphlogistic Phagocytosis of Apoptotic Neutrophils by Monocyte-Derived Macrophages. *J. Immunol.* 164, 1663–1667 (2000).

202. Bourke et al. IL-1 Scavenging by the Type II IL-1 Decoy Receptor in Human Neutrophils. *J. Immunol.* 170, 5999–6005 (2003).

203. McKimmie et al. Hemopoietic cell expression of the chemokine decoy receptor D6 is dynamic and regulated by GATA1. *J. Immunol.* 181, 3353–3363 (2008).

204. Savill. Apoptosis in resolution of inflammation. *J. Leukoc. Biol.* 61, 375–380 (1997).

205. Shi et al. Role of the liver in regulating numbers of circulating neutrophils. *Blood* 98, 1226–1230 (2001).

206. Boxer et al. The role of the neutrophil in inflammatory diseases of the lung. *Blood Cells* 16, 25—42 (1990).

207. Edwards et al. Seeing the wood for the trees: The forgotten role of neutrophils in rheumatoid arthritis. *Immunol. Today* 18, 320–324 (1997).

208. Savill et al. Macrophage Phagocytosis of Aging Neutrophils in Inflammation. *J. Clin. Invest.* 83, 865–875 (1989).

209. Ren et al. Nonphlogistic Clearance of Late Apoptotic Neutrophils by Macrophages: Efficient Phagocytosis Independent of 2 Integrins. *J. Immunol.* 166, 4743–4750 (2001).

210. Ortiz-Masià et al. Induction of CD36 and Thrombospondin-1 in Macrophages by Hypoxia-Inducible Factor 1 and Its Relevance in the Inflammatory Process. *PLoS One* 7, e48535 (2012).

211. Piccard et al. On the dual roles and polarized phenotypes of neutrophils in tumor development and progression. *Crit. Rev. Oncol. Hematol.* 82, 296–309 (2012).

212. Fridlender et al. Polarization of Tumor-Associated Neutrophil Phenotype by TGF-β: 'N1' versus 'N2' TAN. *Cancer Cell* 16, 183–194 (2009).

213. Perobelli et al. Plasticity of neutrophils reveals modulatory capacity. *Brazilian J. Med. Biol. Res.* 48, 665–675 (2015).

214. Mayadas et al. The Multifaceted Functions of Neutrophils. *Annu Rev Pathol* 9, 181–218 (2014).

215. Vilboux et al. A Congenital Neutrophil Defect Syndrome Associated with Mutations in VPS45 . *N. Engl. J. Med.* 369, 54–65 (2013).

216. Harris et al. Lessons from rare maladies: Leukocyte adhesion deficiency syndromes. *Curr. Opin. Hematol.* 20, 16–25 (2013).

217. Zeidler et al. Clinical implications of ELA2-, HAX1-, and G-CSF-receptor (CSF3R) mutations in severe congenital neutropenia. *Br. J. Haematol.* 144, 459–467 (2008).

218. Hoarau et al. TLR9 Activation Induces Normal Neutrophil Responses in a Child with IRAK-4 Deficiency: Involvement of the Direct PI3K Pathway. *J. Immunol.* 179, 4754–4765 (2007).

219. Singh et al. Impaired Priming and Activation of the Neutrophil NADPH Oxidase in Patients with IRAK4 or NEMO Deficiency. *J. Immunol.* 182, 6410–6417 (2009).

220. McDonald et al. Differential Dependencies of Monocytes and Neutrophils on Dectin-1, Dectin-2 and Complement for the Recognition of Fungal Particles in Inflammation. *PLoS One* 7, e45781 (2012).

221. Filler. Insights from human studies into the host defense against candidiasis. *Cytokine* 58, 129–132 (2012).

222. Kaplan et al. Chediak-Higashi syndrome. *Curr. Opin. Hematol.* 15, 22–29 (2008).

223. Dri et al. Increased degranulation of human myeloperoxidase- deficient polymorphonuclear leucocytes. *Br. J. Haematol.* 59, 115–125 (1985).

224. Stendahl et al. Myeloperoxidase modulates the phagocytic activity of polymorphonuclear neutrophil leukocytes. Studies with cells from a myeloperoxidase-deficient patient. *J. Clin. Invest.* 73, 366–373 (1984).

225. Hansson et al. Biosynthesis, processing, and sorting of human myeloperoxidase. *Arch. Biochem. Biophys.* 445, 214–224 (2006).

226. Tagami et al. Psoriasis and leukocyte chemotaxis. *J. Invest. Dermatol.* 88, 18–23 (1987).

227. Cassatella. Neutrophil-Derived Proteins: Selling Cytokines by the Pound. *Adv. Immunol.* 73, 369–509 (1999).

228. Tecchio et al. Neutrophil-derived cytokines: Facts beyond expression. *Front. Immunol.* 5, doi: 10.3389/fimmu.2014.00508 (2014).

229. Schön et al. Sexy again: the renaissance of neutrophils in psoriasis. *Exp. Dermatol.* 26, 305–311 (2017).

230. Clancy et al. Extracellular Neutrophil Proteases Are Efficient Regulators of IL-1, IL-33, and IL-36 Cytokine Activity but Poor Effectors of Microbial Killing. *Cell Rep.* 22, 2937–2950 (2018).

231. Sørensen et al. Human cathelicidin, hCAP-18, is processed to the antimicrobial peptide LL-37 by extracellular cleavage with proteinase 3. *Blood* 97, 3951–3959 (2001).

232. Meyer-Hoffert et al. Human leukocyte elastase induces keratinocyte proliferation by epidermal growth factor receptor activation. *J. Invest. Dermatol.* 123, 338–345 (2004).

233. Benelli et al. Neutrophils as a key cellular target for angiostatin: implications for regulation of angiogenesis and inflammation. *FASEB J.* 10.1096/fj.01-0651fje (2001).

234. Marzano et al. Mechanisms of Inflammation in Neutrophil-Mediated Skin Diseases. *Front. Immunol.* 10, doi: 10.3389/fimmu.2019.01059 (2019).

235. Miller et al. A simple salting out procedure for extracting DNA from human nucleated cells. *Nucleic Acids Res.* 16, 55404 (1988).

236. Livak et al. Analysis of relative gene expression data using real-time quantitative PCR and and the 2(-Delta Delta C(T)) Method. *Methods* 25, 402–408 (2001).

237. Abbott. Europe to map the human epigenome. *Nature* 477, 518 (2011).

238. Noguchi. Data Descriptor: FANTOM5 CAGE profiles of human and mouse samples Background & Summary. *Sci. data* 4:170112, doi: 10.1038/sdata.2017.112 (2017).

239. Kapushesky et al. Gene Expression Atlas update - Value-added database of microarray and sequencing-based functional genomics experiments. *Nucleic Acids Res.* 40, d1077–d1081 (2012).

240. Buniello et al. The NHGRI-EBI GWAS Catalog of published genome-wide association studies, targeted arrays and summary statistics 2019. *Nucleic Acids Res.* 47, d1005–d1012 (2019).

241. Zerbino et al. Ensembl 2018. *Nucleic Acids Res.* 46, d754–d761 (2018).

242. Weisburd et al. Analysis of protein-coding genetic variation in 60,706 humans. *Nature* 536, 285–291 (2016).

243. Online Mendelian Inheritance in Man, OMIM® [Online], Available at: https://omim.org/. Accessed on 19/07/2019.

244. Canela-Xandri et al. An atlas of genetic associations in UK Biobank. *Nat. Genet.* 50, 1593–1599 (2018).

245. Li et al. The Sequence Alignment/Map format and SAMtools. *Bioinformatics* 25, 2078–2079 (2009).

246. Wang et al. ANNOVAR: Functional annotation of genetic variants from high-throughput sequencing data. *Nucleic Acids Res.* 38, e164 (2010).

247. Robinson et al. Integrative genomics viewer. *Nat. Biotechnol.* 29, 24–26 (2011).

248. Sievers et al. Fast, scalable generation of high-quality protein multiple sequence alignments using Clustal Omega. *Mol. Syst. Biol.* 7, doi:10.1038/msb.2011.75 (2011).

249. Choi et al. Predicting the Functional Effect of Amino Acid Substitutions and Indels. *PLoS One* 7, e46688 (2012).

250. Kumar et al. Predicting the effects of coding non-synonymous variants on protein function using the SIFT algorithm. *Nat. Protoc.* 4, 1073–1081 (2009).

251. Adzhubei et al. Predicting Functional Effect of Human Missense Mutations Using PolyPhen-2. *Curr Protoc Hum Genet.* 2, doi:10.1002/0471142905.hg0720s76 (2015).

252. Schwarz et al. MutationTaster evaluates disease-causing potential of sequence alterations. *Nat. Methods* 7, 575–576 (2010).

253. Kircher et al. A general framework for estimating the relative pathogenicity of human genetic variants. *Nat. Genet.* 46, 310–315 (2014).

254. Yeo et al. Maximum Entropy Modeling of Short Sequence Motifs with Applications to RNA Splicing Signals. *J. Comput. Biol.* 11, 377–394 (2004).

255. Lim et al. Spliceman-A computational web server that predicts sequence

variations in pre-mRNA splicing. *Bioinformatics* 28, 1031–1032 (2012).

256. Itan et al. The human gene damage index as a gene-level approach to prioritizing exome variants. *Proc. Natl. Acad. Sci.* 112, 13615–13620 (2015).

257. Petrovski et al. Genic Intolerance to Functional Variation and the Interpretation of Personal Genomes. *PLoS Genet.* 9, e1003709 (2013).

258. Trapnell et al. TopHat: Discovering splice junctions with RNA-Seq. *Bioinformatics* 25, 1105–1111 (2009).

259. Langmead et al. Fast gapped-read alignment with Bowtie 2. *Nat. Methods* 9, 357–359 (2012).

260. Anders et al. HTSeq-A Python framework to work with high-throughput sequencing data. *Bioinformatics* 31, 166–169 (2015).

261. Tutino et al. Circulating neutrophil transcriptome may reveal intracranial aneurysm signature. *PLoS One* 13, e0191407 (2018).

262. Jiang et al. RNA sequencing from human neutrophils reveals distinct transcriptional differences associated with chronic inflammatory states. *BMC Med. Genomics* 8, 1–13 (2015).

263. RStudio Team. RStudio: Integrated Development for R. (2015).

264. Love et al. Moderated estimation of fold change and dispersion for RNA-seq data with DESeq2. *Genome Biol.* 15, doi: 10.1186/s13059-014-0550-8 (2014).

265. Benjamini et al. Controlling the False Discovery Rate: a Practical and Powerful Approach to Multiple Testing. *J. R. Stat. Soc.* B, 289 –300 (1995).

266. Li et al. Molecular signatures of antibody responses derived from a systems biology study of five human vaccines. *Nat. Immunol.* 15, 195–204 (2014).

267. Rice et al. Assessment of interferon-related biomarkers in Aicardi-Goutières

syndrome associated with mutations in TREX1, RNASEH2A, RNASEH2B, RNASEH2C, SAMHD1, and ADAR: A case-control study. *Lancet Neurol.* 12, 1159–1169 (2013).

268. Pfeffer et al. An interferon response gene signature is associated with the therapeutic response of hepatitis C patients. *PLoS One* 9, e104202 (2014).

269. Dunn. Multiple Comparisons Among Means. *J. Am. Stat. Assoc.* 56, 52–64 (1961).

270. The National Genomics Research and Healthcare Knowledgebase v5, Genomics England. doi:10.6084/m9.figshare.4530893.v5 (2019).

271. Astle et al. The Allelic Landscape of Human Blood Cell Trait Variation and Links to Common Complex Disease. *Cell* 167, 1415–1429 (2016).

272. Wan et al. Landscape and variation of RNA secondary structure across the human transcriptome. *Nature* 505, 706–709 (2014).

273. Zhang et al. regSNPs-splicing: a tool for prioritizing synonymous single-nucleotide substitution. *Hum. Genet.* 136, 1279–1289 (2017).

274. Papadaki et al. Correlation of BRCA1, TXR1 and TSP1 mRNA expression with treatment outcome to docetaxel-based first-line chemotherapy in patients with advanced/metastatic non-small-cell lung cancer. *Br. J. Cancer* 104, 316–323 (2011).

275. Lih et al. Txr1 : a transcriptional regulator of thrombospondin-1 that modulates cellular sensitivity to taxanes. *Genes Dev.* 20, 2082–2095 (2006).

276. Pontikakis et al. Predictive value of ATP7b, BRCA1, BRCA2, PARP1, UIMC1 (RAP80), HOXA9, DAXX, TXN (TRX1), THBS1 (TSP1) and PRR13 (TXR1) genes in patients with epithelial ovarian cancer who received platinum-taxane first-line therapy. *Pharmacogenomics J.* 17, 506–514 (2017).

277. Bi et al. Txr1: An important factor in oxaliplatin resistance in gastric cancer. *Med.*

Oncol. 31, doi: 10.1007/s12032-013-0807-1 (2014).

278. Papadaki et al. Tumoral expression of TXR1 and TSP1 predicts overall survival of patients with lung adenocarcinoma treated with first-line docetaxel-gemcitabine regimen. *Clin. Cancer Res.* 15, 3827–3833 (2009).

279. Chi et al. Taxol-Resistant Gene 1 (Txr1) Mediates Oxaliplatin Resistance by Inducing Autophagy in Human Nasopharyngeal Carcinoma Cells. *Med. Sci. Monit.* 25, 475–483 (2019).

280. Deretic et al. Autophagy in infection, inflammation, and immunity. *Nat Rev Immunol.* 13, 722–737 (2013).

281. Yin et al. The Therapeutic and Pathogenic Role of Autophagy in Autoimmune Diseases. *Front. Immunol.* 9, doi: 10.3389/fimmu.2018.01512 (2018).

282. Lee et al. Autophagy Negatively Regulates Keratinocyte Inflammatory Responses via Scaffolding Protein p62/SQSTM1. *J. Immunol.* 186, 1248–1258 (2011).

283. Park et al. Autophagy primes neutrophils for neutrophil extracellular trap formation during sepsis. *Am. J. Respir. Crit. Care Med.* 196, 577–589 (2017).

284. Bhattacharya et al. Autophagy Is Required for Neutrophil-Mediated Inflammation. *Cell Rep.* 12, 1731–1739 (2015).

285. Zhang et al. Thrombospondin-1 modulates vascular endothelial growth factor activity at the receptor level. *FASEB J.* 23, 3368–3376 (2009).

286. Rodríguez-Manzaneque et al. Thrombospondin-1 suppresses spontaneous tumor growth and inhibits activation of matrix metalloproteinase-9 and mobilization of vascular endothelial growth factor. *PNAS* 98, 12485–12490 (2001).

287. Smadja et al. Thrombospondin-1 Is a Plasmatic Marker of Peripheral Arterial Disease That Modulates Endothelial Progenitor Cell Angiogenic Properties. *Arterioscler. Thromb. Vasc. Biol.* 31, 551–559 (2011).

288. Heidenreich et al. Angiogenesis drives psoriasis pathogenesis. *Int. J. Exp. Pathol.* 90, 232–248 (2009).

289. Chua et al. The role of angiogenesis in the pathogenesis of psoriasis. *Autoimmunity* 42, 574–579 (2009).

290. Exome Aggregation Consortium (ExAC) [Online], Available at: http://exac.broadinstitute.org/.

291. Marchetti et al. Genetic Characterization of Myeloperoxidase Deficiency in Italy. *Hum. Mutat.* 23, 496–505 (2004).

292. Stendahl et al. Function of Granulocytes with Deficient Myeloperoxidase-Mediated Iodination in a Patient with Generalized Pustular Psoriasis. *Scand. J. Haematol.* 16, 144–153 (1976).

293. De Argila et al. Pustular psoriasis in a patient with myeloperoxidase deficiency. *Dermatology* 193, 270 (1996).

294. Nguyen et al. Myeloperoxidase deficiency manifesting as pustular candidal dermatitis. *Clin. Infect. Dis.* 24, 258–260 (1997).

295. Disdier et al. Neutrophilic dermatosis despite myeloperoxidase deficiency. *J. Am. Acad. Dermatol.* 24, 654–5 (1991).

296. Sugiura. The genetic background of generalized pustular psoriasis: IL36RN mutations and CARD14 gain-of-function variants. *J. Dermatol. Sci.* 74, 187–192 (2014).

297. Xu et al. Prevalence estimates for pyoderma gangrenosum in the United States: An age- and sex-adjusted population analysis. *J. Am. Acad. Dermatol.* In Press, https://doi.org/10.1016/j.jaad.2019.08.001 (2019).

298. Sudlow et al. UK Biobank: An Open Access Resource for Identifying the Causes of a Wide Range of Complex Diseases of Middle and Old Age. *PLoS Med.* 12,

e1001779 (2015).

299. Denny et al. PheWAS: Demonstrating the feasibility of a phenome-wide scan to discover gene-disease associations. *Bioinformatics* 26, 1205–1210 (2010).

300. DeLeo et al. A novel form of hereditary myeloperoxidase deficiency linked to endoplasmic reticulum/proteasome degradation. *J. Clin. Invest.* 101, 2900–2909 (1998).

301. Nauseef et al. Hereditary myeloperoxidase deficiency due to a missense mutation of arginine 569 to tryptophan. *J. Biol. Chem.* 269, 1212–1216 (1994).

302. Romano et al. Biochemical and Molecular Characterization of Hereditary Myeloperoxidase Deficiency. *Blood* 90, 4126–4134 (1997).

303. Liu et al. PBK/TOPK mediates promyelocyte proliferation via Nrf2-regulated cell cycle progression and apoptosis. *Oncol. Rep.* 34, 3288–3296 (2015).

304. Weissmann et al. Stimulation of Soluble Guanylate Cyclase Prevents Cigarette Smoke – induced Pulmonary Hypertension and Emphysema. 189, 1359–1373 (2014).

305. Agner. Verdoperoxidase: a ferment isolated from leukocytes. *Acta. Physiol. Scand* 2, 1– 62 (1941).

306. Klebanoff. Myeloperoxidase: contribution to the microbicidal activity of intact leukocytes. *Science (80-.).* 169, 1095–1097 (1970).

307. Klebanoff. Myeloperoxidase. *Proc. Assoc. Am. Physicians* 111, 383–389 (1999).

308. Nauseef et al. Biosynthesis and processing of myeloperoxidase--a marker for myeloid cell differentiation. *Eur. J. Haematol.* 40, 97–110 (1988).

309. Hurst et al. Leukocytic oxygen activation and microbicidal oxidative toxin. *Crit. Rev. Biochem. Mol. Biol.* 24, 271–328 (1989).

310. Nauseef. Contributions of myeloperoxidase to proinflammatory events: More than an antimicrobial system. *Int. J. Hematol.* 74, 125–133 (2001).

311. Nauseef et al. Impact of missense mutations on biosynthesis of myeloperoxidase. *Redox Rep.* 5, 197–206 (2000).

312. Kutter et al. Consequences of Total and Subtotal Myeloperoxidase Deficiency : Risk or Benefit ? *Acta Haematol.* 104, 10–15 (2000).

313. Glennon-Alty et al. Neutrophils and redox stress in the pathogenesis of autoimmune disease. *Free Radic. Biol. Med.* 125, 25–35 (2018).

314. Bassoy et al. Regulation and function of interleukin-36 cytokines. *Immunol. Rev.* 281, 169–178 (2018).

315. Wang et al. The activation and function of IL-36γ in neutrophilic inflammation in chronic rhinosinusitis. *J. Allergy Clin. Immunol.* 141, 1646–1658 (2018).

316. Foster et al. IL-36 Promotes Myeloid Cell Infiltration, Activation, and Inflammatory Activity in Skin. *J. Immunol.* 192, 6053–6061 (2014).

317. Mcnab et al. Type I interferons in infectious disease. *Nat. Publ. Gr.* 15, 87–103 (2015).

318. Asselin-Paturel et al. Production of type I interferons. *J. Exp. Med.* 202, 461–465 (2005).

319. Chamilos et al. Cytosolic sensing of extracellular self-DNA transported into monocytes by the antimicrobial peptide LL37. *Blood* 120, 3699–3707 (2012).

320. Talukder et al. Phospholipid Scramblase 1 regulates Toll-like receptor 9-mediated type I interferon production in plasmacytoid dendritic cells. *Nat. Publ. Gr.* 22, 1129–1139 (2012).

321. Zhang et al. Evidence of STAT1 phosphorylation modulated by MAPKs, MEK1 and

MSK1. *Carcinogenesis* 25, 1165–1175 (2004).

322. Swindell et al. RNA-seq analysis of IL-1B and IL-36 responses in epidermal keratinocytes identifies a shared MyD88-dependent gene signature. *Front. Immunol.* 9, doi: 10.3389/fimmu.2018.00080 (2018).

323. Calzetti et al. The importance of being "pure" neutrophils. *J. Allergy Clin. Immunol.* 139, 352–355 (2017).

324. Stephan et al. LL37:DNA complexes provide antimicrobial activity against intracellular bacteria in human macrophages. *Immunology* 148, 420–432 (2016).

325. Yamanaka et al. Neutrophils are not the dominant interleukin-17 producer in psoriasis. *J. Dermatol.* 44, e170–e171 (2017).

326. Lee-Kirsch. The Type I Interferonopathies. *Annu. Rev. Med.* 68, 297–315 (2017).

327. Rodero et al. Type I interferon – mediated monogenic autoinflammation: The type I interferonopathies, a conceptual overview. *J. Exp. Med.* 213, 2527–2538 (2016).

328. Lachmann. Periodic fever syndromes. *Best Pract. Res. Clin. Rheumatol.* 31, 596–609 (2017).

329. Tortola et al. Psoriasiform dermatitis is driven by IL-36-mediated DC-keratinocyte crosstalk. *J. Clin. Invest.* 122, 3965–3976 (2012).

330. Blumberg et al. IL-1RL2 and Its Ligands Contribute to the Cytokine Network in Psoriasis. *J. Immunol.* 185, 4354–4362 (2010).

331. Blumberg et al. Opposing activities of two novel members of the IL-1 ligand family regulate skin inflammation. *J. Exp. Med.* 204, 2603–2614 (2007).

332. Carrier et al. Inter-regulation of Th17 cytokines and the IL-36 cytokines in vitro and in vivo: Implications in psoriasis pathogenesis. *J. Invest. Dermatol.* 131, 2428–

2437 (2011).

333. Furue et al. Highlighting interleukin-36 signalling in plaque psoriasis and pustular psoriasis. *Acta Derm. Venereol.* 98, 5–13 (2018).

334. Zhou et al. Transcriptional control of the human plasma membrane phospholipid scramblase 1 gene is mediated by interferon-a. *Blood* 95, 2593–2600 (2000).

335. Dong et al. Phospholipid Scramblase 1 Potentiates the Antiviral Activity of Interferon. *J. Virol.* 78, 8983–8993 (2004).

336. Kodigepalli et al. Roles and regulation of phospholipid scramblases. *FEBS Lett.* 589, 3–14 (2015).

337. Shah et al. Real-world burden of comorbidities in US patients with psoriasis. *J. Am. Acad. Dermatol.* 3, e000588 (2017).

338. Reich. The concept of psoriasis as a systemic inflammation: Implications for disease management. *J. Eur. Acad. Dermatology Venereol.* 26, (Suppl. 2), 3-11 (2012).

339. König et al. Familial chilblain lupus due to a gain-of-function mutation in STING. *Ann. Rheum. Dis.* 76, 468–472 (2017).

340. Wilson et al. Blockade of Chronic Type I Interferon Signaling to Control Persistent LCMV Infection. *Science* 340, 202–207 (2013).

341. Lauwerys et al. Type I interferon blockade in systemic lupus erythematosus: Where do we stand? *Rheumatology (Oxford).* 53, 1369–1376 (2014).

342. Mathian et al. Targeting interferons in systemic lupus erythematosus: Current and future prospects. *Drugs* 75, 835–846 (2015).

343. Furie et al. Anifrolumab, an Anti–Interferon-α Receptor Monoclonal Antibody, in Moderate-to-Severe Systemic Lupus Erythematosus. *Arthritis Rheumatol.* 69,

376–386 (2017).

344. Kalunian et al. A phase II study of the efficacy and safety of rontalizumab (rhuMAb interferon-α) in patients with systemic lupus erythematosus (ROSE). *Ann. Rheum. Dis.* 75, 196–202 (2015).

345. Khamashta et al. Sifalimumab, an anti-interferon-α monoclonal antibody, in moderate to severe systemic lupus erythematosus: A randomised, double-blind, placebo-controlled study. *Ann. Rheum. Dis.* 75, 1909–1916 (2016).

346. Li et al. Transcriptome Analysis of Psoriasis in a Large Case–Control Sample: RNA-Seq Provides Insights into Disease Mechanisms. *J. Invest. Dermatol.* 134, 1828–1838 (2014).

347. Bissonnette et al. A randomized, double-blind, placebo-controlled, phase I study of MEDI-545, an anti-interferon-alfa monoclonal antibody, in subjects with chronic psoriasis. *J. Am. Acad. Dermatol.* 62, 427–436 (2010).

348. Mylonas et al. Psoriasis: Classical vs. Paradoxical. The Yin-Yang of TNF and Type I Interferon. *Front. Immunol.* 9, doi: 10.3389/fimmu.2018.0274 (2018).

349. European Rare And Severe Psoriasis Expert Network [Online], Available at: http://eraspen.eu/.

350. Landrum et al. ClinVar: Public archive of relationships among sequence variation and human phenotype. *Nucleic Acids Res.* 42, d980–d985 (2014).

351. Sobreira et al. GeneMatcher: A Matching Tool for Connecting Investigators with an Interest in the Same Gene. *Hum. Mutat.* 36, 928–930 (2015).

352. Boutet et al. Distinct expression of interleukin (IL)-36α, β and γ, their antagonist IL-36Ra and IL-38 in psoriasis, rheumatoid arthritis and Crohn's disease. *Clin. Exp. Immunol.* 184, 159–173 (2016).

353. Wright et al. Interferon gene expression signature in rheumatoid arthritis

neutrophils correlates with a good response to TNFi therapy. *Rheumatology (Oxford).* 54, 188–193 (2014).

354. Boutet et al. SAT0024 IL-36 axis is an emerging therapeutic target in psoriatic arthritis synovial tissue. *Ann Rheum Dis* 77, 885 (2018).

355. Mai et al. Increased serum IL-36α and IL-36γ levels in patients with systemic lupus erythematosus: Association with disease activity and arthritis. *Int. Immunopharmacol.* 58, 103–108 (2018).

356. Nauseef et al. Neutrophils at work. *Nat. Immunol.* 15, 602–611 (2014).

357. Zhang et al. Neutrophil ageing is regulated by the microbiome. *Nature* 525, 528–532 (2015).

358. Hacbarth et al. Low density neutrophils in patients with systemic lupus erythematosus, rheumatoid arthritis, and acute rheumatic fever. *Arthritis Rheum.* 29, 1334–1342 (1986).

359. Sagiv et al. Phenotypic diversity and plasticity in circulating neutrophil subpopulations in cancer. *Cell Rep.* 10, 562–573 (2015).

360. Denny et al. A Distinct Subset of Proinflammatory Neutrophils Isolated from Patients with Systemic Lupus Erythematosus Induces Vascular Damage and Synthesizes Type I IFNs. *J. Immunol.* 184, 3284–3297 (2010).

361. Martinelli et al. Induction of Genes Mediating Interferon-dependent Extracellular Trap Formation during Neutrophil Differentiation. *J. Biol. Chem.* 279, 44123–44132 (2004).

362. Villanueva et al. Netting Neutrophils Induce Endothelial Damage, Infiltrate Tissues, and Expose Immunostimulatory Molecules in Systemic Lupus Erythematosus. *J. Immunol.* 187, 538–552 (2011).

363. Teague et al. Neutrophil Subsets, Platelets, and Vascular Disease in Psoriasis. *JACC*

Basic Transl Sci. 4, 1–14 (2019).

364. Wright et al. Neutrophil biomarkers predict response to therapy with tumor necrosis factor inhibitors in rheumatoid arthritis. *J. Leukoc. Biol.* 101, 785–795 (2017).

365. Eulenberg-Gustavus et al. Gene silencing and a novel monoallelic expression pattern in distinct CD177 neutrophil subsets. *J. Exp. Med.* 214, 2089–2101 (2017).

366. Döhrmann et al. Conquering Neutrophils. *PLoS Pathog.* 12, e1005682 (2016).

367. Yaseen et al. Antimicrobial activity of HL-60 cells compared to primary blood-derived neutrophils against Staphylococcus aureus. *J. Negat. Results Biomed.* 16, doi: 10.1186/s12952-017-0067-2 (2017).

368. Stolfa et al. Using CRISPR-Cas9 to quantify the contributions of O-glycans, N-glycans and Glycosphingolipids to human leukocyte-endothelium adhesion. *Sci. Rep.* 6:30392, doi: 10.1038/srep30392 (2016).

369. Nasri et al. CRISPR/Cas9 mediated ELANE knockout enables neutrophilic maturation of primary hematopoietic stem and progenitor cells and induced pluripotent stem cells of severe congenital neutropenia patients. *Haematologica* doi: 10.3324/haematol.2019.221804 (2019).

370. Cullere et al. Neutrophil-selective CD18 silencing using RNA interference in vivo. *Blood* 111, 3591–3598 (2008).

371. Wrona et al. CRISPR/Cas9-generated p47 phox -deficient cell line for Chronic Granulomatous Disease gene therapy vector development. *Sci. Rep.* 7:44187, doi: 10.1038/srep44187 (2017).

372. Zhou et al. Neutrophil-specific knockout demonstrates a role for mitochondria in regulating neutrophil motility in zebrafish. *Dis. Model. Mech.* 11, doi: 10.1242/dmm.033027 (2018).

373. Makaryan et al. CRISPR/Cas9 Knock-in HL60 Cells Closely Simulate Cellular and Functional Abnormalities of ELANE associated Neutropenia; Phenotype Rescue with MK-0339 Neutrophil Elastase Inhibitor. *Blood* 132, https://doi.org/10.1182/blood-2018-99-113054 (2018).

374. Basit et al. shRNA-Induced Gene Knockdown In Vivo to Investigate Neutrophil Function. *Methods Mol. Biol.* 1407, 169–177 (2016).

375. Mestas et al. Of Mice and Not Men: Differences between Mouse and Human Immunology. *J. Immunol.* 172, 2731–2738 (2004).

376. An et al. Marked reduction of LL-37/hCAP-18, an antimicrobial peptide, in patients with acute myeloid leukemia. *Int. J. Hematol.* 81, 45–47 (2005).

377. Nordenfelt et al. Phagocytosis of streptococcus pyogenes by all-trans retinoic acid-differentiated HL-60 cells: Roles of azurophilic granules and NADPH oxidase. *PLoS One* 4, e7363 (2009).

378. Herwig et al. Distinct temporal patterns of defensin mRNA regulation during drug-induced differentiation of human myeloid leukemia cells. *Blood* 87, 350–364 (1996).

Appendix I: PLUM Case Report Form

VISIT DATE		Participant ID	

PLUM Case Report Form

REGISTRATION

Participant Name	
NHS Number	
Date of birth (dd/mm/yyyy)	/ /
Date of consent (dd/mm/yyyy)	/ /

Has consent also been given for:

	Yes	No
Recall		
Skin microbiopsies		

DEMOGRAPHICS

Sex		Male
		Female

Patient's ethnic group		White
		Asian or Asian British (Indian Subcontinent)
		Black or Black British
		Chinese, Japanese, Korean, Indochinese
		Mixed race
		Other
If "Other" please provide details		
Country of Origin		

VISIT DATE		Participant ID	

HISTORY

CLINICAL DIAGNOSIS

More than one may apply

	Yes	No	Date of onset	Date diagnosed by a dermatologist
Generalised pustular psoriasis				
Palmo-plantar pustulosis				
Acrodermatitis continua of Hallopeau				
Subacute annular pustular psoriasis				
Plaque psoriasis with pustulation within plaques				
Palmoplantar psoriasis with pustulation				
Acute generalised exanthematous pustulosis				
Chronic plaque psoriasis				
Flexural/intertriginous				
Seborrhoeic psoriasis				
Scalp psoriasis				
Psoriasis of palms/soles (non-pustular)				
Nail involvement				
Fissured tongue				
Guttate psoriasis				
Unstable psoriasis				
Psoriatic arthritis				
Reactive arthritis				
Other				
If other please provide details:				

Phenotype completed by (clinician name and signature)	

VISIT DATE		Participant ID	

FAMILY HISTORY:

Does the participant have any family history of the following?

	Yes	No	Affected relative(s)
Plaque-type psoriasis			
Pustular psoriasis			
	Yes	**No**	**Affected relative(s)**
Other psoriasis:			

Information on parental relatedness can really help genetic studies particularly in rare diseases such as pustular psoriasis but is a sensitive topic. The next question should be addressed carefully.

Phrases such as: "Are your parents related (except by marriage)?" "Are there any surnames or maiden names in common in your family?" and "Did your parents have the same surname before they were married?" may be helpful.

Are the participants' parents related to each other?		Have not asked
		Yes
		No
		Participant doesn't know
If "Yes" please describe relatedness (e.g. first cousins)		

MEDICAL HISTORY

CO-MORBIDITIES:

Does the participant have any co-morbidities? Please provide details

Co-morbidity	Year of onset

VISIT DATE		Participant ID	

TREATMENT HISTORY

Has the participant ever been treated with the following systemic therapies and what was its effect on the participants' pustular psoriasis during last use, if any?

Please provide details of the **most recent period of use including current**

	Start Date	Freq.	Dose	First Biologic?	End Date	Reason for stopping	Drug route
Etanercept							
Infliximab							
Adalimumab							
Ustekinumab							
Secukinumab							
Ixekizumab							
UVB/PUVA							
Acitretin							
Ciclosporin							
Methotrexate							

Is the participant **currently** using any topical therapies?

	Topical	Start date
1		
2		
3		
4		
5		
6		

VISIT DATE		Participant ID	

CONCOMITANT MEDICATIONS

Please list any **current** concomitant medication

Medication prescribed	Indication	Dose	Freq.	Date Started

COURSE of DISEASE

What best describes the participant's current pustular psoriasis?

	Yes	No
Persistent (ie >3 months)		
Relapsing remitting		
Single flare		

FLARES

If disease is relapsing:

Average number of flares per year	
Nature of flares (e.g generalised pustular)	
Date of last flare	

VISIT DATE		Participant ID	

Do any of the below apply during a **disease flare**? If yes, please provide the **maximum ever recorded** values if available.

	Yes	No	Not applicable	Unknown
Malaise/fatigue				
Increased CRP				
If yes, max CRP:				
Increased blood count				
If yes, max Leukocytes:			**max Neutrophils:**	
Fever				
If yes, max temperature:				

For all participants, does their pustular psoriasis get worse with any of the following:

	Yes	No	Not applicable	Unknown
Alcohol intake				
Episodes of stress				
Pregnancy				
Viral infection				
Streptococcal infection/cough/sore throat/fever				
If yes to strep infection was it confirmed by ASOT/throat swab?				
Drug (please name):				
Other (please detail):				

VISIT DATE		Participant ID	

CLINICAL ASSESSMENTS

Date assessed	/ /
Weight (kg)	
Height (cm)	

	Yes	No	Previously	Details
Smoker?				

CURRENT DISEASE SEVERITY

Body Surface Area	
DLQI	
PGA	
PASI score	
ppPASI (if applicable)	

LOCATION OF PUSTULES

(as assessed and currently visible)

	Yes	No
Head/neck		
Trunk		
Upper limbs		
Lower limbs		
Flexural areas		

VISIT DATE		Participant ID	

	Yes	No
Oral mucosa		
Palms/soles		
Nail apparatus		
Distal phalanx		
Subungual hyperkeratosis		
Permanent nail loss		
Number of digits involved		

Are any of the following available?

	Yes	No	Confirming diagnosis? Lesional? Please provide details
Clinical photos			
Histology			
Histology report			
Histology block			

[continued on next page]

VISIT DATE		Participant ID	

BLOOD SAMPLES

	Yes	No	Date taken
DNA (8ml) PURPLE top			
RNA (3ml) BLUE Tempus			
Plasma (5ml) PURPLE top			
Neutrophils (5ml) PURPLE top			
FBC			

Please phone Marta when blood samples have been collected – Neutrophils are TIME CRITICAL

COMPLETED BY

Signed	
Print name	
Date	

[End of document]

Appendix II: Table of all PCR and real-time PCR primers

Target	Primer ID	Sequence (5' to 3')	Annealing T (°C)	Application
GLI3 Exon 15	GLI3 Ex15 F	CCAGCAGTACCGCCTCAA	62	PCR and Sanger sequencing
	GLI3 Ex15 R	CCGCGTGTAATTCTGAAGCA		
ITGB6 Exon 11	ITGB6 Ex11 F	CCCCTCAAATCTGCAAGTGT	62	PCR and Sanger sequencing
	ITGB6 Ex11 R	TGGAGACCAAACCAGCAAAT		
MAN2B2 Exon 18	MAN2B2 Ex18 F	GAGTTCGTGGTGTGTCTGC	64	PCR and Sanger sequencing
	MAN2B2 Ex18 R	GTTCAGAGTAGGAAAGCAGCC		
MPO Exon 1	MPO Ex1 F	CTTCCTCTACCTCACCCCAC	62	PCR and Sanger sequencing
	MPO Ex1 R	CTATCAGGCCCCAGAGCTAG		
MPO Exon 2	MPO Ex2 F	TTCCTAGCTCTGGGGCCT	62	PCR and Sanger sequencing
	MPO Ex2 R	CCTCTCCCACCTTCAAGCT		
MPO Exon 3	MPO Ex3 F	CAAAGCCTTGCCTCTGTCTG	62	PCR and Sanger sequencing
	MPO Ex3 R	TGGAGGAAGAAGTTGAGGGG		
MPO Exon 4-5	MPO Ex4-5 F	CCCCTCAACTTCTTCCTCCA	62	PCR and Sanger sequencing
	MPO Ex4-5 R	TCAGCTGATCAGTGGGGAAG		

MPO Exon 6	MPO Ex6 F	GCCAGCTGATCTCCGTGT	62	PCR and Sanger sequencing
	MPO Ex6 R	CAGCGTCTGGGAAAGGAAAC		
MPO Exon 7	MPO Ex7 F	CTGCTCATTAACCCTGCACC	62	PCR and Sanger sequencing
	MPO Ex7 R	CCACAAGCTGCTCACAAACA		
MPO Exon 8	MPO Ex8 F	GGGGTTTCAGTGGAGCAAAT	62	PCR and Sanger sequencing
	MPO Ex8 R	TCAACCCTCCCAACACCAAT		
MPO Exon 9	MPO Ex9 F	CCAAGAGCAGGCAGAGACT	64	PCR and Sanger sequencing
	MPO Ex9 R	AGGCTAGAGAGTCAGACCAGA		
MPO Exon 10	MPO Ex10 F	TCTCGAATCCTCCTGACCCT	64	PCR and Sanger sequencing
	MPO Ex10 R	TCTAATATGCTTTGGAGAGGGC		
MPO Exon 11	MPO Ex11 F	TCTCCAGTGACCTCCCCA	62	PCR and Sanger sequencing
	MPO Ex11 R	AGGAGGAAATTTGGGCTCCA		
MPO Exon 12	MPO Ex12 F	ATATCCTGGGAGCAGCACAA	62	PCR and Sanger sequencing
	MPO Ex12 R	CATTTTCTCAGCTGCACCCA		
PITPNM3 Exon 8	PITPNM3 Ex8 F	ATGAAGGGGTTGGTTTGTGC	64	PCR and Sanger sequencing
	PITPNM3 Ex8 R	AGTGCTTATCTATGGGCCCC		

PRR13 Exon 2	PRR13 Ex2 F	CTGTGGGGTGGAAGACGTTA	62	PCR and Sanger sequencing
	PRR13 Ex2 R	GCACTGGTCAGCTCTAGACT		
PRR13 Exon 3	PRR13 Ex3 F	TGTCTCCCCTACCCTCCATT	62	PCR and Sanger sequencing
	PRR13 Ex3 R	ATTGTCATCCCTCACGTCCA		
PRR13 Exon 4	PRR13 Ex4 F	TCAAGACTCCTGACCTTCTTAG	62	PCR and Sanger sequencing
	PRR13 Ex4 R	CCATGGCAATCCTCTTCCCA		
PTCH1 Exon 14	PTCH1 Ex14 F	GTCAGAGCTGTGTAAAATGGGT	64	PCR and Sanger sequencing
	PTCH1 Ex14 R	CTGATGAACTCCAAAGGTTCTGT		
SDK1 Exon 18	SDK1 Ex18 F	ACACTTCCTCGGTCTCAGTG	64	PCR and Sanger sequencing
	SDK1 Ex18 R	CAAGGTCAAGACGCCCTGTA		
SVIL Exon 18	SVIL Ex18 F	TCACTCATGAAATGCTGCAGG	64	PCR and Sanger sequencing
	SVIL Ex18 F	ATGGACACACACACACTGAC		
TMEM184A Exon 9	TMEM184A Ex9 F	GATGGTGGGGCTCATACACT	62	PCR and Sanger sequencing
	TMEM184A Ex9 F	CTGGGTCCCTACAGCACTG		
IFI6	IFI6 qF	CCATCTATCAGCAGGCTCCG	60	Real time PCR
	IFI6 qR	TTTCTTACCTGCCTCCACCC		

IFIT3	IFIT3 qF	GCACAGACCTAACAGCACCC	60	Real time PCR
	IFIT3 qR	TTGGTGACCTCACTCATGATGG		
IFITM3	IFITM3 qF	TCGCCTACTCCGTGAAGTCTA	60	Real time PCR
	IFITM3 qR	CACTGGGATGACGATGAGCA		
IL8	IL8 qF	TTGGCAGCCTTCCTGATTTC	60	Real time PCR
	IL8 qR	AACTTCTCCACAACCCTCT		
OASL	OASL qF	GTACCAGCAGAGGGCACG	60	Real time PCR
	OASL qR	GGAACCTGGAAGGACAGACG		
PLSCR1	PLSCR1 qF	CGGCAGCCAGAGAACTGTTTTA	60	Real time PCR
	PLSCR1 qR	AGGAGGATACCCAACTGGCA		

Appendix III: Stepwise filtering of whole-exome sequence profiles from family 8GPP

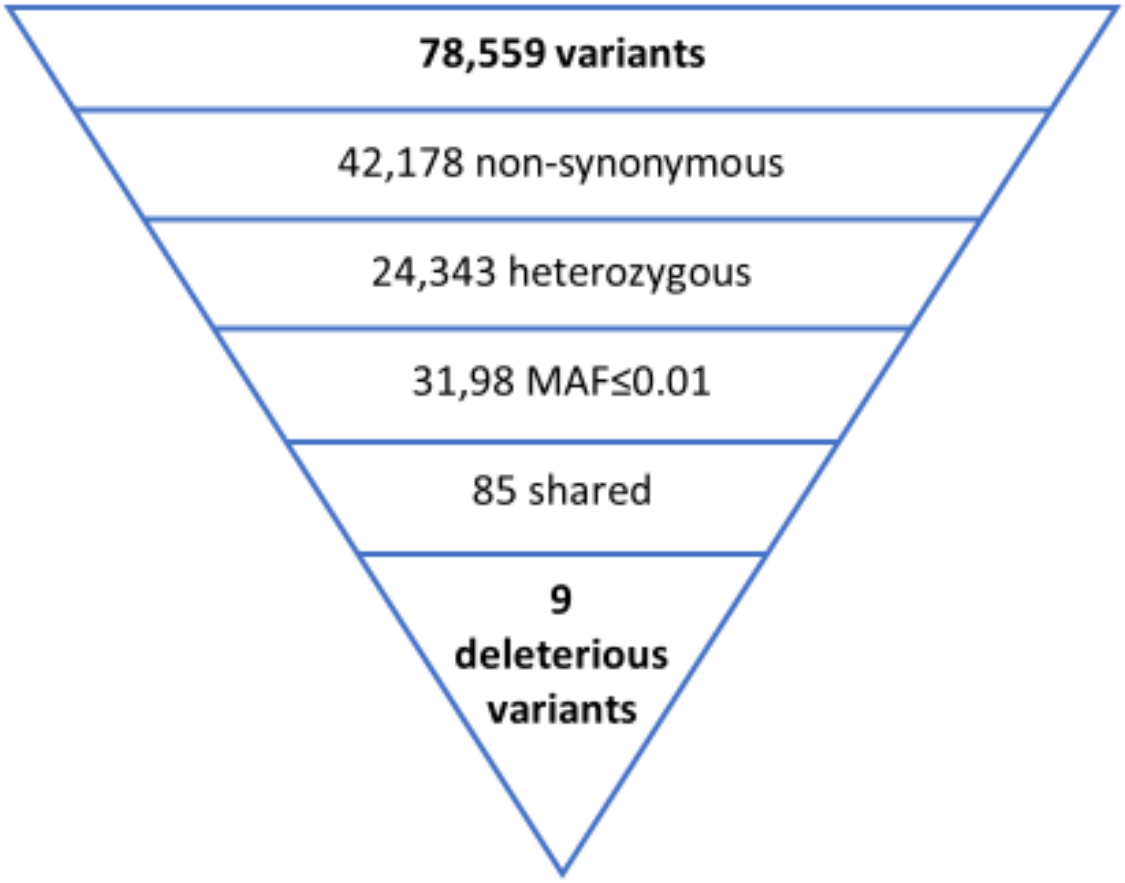

Appendix IV: Stepwise filtering of whole-exome sequence profiles from the 19 unrelated GPP cases

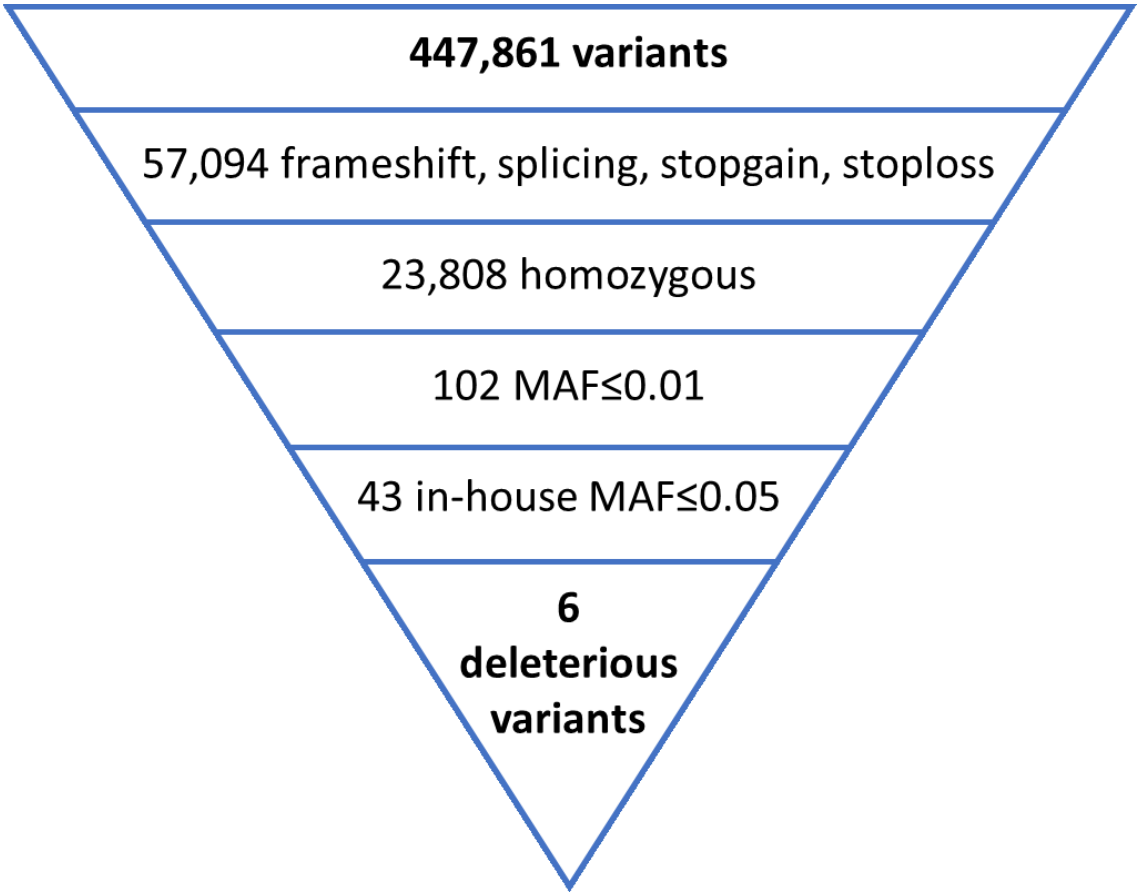

Appendix V: Differentially expressed genes detected in the neutrophils of the 2031-2A>C homozygous GPP patient

Symbol	log2FoldChange	FDR
PBK	5.044394	1.7E-155
GPR33	5.044394	1.7E-155
COL14A1	4.78136	1.2E-105
GUCY1A2	4.459432	3.77E-65
SLC10A4	4.459432	3.77E-65
DEFB1	4.459432	3.77E-65
DPP10	4.459432	3.77E-65
PURG	4.459432	3.77E-65
CALCB	4.459432	3.77E-65
DUOXA1	4.459432	3.77E-65
BDKRB2	4.459432	3.77E-65
DEFA3	4.430254	2.58E-62
METTL7B	3.944858	5.82E-29
NNMT	3.944858	5.82E-29
SLC22A16	3.718818	8.89E-20
CES1	3.702288	3.24E-19
USP2	3.459432	2.4E-12
C11orf45	3.459432	2.4E-12
CLEC3B	3.459432	2.4E-12
MAGEL2	3.459432	2.4E-12
FRAS1	3.459432	2.4E-12
MUC12	3.459432	2.4E-12
SLIT3	3.459432	2.4E-12
ALPK2	3.459432	2.4E-12
HCN4	3.459432	2.4E-12
IGFBP5	3.459432	2.4E-12
C9orf47	3.459432	2.4E-12
GLRA3	3.459432	2.4E-12
TERT	3.459432	2.4E-12
CLDN1	3.459432	2.4E-12
PLEKHS1	3.459432	2.4E-12
MISP	3.459432	2.4E-12
KSR2	3.459432	2.4E-12
PRSS16	3.459432	2.4E-12
LRRC66	3.459432	2.4E-12
SLC26A7	3.459432	2.4E-12
MUSK	3.459432	2.4E-12
PDYN	3.459432	2.4E-12
SCG2	3.459432	2.4E-12
MEPE	3.459432	2.4E-12
SLC7A13	3.459432	2.4E-12
ZNF474	3.459432	2.4E-12
SHC2	3.459432	2.4E-12

SUN3	3.459432	2.4E-12
EN2	3.459432	2.4E-12
ATP4B	3.459432	2.4E-12
BMP4	3.459432	2.4E-12
RASGEF1C	3.459432	2.4E-12
ACTL6B	3.459432	2.4E-12
SLC22A3	3.459432	2.4E-12
KLRC2	3.459432	2.4E-12
CXCL13	3.459432	2.4E-12
VCX	3.459432	2.4E-12
OR5K2	3.459432	2.4E-12
KITLG	3.459432	2.4E-12
TTC36	3.459432	2.4E-12
IFNB1	3.459432	2.4E-12
DPPA5	3.459432	2.4E-12
C6orf99	3.459432	2.4E-12
SLC10A6	3.459432	2.4E-12
LHB	3.459432	2.4E-12
CXCL11	3.459432	2.4E-12
WFDC2	3.459432	2.4E-12
CAPN11	3.459432	2.4E-12
XAGE3	3.459432	2.4E-12
MLN	3.459432	2.4E-12
IGFL3	3.459432	2.4E-12
SPINK1	3.459432	2.4E-12
HIST1H2BM	3.459432	2.4E-12
SLC22A31	3.459432	2.4E-12
DIRAS2	3.459432	2.4E-12
PGA3	3.459432	2.4E-12
FIGNL2	3.459431	2.4E-12
BCAR1	3.211504	1.93E-07
CRYGD	3.169925	8.83E-07
AZU1	3.163082	1.12E-06
NRP1	3.137504	2.72E-06
ELANE	3.090839	1.25E-05
PXMP2	3.044394	5.17E-05
LURAP1L	3.044394	5.17E-05
ABCA8	2.974005	0.000371
TPSD1	2.974005	0.000371
EDA2R	2.974005	0.000371
CABP1	2.974005	0.000371
GPR15	2.954196	0.000623
BUB1B	2.888275	0.003144
PTCRA	2.874469	0.004326
C2orf80	2.874469	0.004326
MARCH2	2.874469	0.004326
NDNF	2.874469	0.004326
STEAP1B	2.874469	0.004326

OR52I2	2.874469	0.004326
GRK1	2.874469	0.004326
SMIM10	2.78136	0.031601
CTSG	2.779864	0.032555

Appendix VI: 231 genes differentially expressed in neutrophils from 8 GPP vs. 11 healthy controls

Symbol	log2FoldChange	P value	FDR
CYP26B1	9.172412148	6.27E-06	0.002025496
OTOF	5.119228745	4.50E-08	0.000137377
OAS2	3.971808127	3.38E-07	0.000375607
SIGLEC1	3.947811981	2.34E-05	0.004503355
USP18	3.841053847	5.04E-06	0.001709095
RSAD2	3.663108849	2.90E-07	0.000354599
IFI44L	3.563097345	6.66E-07	0.000488218
OAS1	3.523123021	3.76E-06	0.001444593
OAS3	3.41407656	2.19E-06	0.001028476
GBP1P1	3.328636236	2.35E-07	0.000318987
LY6E	3.308108285	3.40E-06	0.001434257
SPATS2L	3.271775597	9.52E-07	0.000567181
IFI44	3.21792139	7.32E-07	0.000488218
RTP4	3.105936328	4.81E-07	0.000419908
CMPK2	3.055439406	2.77E-06	0.001208097
ISG15	3.028183431	7.59E-07	0.000488218
EPSTI1	3.003631939	9.98E-06	0.002836422
SEPT4	2.944237993	2.08E-08	8.48E-05
FSTL4	2.764056435	0.000400287	0.026431925
AGRN	2.755875361	4.16E-05	0.006279419
DDX60	2.538926661	4.51E-06	0.001666504
MT2A	2.514422494	5.75E-08	0.000140394
IFI6	2.507376228	1.99E-05	0.004267589
NRIR	2.458692631	5.80E-05	0.00762578
RMI2	2.412486832	2.11E-07	0.000318987
IFIT1	2.341066217	8.61E-05	0.009744028
LAMP3	2.310196414	0.000298783	0.02212082
HERC5	2.243206042	3.41E-05	0.005449044
XAF1	2.21414774	3.34E-05	0.005445064
MTRNR2L8	2.074454003	0.00032389	0.023274373
SERPING1	2.054662518	1.38E-06	0.000702275
MX1	2.008222687	0.00063619	0.035649963
BATF2	2.002474113	8.48E-06	0.002590667
OASL	1.955295475	6.84E-07	0.000488218
CARD17	1.89526733	2.60E-05	0.00472263
ATF3	1.87642956	1.84E-05	0.004008361
TRIM22	1.837133962	1.09E-07	0.000222672
PNPT1	1.827403125	0.000146834	0.014235937
ZNF496	1.767046002	6.03E-05	0.007840177

SOCS1	1.762221129	6.50E-06	0.002035366
DHX58	1.745220861	8.79E-05	0.009765761
TIMM10	1.737338305	0.00038316	0.026043408
IFIT3	1.73483868	6.51E-05	0.008112721
FRMD3	1.711113474	6.39E-05	0.008047376
GBP5	1.680531557	2.37E-05	0.004503355
BST2	1.619525415	2.19E-05	0.004369047
GBP1	1.611339308	1.15E-05	0.003096475
HERC6	1.597937324	0.000179746	0.016265027
PLSCR1	1.544410476	2.40E-05	0.004503355
CASP7	1.534666214	8.90E-05	0.009800224
LHFPL2	1.523816094	4.64E-06	0.001666504
TFEC	1.510789858	0.000357379	0.02500654
MOV10	1.502862096	1.17E-05	0.003096475
FGF13	1.502339718	0.000287129	0.02178617
PDCD1LG2	1.498961218	0.000514936	0.030987477
KCNH3	1.49789933	0.00051133	0.030922786
IFIT5	1.492253759	0.000198352	0.017278784
PARP12	1.476740184	0.0001245	0.012569356
RSPH9	1.470266601	0.000132769	0.013079894
GADD45A	1.458655659	0.000609295	0.034840457
EXOC3L1	1.458276278	0.000362168	0.025137738
IFI35	1.443433488	2.67E-05	0.00472263
GPR84	1.441671885	0.000999832	0.04644086
FBXO6	1.440837799	1.31E-06	0.000698126
PLVAP	1.439279424	0.00065625	0.036150616
GYG1	1.433990899	0.000893309	0.043625102
ANKRD22	1.433983216	4.50E-07	0.000419908
PPM1K	1.427949724	0.000732806	0.039091511
OLAH	1.405226179	0.000774575	0.040675997
LINC00968	1.399872758	8.08E-05	0.0093955
CD2AP	1.397288889	2.15E-05	0.004369047
APOL6	1.396735209	4.14E-05	0.006279419
CD274	1.372119138	2.50E-05	0.004621926
GBP6	1.365253514	2.06E-05	0.004337684
SPATC1	1.354692662	0.000868531	0.043120296
IFIT2	1.344909309	0.000275355	0.021289443
P2RY14	1.326831635	0.000113672	0.012041279
PARP10	1.325405223	3.78E-06	0.001444593
ZBP1	1.32482501	9.29E-06	0.002766958
FCGR1A	1.317629758	4.49E-05	0.006399585
ANXA2R	1.311304513	1.02E-06	0.000567181
SAMD9L	1.309580254	2.98E-05	0.00505346
KIAA0895L	1.302366152	0.00050729	0.030846181

CMAHP	1.280619965	0.000170584	0.015551166
STAT2	1.279120204	7.63E-05	0.009067873
TMEM62	1.278234659	1.39E-05	0.003276561
AIM2	1.272582865	0.000126204	0.012636938
GCH1	1.268234096	3.52E-05	0.005449044
UBE2L6	1.267529814	1.60E-05	0.003564108
AANAT	1.266669793	3.50E-05	0.005449044
KPTN	1.252416073	7.44E-05	0.009067873
PML	1.220691205	0.000280986	0.021588219
GRAMD1B	1.213561027	4.43E-05	0.006399585
EIF2AK2	1.212456821	0.000120418	0.012466353
RNF144A	1.2106128	0.000284576	0.021727356
SP140	1.20790437	0.00010958	0.011809536
LILRA5	1.200638097	0.000217577	0.018330454
TLDC2	1.192035868	0.000313643	0.022942887
CMTR1	1.185436073	0.000486149	0.03050535
EFCAB2	1.18052117	2.88E-05	0.004960046
FRMD4B	1.167068583	0.000823488	0.041840852
PCGF5	1.165649202	5.81E-05	0.00762578
C5	1.162588266	1.31E-05	0.003248412
SYNPO2	1.130480611	0.000557197	0.032882701
CARD14	1.127423802	0.000397318	0.02637844
RNF213	1.120286036	0.000210641	0.018090676
EXT1	1.092510749	1.12E-05	0.003096475
SAMHD1	1.088511452	0.000496936	0.03050535
ASPHD2	1.077181925	8.54E-05	0.009744028
ZCCHC2	1.071297761	0.00111444	0.049868115
SSPN	1.052259363	8.45E-05	0.009739882
ANXA5	1.051622007	0.000245605	0.019609877
DDX58	1.047786872	0.000229388	0.018806751
STOML1	1.047490268	0.000548996	0.032555971
TNFAIP6	1.041869796	0.000495858	0.03050535
SPTSSA	1.038312831	0.000870785	0.043120296
VAMP5	1.038295865	0.000143683	0.014041867
IRF7	1.037956611	0.000224668	0.018544223
NT5C3A	1.037285357	1.78E-07	0.000310716
KLF4	1.023918066	0.000829156	0.041840852
RARRES3	1.012704298	0.000486544	0.03050535
CACNA1A	1.008040885	2.20E-05	0.004369047
TNFSF13B	1.003385229	0.000532886	0.0317548
SCO2	0.998373457	0.000198592	0.017278784
RHBDF2	0.991076103	1.31E-05	0.003248412
FCGR1B	0.987986558	0.000471187	0.029979297
TOR1B	0.983658892	0.000488411	0.03050535

UBE2F	0.982310352	0.000586514	0.033796465
LINC01270	0.970905226	0.000997495	0.04644086
GIMAP2	0.965919995	8.00E-05	0.009395055
NEK11	0.940478444	0.000318401	0.023152279
ODF3B	0.928607387	0.000123543	0.012569356
ZC3HAV1	0.925168614	0.000167536	0.015504698
FANCL	0.913034414	0.000254294	0.020041653
FANCA	0.912148836	0.000812271	0.041517588
MDK	0.91128109	0.001104422	0.049784564
VPS9D1	0.905923093	6.60E-05	0.008147868
CNP	0.904153596	0.000993786	0.04644086
DRAP1	0.878907907	0.000391563	0.02637844
KLHDC7B	0.877180454	1.36E-05	0.003258484
STAT1	0.869897453	0.000628592	0.035649963
CNIH4	0.869149679	0.000117527	0.01227099
VPS9D1-AS1	0.868483281	8.73E-05	0.009765761
GPR160	0.86503306	1.60E-05	0.003564108
TMSB10	0.860653865	1.33E-05	0.003248412
PARP9	0.858895586	0.000103644	0.01130458
NASP	0.857743411	2.22E-05	0.004369047
ISG20	0.840318544	2.65E-05	0.00472263
COPG2	0.838048423	0.000967808	0.045647637
NLRC5	0.836908327	1.25E-05	0.003248412
KIAA1958	0.833798743	0.000924866	0.044395601
IFI16	0.832350065	0.000373172	0.025755225
ARHGAP24	0.830986669	0.000153733	0.014446194
TDRD7	0.823932363	0.000829064	0.041840852
RBM43	0.811593154	0.000571785	0.033268441
CARD16	0.802449754	0.000528426	0.031643362
MSL3	0.795148856	0.000455724	0.029147276
IL18R1	0.784017801	0.000752002	0.039941094
EPAS1	0.778843151	0.000779788	0.040708915
SESTD1	0.773683913	0.000231977	0.018892219
DUSP3	0.769938634	5.05E-05	0.006803082
NOD1	0.751345287	0.000448603	0.028861116
SNX20	0.738685074	7.65E-05	0.009067873
EPB41L5	0.737614314	0.000122092	0.012533433
PHF11	0.736538584	0.000189075	0.016737288
OBFC1	0.729353987	0.000656961	0.036150616
STX11	0.725850843	2.02E-06	0.000989427
GIMAP4	0.709501528	0.000492613	0.03050535
PSMB9	0.705399798	0.00018206	0.016353292
TRIM69	0.702990532	6.18E-05	0.007946945
GBP2	0.697778501	4.87E-05	0.006686955

TAP1	0.694168739	0.000242001	0.019449252
LGALS3BP	0.68711756	0.000801578	0.041425218
CASP1	0.668810281	6.25E-05	0.007946945
TRIM38	0.665362102	0.000114341	0.012041279
TMEM170B	0.661466083	0.000188423	0.016737288
C18orf25	0.655366038	3.75E-07	0.000381997
PHACTR2	0.650048481	0.000997671	0.04644086
SRBD1	0.643872457	0.001078789	0.049173475
ACOT9	0.635180714	0.000322153	0.023274373
LRRC46	0.634002664	3.27E-05	0.005398871
GSTK1	0.626735822	0.000507538	0.030846181
TXN	0.625004267	0.000110207	0.011809536
AFF1	0.615612791	4.85E-05	0.006686955
SIAH2	0.596116122	9.53E-06	0.002770752
C4orf3	0.584110058	0.001004416	0.046477048
SPATA13	0.583286873	2.88E-05	0.004960046
JAG1	0.580393657	0.000394962	0.02637844
DAPP1	0.55931579	0.000337492	0.024073345
TYMP	0.558459135	0.000808486	0.041497774
HEXDC	0.553808905	0.000291449	0.021895219
RAB12	0.547963099	0.000787092	0.040915392
TCAIM	0.543945782	0.000896357	0.043625102
FAM46C	0.543479462	0.000293581	0.021895219
ERLIN1	0.542717998	0.00043665	0.028372938
CLEC2B	0.542113635	0.000382774	0.026043408
CARS2	0.536302284	4.26E-05	0.006342136
TIPARP	0.520407717	0.000922971	0.044395601
DPYD	0.513882555	4.51E-05	0.006399585
LY96	0.501502866	0.000855325	0.042822351
PDCD11	-0.5037905	0.000666236	0.036496611
SYNGAP1	-0.506270024	0.000887589	0.04354535
SLBP	-0.515947183	0.000803682	0.041425218
C2CD2L	-0.547227699	4.31E-05	0.006342136
CEP104	-0.575412769	0.000358231	0.02500654
GNPDA1	-0.593530531	0.000293944	0.021895219
MFNG	-0.59705505	0.000340921	0.024073345
DDX28	-0.613373428	0.000267114	0.020917076
SEMA6C	-0.630243096	0.000571903	0.033268441
SSBP3	-0.634790609	0.000922404	0.044395601
AGAP3	-0.675683931	0.000775827	0.040675997
NFATC3	-0.701629022	1.39E-09	8.50E-06
BOD1	-0.70236116	1.60E-05	0.003564108
OBSCN	-0.807600057	7.63E-05	0.009067873
FBXL16	-0.954345541	0.000768664	0.040649346

ZAP70	-1.043941491	0.000688563	0.03738438
P2RY10	-1.103321241	0.000634441	0.035649963
HSPG2	-1.105324054	0.000491941	0.03050535
MYCL	-1.148689702	0.000150584	0.014371374
CD5	-1.299678648	4.99E-06	0.001709095
RHPN2	-1.301153916	0.000221208	0.018508707
ESRP2	-1.331327558	3.45E-05	0.005449044
CCDC163P	-1.377483528	5.07E-05	0.006803082
FADS1	-1.438401712	3.56E-06	0.001444593
CD160	-1.452242814	0.000698563	0.037759519
CLIC3	-1.465532635	0.00093954	0.044486117
GSTM4	-1.475580157	0.000718722	0.03867799
GSTM2	-1.717932525	3.15E-05	0.005268772
MYOM2	-2.019043881	0.000418001	0.027306408
FAM3B	-3.637480697	0.000678806	0.037019155
FADS2	-3.768072503	4.43E-12	5.42E-08

PUBLICATION ARISING FROM THIS THESIS

Journal of Investigative Dermatology

Decision Letter (JID-2019-0205.R2)

From: JIDOffice@sidnet.org

To: marika.catapano@kcl.ac.uk, marta.vergnano@kcl.ac.uk, marco.romano@kcl.ac.uk, satveer.mahil@kcl.ac.uk, choonse@yahoo.co.uk, David.Burden@glasgow.ac.uk, helen.s.young@manchester.ac.uk, i.m.carr@leeds.ac.uk, h.lachmann@ucl.ac.uk, giovanna.lombardi@kcl.ac.uk, catherine.smith@kcl.ac.uk, francesca.ciccarelli@crick.ac.uk, jonathan.barker@kcl.ac.uk, francesca.capon@kcl.ac.uk

CC:

Subject: Decision: Accepted for Publication (JID-2019-0205.R2)

Body: 06-Aug-2019

RE: MS# JID-2019-0205.R2

TITLE: Interleukin-36 promotes systemic Type-I IFN responses in severe forms of psoriasis

Dear Dr. Capon:

Your manuscript has been favorably reviewed and is accepted for publication in The Journal of Investigative Dermatology. We look forward to future submissions from you and your colleagues.

YOU WILL RECEIVE AN ADDITIONAL MESSAGE FROM THE EDITORIAL OFFICE WITHIN 2 WEEKS REGARDING ANY SPECIAL REQUIREMENTS WE MAY HAVE BEFORE PUBLICATION. This may include the possibility of publishing some materials online-only, due to limited space in the Journal. Please wait for this message before submitting publication materials.

We are accepting this manuscript for publication on the condition that neither the substance of the manuscript nor the text or data in this manuscript have been published, accepted for publication, or submitted for publication elsewhere. In signing the copyright agreement, the authors agree with this condition.

Publication of this article remains at the discretion of the editor; if substantial issues (e.g., authorship disputes, failure to fulfill ethics publication requirements, etc.) arise during the publication process, the editor may withdraw acceptance.

It is the policy of the Journal that unique non-proprietary reagents described (e.g., cells, DNA, antibodies) and instruments created for surveys must be made freely available to qualified scientists. Only under this condition is the information useful to the scientific community, and only in this way can results be reproduced by other scientists.

PUBLICATION MATERIALS
Publication materials should be received within 2 weeks; any delay will result in a delay in the publication of your article. See important information below regarding publication materials.

MAKING YOUR WORK CITABLE WITHIN DAYS
JID publishes all Original Articles and Letters to the Editor four business days following the transmission of final publication materials to the publisher. The publication is a .pdf of the accepted article's text and figures, and it includes a covering page with a disclaimer, along with a watermark and headers, that identifies the article as an unedited version of a peer-reviewed manuscript that has been accepted for publication. The covering page also includes instructions on how the article should be cited. Once the copyedited, typeset, and proofed version is published online, the manuscript version of the article will be removed. Both versions bear the same digital object identifier (DOI), allowing articles to be referenced as soon as they appear online and ensuring that all references to the article will be consistent.

USING THE DOI TO CITE ARTICLES PUBLISHED AHEAD OF PRINT:
[Author(s)]. [Title]. Journal of Investigative Dermatology accepted article preview, [publication date]; doi:[DOI]

OPEN ACCESS
Authors of research articles may choose to publish their accepted articles open access (i.e., free to all readers, regardless of whether they have a subscription) online immediately upon publication. After publication materials have been transmitted to the publisher, authors will be asked whether they wish to publish the article under JID's immediate open access options. The cost of immediate open access publication is $3200 ($2600 for ESDR and SID members).

MEET THE INVESTIGATOR
JID has initiated a new Facebook feature called "Meet the Investigator", in which we hope to introduce the Dermatology community to up-and-coming investigators. We invite you to recommend one of your junior co-authors for this feature; to do so, please send your nomination by return email;

this can be brief, but a sentence or two describing how this individual will impact investigative dermatology in the future would be welcome. Please also include the nominee's email address and CV. Nominations will be reviewed by our "Meet the Investigator" Editor, and at least one profile will be selected each month.

We are delighted to publish your work in the JID.

Sincerely,

Mark C. Udey, MD, PhD
Editor
Journal of Investigative Dermatology

Editor comments:
Section/Deputy Editor: 1
Comments to the Author:
(There are no comments.)

Reviewer Comments:
Reviewer: 2

Comments to the Author
(There are no comments.)

PUBLICATION MATERIALS
The Publication Checklist (attached) contains important information about publication materials. The Editorial Office will email the submitting author within the next two weeks with a list of specific instructions for preparing the final materials for publication.

Remember that your file is not complete until the Editorial Office has received the License to Publish form completed by the CORRESPONDING AUTHOR. We also require an authorship form completed by EACH AUTHOR. All authors were sent an email containing a link to their own form. If these forms have already been submitted, they remain on file; there is no need to submit them again.

Date Sent: 06-Aug-2019

File 1: * JID-Publication-Checklist-February-2019-Final.pdf

Close Window

Interleukin-36 promotes systemic Type-I IFN responses in severe forms of psoriasis

Marika Catapano[1,11], Marta Vergnano[1,11], Marco Romano[2], Satveer K Mahil[3], Siew-Eng Choon[4], A David Burden[5], Helen S Young[6], Ian M Carr[7], Helen J Lachmann[8], Giovanna Lombardi[2], Catherine H Smith[3], Francesca D. Ciccarelli[9,10], Jonathan N Barker[3], Francesca Capon[1]*.

M. Catapano: 0000-0003-2344-6067, M. Vergnano: 0000-0003-4654-5519, M. Romano: 0000-0001-6089-5828, S. K. Mahil: 0000-0003-4692-3794, S.E. Choon: 0000-0002-7796-5746, A. D. Burden: 0000-0001-7395-9931, H. S. Young: 0000-0003-1538-445X, I. M. Carr: 0000-0001-9544-1068, H. J. Lachmann: 0000-0001-8378-2498, G. Lombardi: 0000-0003-4496-3215, C. H. Smith: 0000-0001-9918-1144, F. D. Ciccarelli: 0000-0002-9325-0900, J. N. Barker: 0000-0002-9030-183X, F. Capon: 0000-0003-2432-5793

[1]Department of Medical and Molecular Genetics, School of Basic & Medical Biosciences, King's College London, London, UK; [2]Department of Immunobiology, School of Immunology & Microbial Sciences, King's College London, London, UK; [3]St John's Institute of Dermatology; School of Basic & Medical Biosciences, King's College London, London, UK; [4]Department of Dermatology, Sultanah Aminah Hospital, Johor Bahru, Malaysia; [5]Department of Dermatology, University of Glasgow, Glasgow, UK; [6]Division of Musculoskeletal and Dermatological sciences, University of Manchester, Manchester, UK; [7]School of Medicine, University of Leeds, Leeds, UK; [8]National Amyloidosis Centre and Centre for Acute Phase Proteins, Division of Medicine, University College London, London, UK; [9]Cancer Systems Biology Laboratory, The Francis Crick Institute, London, UK; [10]School of Cancer & Pharmaceutical Sciences, King's College London, London, UK.

[11]These authors contributed equally. *Corresponding author: Francesca Capon, Department of Medical and Molecular Genetics, School of Basic and Medical Biosciences, King's College London, 9th floor Tower Wing Guy's Hospital, London SE1 9RT, United Kingdom. E-mail: francesca.capon@kcl.ac.uk; Twitter handle: @FranciCapon

Short title: An IL-36/Type I IFN axis in psoriasis

ABSTRACT

Psoriasis is an immune-mediated skin disorder associated with severe systemic co-morbidities. While IL-36 is a key disease driver, the pathogenic role of this cytokine has mainly been investigated in skin. Thus, its effects on systemic immunity and extra-cutaneous disease manifestations remain poorly understood.

To address this issue, we investigated the consequences of excessive IL-36 activity in circulating immune cells. We initially focused our attention on generalised pustular psoriasis (GPP), a clinical variant associated with pervasive up-regulation of IL-36 signalling. By undertaking blood and neutrophil RNA-sequencing, we demonstrated that affected individuals display a prominent Type-I IFN signature, which correlates with abnormal IL-36 activity. We then validated the association between IL-36 de-regulation and Type-I IFN over-expression in patients with severe psoriasis vulgaris (PsV). We also found that the activation of Type-I IFN genes was associated with extra-cutaneous morbidity, in both GPP and PsV. Finally, we undertook mechanistic experiments, demonstrating that IL-36 acts directly on plasmacytoid dendritic cells (pDCs), where it potentiates Toll-like Receptor (TLR)-9 activation and IFN-α production. This effect was mediated by the up-regulation of PLSCR1, a phospholipid scramblase mediating endosomal TLR-9 translocation.

These findings identify an IL-36/Type-I IFN axis contributing to extra-cutaneous inflammation in psoriasis.

Key words:

Generalized pustular psoriasis, psoriasis vulgaris, systemic inflammation, IL-36, Type-I IFN, PLSCR1

Abbreviations: CAPS, cryopyrin associated periodic syndrome; DEG, differentially expressed genes; FC, fold change; GPP, generalised pustular psoriasis; IFN, interferon; IL-36, interleukin-36; IL36R, IL-36 receptor; *IL36RN*: IL-36 receptor antagonist; MAPK, mitogen-activated protein kinases; pDCs, plasmacytoid dendritic cells; *PLSCR1*, Phospholipid Scramblase 1; PsV: psoriasis vulgaris; TLR- 9: Toll-like receptor- 9

INTRODUCTION

Interleukin-36α, -β and -γ (hence IL-36) are group of IL-1 family cytokines that are mainly produced by keratinocytes, monocytes and dendritic cells (Bassoy et al., 2018). IL-36 signalling plays an important role in epithelial immune homeostasis and its de-regulation has been repeatedly implicated in the pathogenesis of psoriasis vulgaris (PsV), a common and chronic, immune-mediated skin disorder (Bassoy et al., 2018).

Numerous studies have shown that IL-36 responses are elevated in PsV skin (Mahil et al., 2017, Quaranta et al., 2014, Swindell et al., 2015) where they stimulate chemokine production and amplify the effects of IL-17 signalling (Mahil et al., 2017). Animal studies have also demonstrated that IL-36 promotes the activation of dendritic cells and the polarization of T lymphocytes into Th17 cells (Tortola et al., 2012). Thus, the mechanisms whereby IL-36 contributes to cutaneous inflammation have been extensively investigated. Its effects on circulating leukocytes, however, remain poorly understood.

We and others have shown that recessive mutations of the IL-36 receptor antagonist (*IL36RN*) are associated with generalised pustular psoriasis (GPP), a disease variant characterized by severe extra-cutaneous symptoms (Marrakchi et al., 2011, Onoufriadis et al., 2011). In fact, GPP patients suffer from flares of skin pustulation that are often accompanied by systemic upset (fever, elevation of acute phase reactants and neutrophilia) (Burden and Kirby, 2016). This suggests that IL-36 signalling is likely to influence immune responses beyond skin.

Extra-cutaneous co-morbidities are also well documented in PsV, as individuals suffering from severe disease are at high risk of psoriatic arthritis, metabolic syndrome and atherosclerosis (Burden and Kirby, 2016, Fang et al., 2016, Shah et al., 2017). It has therefore been proposed that PsV is a systemic disease, manifesting with skin, joint and vascular inflammation (Davidovici et al., 2010, Reich, 2012).

In this context, we hypothesise that abnormal IL-36 signalling has extra-cutaneous effects in both GPP and PsV, driving acute systemic flares in the former and contributing to a state of chronic systemic inflammation in the latter. To explore this model, we integrated the transcription profiling of patient leukocytes with ex-vivo IL-36 stimulations. We show that IL-36 potentiates Toll-like receptor (TLR)-9 activation and enhances the production of Type-I IFN, a cytokine that contributes to systemic immunity, arthritis and atherosclerosis.

RESULTS

Expression profiling identifies a Type-I IFN signature in GPP and PsV whole-blood samples

We reasoned that GPP would represent an ideal model in which to investigate the systemic effects of IL-36, given the well-established link with *IL36RN* mutations (Marrakchi et al., 2011, Onoufriadis et al., 2011) and enhanced IL-36 activity (Johnston et al., 2016). We therefore undertook whole-blood RNA-sequencing in 9 affected individuals and 7 healthy controls (Supplementary Table S1 a). While the deconvolution of transcription profiles showed that leukocyte frequencies were comparable in cases vs. controls (Supplementary Table S1 b), differential expression analysis identified 111 genes that were over-expressed (fold change≥1.5; FDR< 0.05) in patients (Figure 1 a, Supplementary Table S2 a). As expected, genes that can be induced by IL-36 (*IL1B, PI3, VNN2, TNFAIP6, SERPINB1*) were collectively up-regulated in cases vs. controls (P=0.019) (Figure 1 b). Of note, the analysis of a publicly available PsV dataset (Wang et al., 2014) identified a moderate, but statistically significant, over-expression of the same genes in patient whole-blood (P=0.001) (Figure 1 b), suggesting that IL-36 may have systemic effects in PsV.

To further explore the biological significance of our findings, we mapped the genes up-regulated in GPP to the blood co-expression modules described by Li et al (Li et al., 2014). We found that the over-expressed genes were significantly enriched among modules related to innate immune activation (e.g. *enriched in activated dendritic cells*, FDR<0.005) and antiviral responses (e.g. *type I IFN response*; FDR<0.05) (Figure 1 c). These findings were validated by Ingenuity Pathway Analysis (IPA), which identified *interferon signalling* as the most significantly enriched pathway (FDR<5×10^{-6}) (Figure 1 d). An upstream regulator analysis also highlighted IRF7, STAT1 and STAT3 as the transcriptional activators that are most strongly associated with gene over-expression (FDR<10^{-10} for all) (Figure 1 e, Supplementary Table S2 c). This is of interest since proteins are critical mediators of IFN signal transduction and IFN-α production by pDCs (Honda et al., 2005).

Finally, the analysis of two publicly available datasets (Liu et al., 2012, Rodero et al., 2017) demonstrated a significant overlap (P<10^{-10}) between the genes that are up-regulated in GPP and those that are over-expressed in autoinflammatory syndromes caused by abnormal activation of Type-I IFN

responses (Figure 1 f). Of note, no overlap was found with the up-regulated genes detected in cryopyrin associated periodic syndrome (CAPS), a disease caused by excessive IL-1 activity, which was analysed as a negative control (Supplementary Figure S1). Thus, the presence of a Type-I IFN signature in GPP leukocytes is supported by several lines of evidence.

To further investigate the relevance of these observations we built an interferon score by measuring the aggregate expression of 5 genes (*IFI6, IFIT3, IFITM3, OASL, PLSCR1*), which were up-regulated in the GPP dataset and annotated as Type-I IFN dependent in the interferome database (Rusinova et al., 2013). As expected, the score was elevated in GPP cases, compared to controls. A similar increase was observed in the publicly available PsV dataset (Figure 1 g). Importantly, we found that the interferon score documented in GPP and PsV significantly correlated with the up-regulation of IL-36 related genes ($P<0.01$) (Figure 1 h). Thus, we have shown that systemic Type-I IFN responses are abnormally active in psoriasis, which may be linked to increased IL-36 production.

The Type-I IFN signature is driven by gene up-regulation in neutrophils

The presence of heterogeneous cell populations in whole-blood can complicate the interpretation of transcription profiling experiments. We therefore sought to validate our results through an independent analysis of a single cell type. We focused our attention on neutrophils, as they play a critical role in systemic inflammation and can be activated by Type-I IFN (Zimmermann et al., 2016).

We obtained fresh blood samples from 8 GPP cases and 11 controls (Supplementary Table S1 a). Following neutrophil isolation and RNA-sequencing, we detected 200 up-regulated genes (Figure 2 a, Supplementary Table S2 b). The analysis of transcriptional networks identified *Type-I interferon response* as the most significantly enriched module (FDR<10^{-12}), followed by *innate antiviral response* and *antiviral interferon signature* (FDR<10^{-10}) (Figure 2 b). IPA also demonstrated a marked enrichment of pathways related to interferon signalling (FDR<10^{-11}) (Figure 2 c) and highlighted IRF7 and STAT1 as the most likely drivers of gene up-regulation (FDR<10^{-30}) (Figure 2 d, Supplementary Table S2 d). In keeping with these findings, interferon scores were elevated in GPP cases compared to controls ($P=0.02$) (Figure 2 e). These observations validate the results obtained in whole-blood and suggest that the Type-I IFN signature is driven at least in part, by gene up-regulation in neutrophils.

The Type-I IFN signature can be validated in extended PsV and GPP datasets

We next sought to validate the type I IFN signature through the analysis of further affected individuals. We examined neutrophils obtained from 17 GPP cases (including 8 newly recruited cases) and 16 PsV patients suffering from severe disease (average Psoriasis Area and Severity Index: 17.9). We also analysed two control groups including 9 individuals affected by CAPS and 26 healthy volunteers. Real-time PCR demonstrated that the interferon score was significantly increased in GPP and PsV cases compared to healthy controls ($P<0.005$). Conversely, and in keeping with the specificity of our observations, the scores of CAPS patients were within the normal range defined in unaffected individuals (Figure 3 a).

Of note, medical records showed that GPP patients with high IFN scores were more likely to experience systemic flares than those with low scores (88% vs 33%; $P=0.049$). Likewise, the prevalence of psoriatic arthritis was higher among PsV subjects with high IFN scores (67% vs 18%; $P=0.03$) (Figure 3 b).

Thus, the Type-I IFN signature detected by RNA-sequencing can be validated in independent PsV and GPP samples, where it is associated with extra-cutaneous morbidity.

The IL-36 receptor is expressed on the surface of plasmacytoid dendritic cells

We next hypothesised that IL-36 has a direct effect on Type-I IFN producing cells. To investigate this possibility, we systematically examined the surface expression of the IL-36 receptor (IL36R) in innate immune cells. In keeping with published findings (Foster et al., 2014), we found that IL36R was barely detectable on the surface of healthy neutrophils (Figure 4 a), suggesting that the effects of IL-36 on these cells are mediated by the activation of different immune population(s).

We also showed that $IL36R^+$ cell numbers were low among innate lymphoid cells (Figure 4 b) and in monocytes (Figure 4 c). Higher IL36R levels were observed in myeloid (mDC) and plasmacytoid dendritic cells (pDCs) (Figure 4 d, Supplementary Figure S2), with the largest percentage of $IL36R^+$ cells detected in the pDCs of GPP patients (Figure 4 e). Thus, we have shown that IL-36R is robustly

expressed in pDCs, which are the main producers of IFN-α (a member of the Type-I IFN family) in the immune system.

IL-36 potentiates IFN-α production in response to Toll-like receptor 9 stimulation

Based on the results obtained in the above experiments, we hypothesised that IL-36 potentiates Type-I IFN production by pDCs. To investigate this possibility, we pre-treated PBMCs obtained from healthy donors with IL-36 or vehicle. We then stimulated the cells with CpG-containing DNA (hence CpG), a TLR-9 ligand which induces IFN-α release by pDCs. Finally, we measured the up-regulation of the IFN signature genes as a readout of Type-I IFN production. While CpG increased the expression of most signature genes, its effect was more pronounced in cells that had been pre-incubated with IL-36 (P<0.05 for *IFIT3, OASL* and *PLSCR1*) (Figure 5 a). This observation was validated by direct measurements of IFN-α production, showing increased cytokine release following IL-36 pre-treatment (Figure 5 b). Finally, flow cytometry documented an increased proportion of $IFN\alpha^+$ pDCs among the cells that had been stimulated with IL-36 and CpG, compared to those that had been exposed to CpG alone (Figure 5 c). Thus, multiple experimental readouts support the notion that IL-36 up-regulates TLR-9 dependent IFN-α release.

IL-36 up-regulates *PLSCR1*, a known TLR-9 transporter

We next sought to define the mechanisms whereby IL-36 enhances cytokine production downstream of TLR-9. A closer inspection of the PBMC stimulation results showed that IL-36 treatment up-regulates *PLSCR1*, even in the absence of CpG. This is of interest, as the gene encodes phospholipid scramblase 1, a protein which regulates TLR-9 trafficking to the endosomal compartment (Talukder et al., 2012). To further explore the link between IL-36 and PLSCR1, we first validated our initial observation in additional donors (Figure 6 a). Next, we demonstrated that IL-36 treatment increases PLSCR1 protein levels in isolated pDCs, showing a direct effect of the cytokine on these cells (P<0.05) (Figure 6 b). Finally, we investigated the mechanism whereby IL-36 up-regulates *PLSCR1*. As expected for an IFN signature gene, an analysis of the *PLSCR1* promoter uncovered a STAT1 binding site. Given that IL-36 can signal through mitogen-activated protein kinases (MAPK) (Bassoy et al., 2018), and that there

have been reports of cross-talk between STAT1 and MAPK signalling (Zhang et al., 2004), we reasoned that the latter pathway was likely to be involved. Real-time PCR experiments confirmed this hypothesis, as the SB-203580 MAPK inhibitor abolished the effect of IL-36 on *PLSCR1* expression (Figure 6 c). Thus, we have demonstrated that IL-36 can act directly on pDCs, where it up-regulates PLSCR1, in a MAPK-dependent fashion.

DISCUSSION

While PsV has been historically described as a dermatological condition, the importance of extra-cutaneous co-morbidities is increasingly recognised (Armstrong et al., 2013). Of note, the prevalence of most co-morbid conditions increases with the severity and the duration of the disease (Burden and Kirby, 2016, Egeberg et al., 2017). There is therefore a dose-dependent association between cutaneous and extra-cutaneous inflammation, which suggests a shared systemic pathogenesis. The underlying pathways, however, remain poorly understood.

Here, we demonstrated that IL-36 signalling is enhanced in the leukocytes of PsV patients, where abnormal IL-36 activity correlates with Type-I IFN over-expression. While many of the genes that are induced by IL-36 are also up-regulated by IL-1, this set of shared targets does not include mediators of Type-I IFN production (Swindell et al., 2018). Accordingly, we found that IFN signature genes are not over-expressed in CAPS, a condition caused by excessive IL-1 signalling. Thus, IL-1 is unlikely to play a significant role in promoting Type-I IFN responses in psoriasis.

Several studies have found that Type-I IFN is a mediator of vascular inflammation, which promotes the recruitment of leukocytes to atherosclerotic plaques (Goossens et al., 2010, Niessner et al., 2007). Experiments carried out in animal models have also shown that TLR-9 dependent Type-I IFN production is a key driver of systemic autoimmunity (Di Domizio et al., 2012).

In keeping with these observations, signatures of excessive Type-I IFN activity have been documented in various diseases presenting with prominent systemic involvement. One notable example is systemic lupus erythematosus (SLE), a disorder associated with skin and joint inflammation, accelerated atherosclerosis and up-regulation of genes such as *IFI6* and *OASL* (El-Sherbiny et al., 2018). Of interest, three independent studies have reported that IL-36 serum levels correlate with disease activity in SLE

(Chu et al., 2015, Ismail et al., 2018, Mai et al., 2018), which further reinforces the link between IL-36 and Type-I IFN. Our work adds to these observations and provides mechanistic insights into the underlying pathways.

Our computational and experimental results implicate pDCs as the most likely mediators of IL-36 activity. First, we identified IRF7 as one of the most significant drivers of differential gene expression in GPP. Second, we demonstrated that IL-36R levels are highest in pDCs, especially among GPP patients. Of note, it has long been established that pDCs accumulate within psoriatic skin lesions, where they contribute to early disease processes alongside slanDC (Hansel et al., 2011, Nestle et al., 2005). It has also been reported that IL36R is abundantly expressed in various classes of skin-resident DC (Dietrich et al., 2016). Thus, it is tempting to speculate that IL-36 mediated pDC activation may also have a pathogenic role in skin.

Our results show that the effects of IL-36 on pDCs are mediated at least in part by PLSCR1 up-regulation. Interestingly, *PLSCR1* siRNA knockout inhibits Type I IFN production by human pDCs (Talukder et al., 2012), so it is reasonable to hypothesise that an increase in gene expression would have the opposite effect. While the PLSCR1 induction observed in our IL-36 stimulation experiments was modest (1.5-2.0 fold), it might be sufficient to activate a feed-forward loop whereby up-regulated PLSCR1 promotes the production of Type-I IFN, which in turn induces further *PLSCR1* transcription. In fact, self-amplifying loops are a key feature of Type-I IFN signalling, as they are required for robust antiviral responses (Hall and Rosen, 2010).

We cannot exclude the possibility that additional IL-36 responsive genes or cell types may also contribute to the up-regulation of Type-I IFN. However, we have found that IL-36 does not affect the expression of *TLR9* or that of key downstream genes (*IRF1*, *IRF3*, *IRF7*; data not shown). We have also observed that genes driving other antiviral pathways (*DDX58*/RIG-I, *IFIH1*/MDA5, *TMEM173*/STING) are not up-regulated in PsV or GPP whole-blood.

While our pDC stimulations were carried out with a synthetic TLR-9 agonist, the identity of the agents that cause IFN-α production in patients remains to be determined. In lesional skin, pDCs are activated by self-nucleic acids released by apoptotic keratinocytes and bound to the LL-37 antimicrobial peptide (Lande et al., 2007). Our transcriptomic data, however, suggests that this mechanism is unlikely to be

relevant at the systemic level. While *CAMP* (the gene encoding LL-37) was up-regulated in psoriatic skin, it was not over-expressed in GPP or PsV whole-blood. Moreover, there was no correlation between *CAMP* whole-blood expression and the up-regulation of Type-I IFN genes ($r<0.1$). Thus, the agents that activate the circulating pDC of psoriatic patients may be different from those that are present in skin.

In conclusion, we have identified an IL-36/TLR-9 axis which up-regulates systemic Type-I IFN production in psoriasis (Figure 6 d). In GPP patients, the effects of IL-36 signalling are amplified by inherited *IL36RN* mutations, a phenomenon which is likely to account for the severe nature of systemic flares. In PsV, the Th17-dependent up-regulation of IL-36 cytokines is associated with a less pronounced transcriptional signature and with signs of chronic systemic inflammation.

Given that IL-36 is down-regulated by IL-17 inhibitors such as secukinumab (Kolbinger et al., 2017), it is possible that treatment of psoriasis with IL-17 antagonists might also modulate Type-I IFN production. Of note, the effects of direct IL-36 inhibition are currently being investigated in clinical trials, with promising results obtained in a Phase I study (Bachelez, 2018). In this context, our work suggests that IL-36 antagonists have the potential to improve systemic Type I IFN up-regulation and extra-cutaneous manifestations of psoriasis.

METHODS

Human subjects

The study was performed according to the principles of the Declaration of Helsinki. Patients were ascertained at St John's Institute of Dermatology and Royal Free Hospital (London, UK), Glasgow Western Infirmary (Glasgow, UK), Salford Royal Foundation Trust (Manchester, UK) and Hospital Sultanah Aminah (Johor Bahru, Malaysia). The study was approved by the ethics committees of participating institutions and written informed consent was obtained from all participants.

Nine unrelated GPP patients and 7 healthy controls were recruited for whole-blood RNA-sequencing, while neutrophil RNA-sequencing was carried out in 8 GPP patients and 11 healthy controls. Five controls and six cases were common to both studies (Supplementary Table S1 a). For the validation of neutrophil RNA-sequencing results, fresh blood was obtained from 17 GPP, 26 control, 9 CAPS and 17 PsV individuals (Supplementary Table S3). All PsV patients suffered from moderate-to-severe

disease (Psoriasis Area Severity Index >10) and were recruited from the same centre (Severe psoriasis service, St John's Institute of Dermatology). Patients presenting with joint pain were referred to an expert rheumatologist, who diagnosed PsA, when applicable. The *IL36RN* gene was screened in all GPP cases and mutations were identified in 4 individuals (Supplementary Table S1 a).

RNA sequencing data analysis

The raw sequence data generated in house and that retrieved from public repositories (Supplementary Table S4) were processed with the same computational pipeline (described in supplementary methods), in order to standardise the data analysis process. Genes were considered up-regulated if the fold change exceeded 1.5 (FDR<0.05). When RNA-sequencing and microarray data were compared, the analysis focused on the 100 genes that were most significantly up-regulated in each sample, in order to account for the different sensitivity of the two platforms.

Genes up-regulated in GPP were used as input for pathway and upstream regulator enrichment analyses (IPA, Qiagen). STAT1- STAT3- and IRF7-centered networks were visualised with the igraph v1.0.1 R Package.

The transcriptional modules that were active in our datasets were selected from the library published by Li et al (Li et al., 2014). The enrichment_test function was then applied to the lists of up-regulated genes.

The interferon score was built using the five Type-I IFN dependent genes that were most up-regulated in GPP whole-blood (*PLSCR1, OALS, IFI6, IFIT3, IFITM3)*. As IL-36 dependent genes have not been systematically characterised in leukocytes, the IL-36 score was based on the analysis of five genes which were strongly induced by IL-36 in keratinocytes (Mahil et al., 2017) and robustly expressed in whole-blood (*IL1B, PI3, VNN2, TNFAIP6, SERPINB1)*. Both scores were derived by normalising RPKM values to a calibrator sample and then computing the median expression of the five genes.

Statistics

Differences between patient and control cytokine scores were assessed using an unpaired t-test or one-way ANOVA, as appropriate. To account for donor variability in cytokine responses, IL-36/CpG

stimulations were analysed with non-parametric methods (Wilcoxon signed-rank test for comparisons between two groups and Friedman's test for comparison between three groups), as these do not assume equal variance among samples. The correlation between cytokine scores was calculated using Spearman method. The significance of overlaps observed in Venn diagrams was computed with a hyper-geometric test and confirmed by bootstrap analysis. Fisher's exact test was used to compare the clinical features of patients with high and low IFN scores.

CREDIT STATEMENT: MC: data curation, formal analysis, investigation, visualization; MV: formal analysis, investigation, validation, visualization; MR: investigation; SKM, SEC, ADB, HSY, IMC, HJL: resources; GL: supervision; CHS: resources, writing-review & editing; FDC: supervision, writing-review & editing; JNB: funding acquisition, resources, writing-review & editing; FC: conceptualization, funding acquisition, project administration, supervision, writing-original draft.

ACKNOWLEDGEMENTS

We are grateful to Paola Di Meglio for her comments and technical advice. We acknowledge support from the Department of Health via the NIHR BioResource Clinical Research Facility and comprehensive Biomedical Research Centre award to Guy's and St Thomas' NHS Foundation Trust in partnership with King's College London and King's College Hospital NHS Foundation Trust (guysbrc-2012-1). The APRICOT clinical trial is funded by the Efficacy and Mechanism Evaluation Programme, an MRC and NIHR partnership (grant EME 13/50/17 to CHS, FC and JNB). MC is supported by the Psoriasis Association, MV by the UK Medical Research Council and SKM by a NIHR Clinical Lectureship.

The views expressed in this publication are those of the author(s) and not necessarily those of the MRC, NHS, NIHR or the Department of Health.

CONFLICT OF INTERESTS

The authors have received funding or fees from Abbvie and Novartis (CHS, HSY, JNB); Almirall, Jansen, Leo Pharma and UCB (HSY, JNB); AnaptysBio (FCa); Aspire Pharma, Johnson and Johnson,

MEDA Pharmaceuticals (HSY); Boehringer Ingelheim (FCa, JNB, ADB); Bristol Myers Squibb, Celegene, Ely Lily, Pfizer, Samsung, Sienna, Sun Pharma (JNB); GSK, Roche, Regeneron, Sanofi (CHS).

DATA AVAILABILITY

The RNA-sequencing data generated in this study are available through the Gene Expression Omnibus (identifier: GSE123787).

REFERENCES

Armstrong EJ, Harskamp CT, Armstrong AW. Psoriasis and major adverse cardiovascular events: a systematic review and meta-analysis of observational studies. Journal of the American Heart Association 2013;2(2):e000062.

Bachelez H. Efficacy and safety of BI 655130, an anti-interleukin-36 receptor antibody, in patients with acute generalised pustular psoriasis. 27th European Academy of Dermatology and Venereology (EADV) Congress Paris2018.

Bassoy EY, Towne JE, Gabay C. Regulation and function of interleukin-36 cytokines. Immunological reviews 2018;281(1):169-78.

Burden AD, Kirby B. Psoriasis and related disorders. In: Griffiths CEM, Barker JN, Bleiker T, Chalmers RJ, Creamer D, editors. Rook's Textbook of Dermatology. Chichester: Wiley-Blackwell; 2016.

Chu M, Wong CK, Cai Z, Dong J, Jiao D, Kam NW, et al. Elevated Expression and Pro-Inflammatory Activity of IL-36 in Patients with Systemic Lupus Erythematosus. Molecules 2015;20(10):19588-604.

Davidovici BB, Sattar N, Prinz J, Puig L, Emery P, Barker JN, et al. Psoriasis and systemic inflammatory diseases: potential mechanistic links between skin disease and co-morbid conditions. J Invest Dermatol 2010;130(7):1785-96.

Di Domizio J, Dorta-Estremera S, Gagea M, Ganguly D, Meller S, Li P, et al. Nucleic acid-containing amyloid fibrils potently induce type I interferon and stimulate systemic autoimmunity. Proc Natl Acad Sci U S A 2012;109(36):14550-5.

Dietrich D, Martin P, Flacher V, Sun Y, Jarrossay D, Brembilla N, et al. Interleukin-36 potently stimulates human M2 macrophages, Langerhans cells and keratinocytes to produce pro-inflammatory cytokines. Cytokine 2016;84:88-98.

Egeberg A, Skov L, Joshi AA, Mallbris L, Gislason GH, Wu JJ, et al. The relationship between duration of psoriasis, vascular inflammation, and cardiovascular events. J Am Acad Dermatol 2017;77(4):650-6 e3.

El-Sherbiny YM, Psarras A, Md Yusof MY, Hensor EMA, Tooze R, Doody G, et al. A novel two-score system for interferon status segregates autoimmune diseases and correlates with clinical features. Scientific reports 2018;8(1):5793.

Fang N, Jiang M, Fan Y. Association Between Psoriasis and Subclinical Atherosclerosis: A Meta-Analysis. Medicine 2016;95(20):e3576.

Foster AM, Baliwag J, Chen CS, Guzman AM, Stoll SW, Gudjonsson JE, et al. IL-36 promotes myeloid cell infiltration, activation, and inflammatory activity in skin. J Immunol 2014;192(12):6053-61.

Goossens P, Gijbels MJ, Zernecke A, Eijgelaar W, Vergouwe MN, van der Made I, et al. Myeloid type I interferon signaling promotes atherosclerosis by stimulating macrophage recruitment to lesions. Cell Metab 2010;12(2):142-53.

Hall JC, Rosen A. Type I interferons: crucial participants in disease amplification in autoimmunity. Nat Rev Rheumatol 2010;6(1):40-9.

Hansel A, Gunther C, Ingwersen J, Starke J, Schmitz M, Bachmann M, et al. Human slan (6-sulfo LacNAc) dendritic cells are inflammatory dermal dendritic cells in psoriasis and drive strong TH17/TH1 T-cell responses. The Journal of allergy and clinical immunology 2011;127(3):787-94 e1-9.

Honda K, Yanai H, Negishi H, Asagiri M, Sato M, Mizutani T, et al. IRF-7 is the master regulator of type-I interferon-dependent immune responses. Nature 2005;434(7034):772-7.

Ismail SM, Abd EMK, Mohamed MS. Serum Levels of Pentraxin3 and Interlukin36 in Patients with Systemic Lupus and their Relation to Disease Activity. The Egyptian journal of immunology 2018;25(1):81-91.

Johnston A, Xing X, Wolterink L, Barnes DH, Yin Z, Reingold L, et al. IL-1 and IL-36 are dominant cytokines in generalized pustular psoriasis. The Journal of allergy and clinical immunology 2016.

Kolbinger F, Loesche C, Valentin MA, Jiang X, Cheng Y, Jarvis P, et al. beta-Defensin 2 is a responsive biomarker of IL-17A-driven skin pathology in patients with psoriasis. The Journal of allergy and clinical immunology 2017;139(3):923-32 e8.

Lande R, Gregorio J, Facchinetti V, Chatterjee B, Wang YH, Homey B, et al. Plasmacytoid dendritic cells sense self-DNA coupled with antimicrobial peptide. Nature 2007;449(7162):564-9.

Li S, Rouphael N, Duraisingham S, Romero-Steiner S, Presnell S, Davis C, et al. Molecular signatures of antibody responses derived from a systems biology study of five human vaccines. Nat Immunol 2014;15(2):195-204.

Liu Y, Ramot Y, Torrelo A, Paller AS, Si N, Babay S, et al. Mutations in proteasome subunit beta type 8 cause chronic atypical neutrophilic dermatosis with lipodystrophy and elevated temperature with evidence of genetic and phenotypic heterogeneity. Arthritis Rheum 2012;64(3):895-907.

Mahil SK, Catapano M, Di Meglio P, Dand N, Ahlfors H, Carr IM, et al. An analysis of IL-36 signature genes and individuals with IL1RL2 knockout mutations validates IL-36 as a psoriasis therapeutic target Science translational medicine 2017;9:eaan2514.

Mai SZ, Li CJ, Xie XY, Xiong H, Xu M, Zeng FQ, et al. Increased serum IL-36alpha and IL-36gamma levels in patients with systemic lupus erythematosus: Association with disease activity and arthritis. International immunopharmacology 2018;58:103-8.

Marrakchi S, Guigue P, Renshaw BR, Puel A, Pei XY, Fraitag S, et al. Interleukin-36-receptor antagonist deficiency and generalized pustular psoriasis. N Engl J Med 2011;365(7):620-8.

Nestle FO, Conrad C, Tun-Kyi A, Homey B, Gombert M, Boyman O, et al. Plasmacytoid predendritic cells initiate psoriasis through interferon-alpha production. The Journal of experimental medicine 2005;202(1):135-43.

Niessner A, Shin MS, Pryshchep O, Goronzy JJ, Chaikof EL, Weyand CM. Synergistic proinflammatory effects of the antiviral cytokine interferon-alpha and Toll-like receptor 4 ligands in the atherosclerotic plaque. Circulation 2007;116(18):2043-52.

Onoufriadis A, Simpson MA, Pink AE, Di Meglio P, Smith CH, Pullabhatla V, et al. Mutations in IL36RN/IL1F5 are associated with the severe episodic inflammatory skin disease known as generalized pustular psoriasis. Am J Hum Genet 2011;89(3):432-7.

Quaranta M, Knapp B, Garzorz N, Mattii M, Pullabhatla V, Pennino D, et al. Intraindividual genome expression analysis reveals a specific molecular signature of psoriasis and eczema. Science translational medicine 2014;6(244):244ra90.

Reich K. The concept of psoriasis as a systemic inflammation: implications for disease management. Journal of the European Academy of Dermatology and Venereology : JEADV 2012;26 Suppl 2:3-11.

Rodero MP, Tesser A, Bartok E, Rice GI, Della Mina E, Depp M, et al. Type I interferon-mediated autoinflammation due to DNase II deficiency. Nature communications 2017;8(1):2176.

Rusinova I, Forster S, Yu S, Kannan A, Masse M, Cumming H, et al. Interferome v2.0: an updated database of annotated interferon-regulated genes. Nucleic acids research 2013;41(Database issue):D1040-6.

Shah K, Paris M, Mellars L, Changolkar A, Mease PJ. Real-world burden of comorbidities in US patients with psoriatic arthritis. RMD open 2017;3(2):e000588.

Swindell WR, Beamer MA, Sarkar MK, Loftus S, Fullmer J, Xing X, et al. RNA-Seq Analysis of IL-1B and IL-36 Responses in Epidermal Keratinocytes Identifies a Shared MyD88-Dependent Gene Signature. Frontiers in immunology 2018;9:80.

Swindell WR, Remmer HA, Sarkar MK, Xing X, Barnes DH, Wolterink L, et al. Proteogenomic analysis of psoriasis reveals discordant and concordant changes in mRNA and protein abundance. Genome medicine 2015;7(1):86.

Talukder AH, Bao M, Kim TW, Facchinetti V, Hanabuchi S, Bover L, et al. Phospholipid scramblase 1 regulates Toll-like receptor 9-mediated type I interferon production in plasmacytoid dendritic cells. Cell research 2012;22(7):1129-39.

Tortola L, Rosenwald E, Abel B, Blumberg H, Schafer M, Coyle AJ, et al. Psoriasiform dermatitis is driven by IL-36-mediated DC-keratinocyte crosstalk. The Journal of clinical investigation 2012;122(11):3965-76.

Wang CQF, Suarez-Farinas M, Nograles KE, Mimoso CA, Shrom D, Dow ER, et al. IL-17 induces inflammation-associated gene products in blood monocytes, and treatment with ixekizumab reduces their expression in psoriasis patient blood. J Invest Dermatol 2014;134(12):2990-3.

Zhang Y, Cho YY, Petersen BL, Zhu F, Dong Z. Evidence of STAT1 phosphorylation modulated by MAPKs, MEK1 and MSK1. Carcinogenesis 2004;25(7):1165-75.

Zimmermann M, Arruda-Silva F, Bianchetto-Aguilera F, Finotti G, Calzetti F, Scapini P, et al. IFNalpha enhances the production of IL-6 by human neutrophils activated via TLR8. Scientific reports 2016;6:19674.

FIGURE LEGENDS

Figure 1. Transcription profiling of GPP and PsV whole-blood uncovers a Type-I IFN signature that correlates with IL-36 activity. (**a**) Identification of genes that are differentially expressed in GPP. Horizontal and vertical lines represent significance and fold change thresholds, respectively. The genes underlying the IFN score are in red. (**b**) Higher expression of IL-36 dependent genes in whole-blood of GPP and PsV patients, compared to controls (CTR). (**c**) Transcriptional modules enriched among genes up-regulated in GPP. The FDR for each module is reported, with the underlying up-regulated genes shown as grey cells. (**d**) Enriched pathways detected among genes over-expressed in GPP. (**e**) Key transcriptional factors driving gene over-expression in GPP. (**f**) Overlap between the genes that are up-regulated in GPP and IFNpathies. (**g**) Elevated IFN score in whole-blood samples of GPP and PsV patients, compared to controls (CTR). (**h**) IL-36 and IFN scores are significantly correlated, in both GPP and PsV patients. Dashed regression lines are plotted with 95% confidence intervals (grey areas). The data in (b) and (g) are presented as mean +/- SD; **P*<0.05, ***P*<0.01 (unpaired t-test).

Figure 2. Transcription profiling of GPP neutrophils confirms the presence of a Type-I IFN signature (**a**) Identification of genes that are differentially expressed in GPP. Horizontal and vertical lines represent significance and fold change thresholds, respectively. (**b**) Transcriptional modules enriched among the genes that are up-regulated in GPP. The FDR for each module is reported, with the underlying up-regulated genes shown as grey cells. (**c**) Enriched pathways detected among the genes that are up-regulated in GPP. IFN-related pathways are highlighted in bold (**d**) Upstream regulator analysis showing that IRF7 and STAT1 drive the up-regulation of numerous genes that are over-expressed in GPP. (**e**) Elevated IFN score in the neutrophils of GPP patients, compared to controls. The data are presented as mean +/- SD; **P*<0.05 (unpaired t-test).

Figure 3. Validation of the Type-I IFN signature in extended datasets (**a**) Elevated IFN score in the neutrophils of GPP and PsV patients, compared to healthy individuals. CAPS cases were analysed as negative controls. The data are presented as mean +/- standard deviation; ***P*<0.01 and ****P*<0.001 (one-way ANOVA followed by Dunnett's post-test). (b) Left: systemic flares are more prevalent in

GPP patients with high interferon scores (n=8) compared to those with low interferon scores (n=9). Right: psoriatic arthritis (PsA) is more prevalent in PsV patients with high interferon scores (n=6) compared to those with low interferon scores (n=11). In both groups, the cut-off between high and low scores was defined as the median +2SD of the values observed in healthy controls. **P*<0.05 (Fisher's exact test).

Figure 4. The IL-36 receptor is preferentially expressed by pDCs. (**a-e**) Representative flow cytometry plots showing IL36R surface expression, compared to fluorescence minus one (FMO) controls. (**a**) neutrophils (gated as $CD14^+$, $CD15^+$, $CD16^+$ cells); (**b**) innate lymphoid cells ($lineage^-$ ($CD3^-$, $CD4^-$, $CD19^-$, $CD20^-$, $CD56^-$), $CD127^+$); (**c**) monocytes ($CD3^-$, $CD20^-$, $CD19^-$, $CD56^-$) separated into classical ($CD16^-$, $CD14^{high}$), intermediate ($CD16^+$, $CD14^+$) and pro-inflammatory ($CD16^{high}$, $CD14^-$) populations; (**d**) pDCs ($lineage^-$, $HLADR^+$, $CD123^+$, $CD11c^-$) and mDCs ($lineage^-$, $HLADR^+$, $CD123^-$, $CD11c^+$). (**e**) Histogram showing the percentage $IL36R^+$ cells in each leukocyte population. Data were obtained in at least 3 GPP cases and 3 sex-matched controls. Results are presented as mean +/- SEM. No significant differences were observed between GPP cases and healthy donors.

Figure 5. IL-36 enhances the production of IFN-α downstream of Toll-like receptor 9. (**a**) PBMCs were stimulated with CpG for 6h, in the presence or absence of IL-36 pre-treatment (6h). The expression of interferon signature genes was measured by real-time PCR. Data represent the mean +/- SEM of results obtained in three independent donors, each stimulated in triplicate. (**b**) Following PBMC stimulation, IFN-α production was measured by ELISA. Data represent the mean +/- SEM of results obtained in two independent donors, each stimulated in triplicate. (**c**) Following PBMC stimulation, the percentage of $IFN\alpha^+$ pDCs was determined by flow cytometry. A representative set of plots is shown (left), together with the data obtained in 3 independent healthy donors (right). **P*<0.05; ***P*<0.01 (Friedman's test, with Dunn's post-test).

Figure 6. IL-36 up-regulates PLSCR1 (**a**) Following treatment of PBMCs with IL-36, *PLSCR1* expression was measured by real-time PCR. (**b**) Following IL-36 treatment of pDCs, PLSCR1 mean fluorescence intensity (MFI) was measured by flow-cytometry, in gated PSLCR1^{+} pDCs. A representative histogram is shown on the left. (**c**) Following pre-treatment with SB203580 (MAPKi), PBMCs where stimulated with IL-36. *PLSCR1* expression was then determined by real-time PCR. (**d**) Proposed pathogenic model. Interleukin-36 produced by mDC up-regulates PLSCR1 in pDCs, potentiating TLR-9 dependent IFN-α release. IFN-α induces further *PLSCR1* transcription, thus propagating an inflammatory feed-forward loop. All data are shown as mean +/- SEM of results obtained in at least 3 donors, each stimulated in triplicate. **P*<0.05 (Wilcoxon signed-rank test (a, b) and Friedman's test with Dunn's post-test (c))

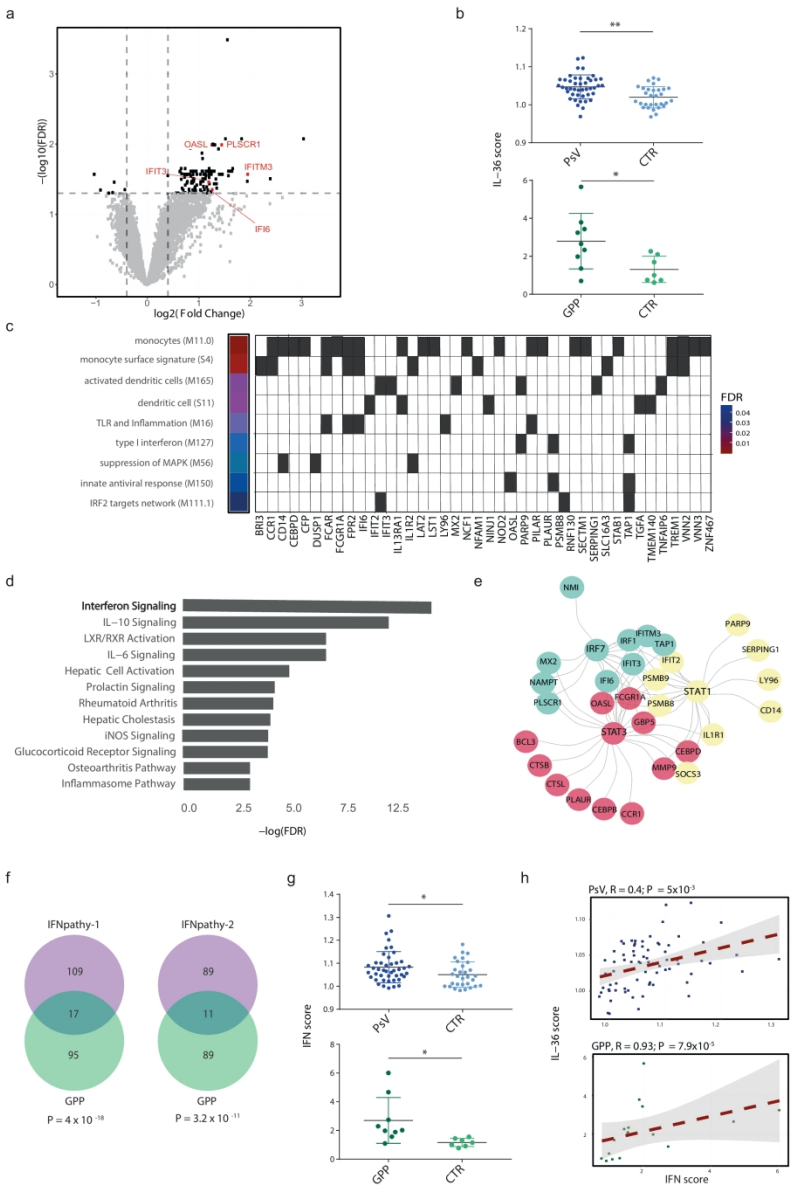

Figure 1

200x297mm (300 x 300 DPI)

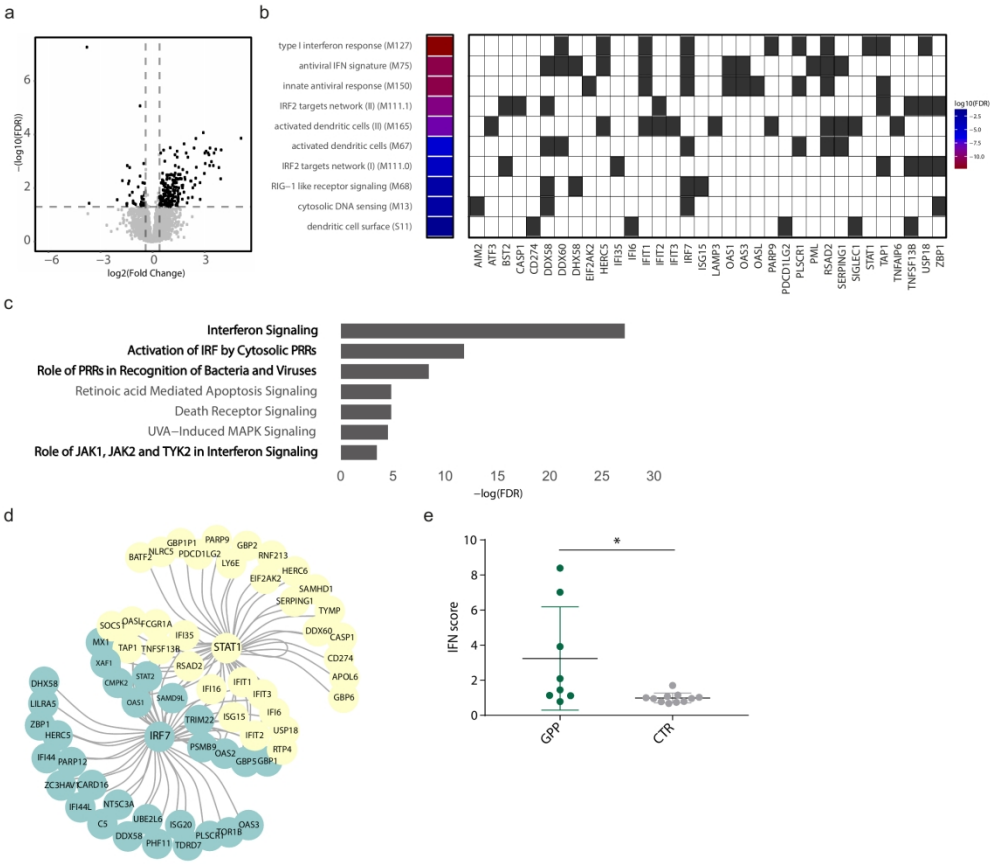

Figure 2

209x185mm (300 x 300 DPI)

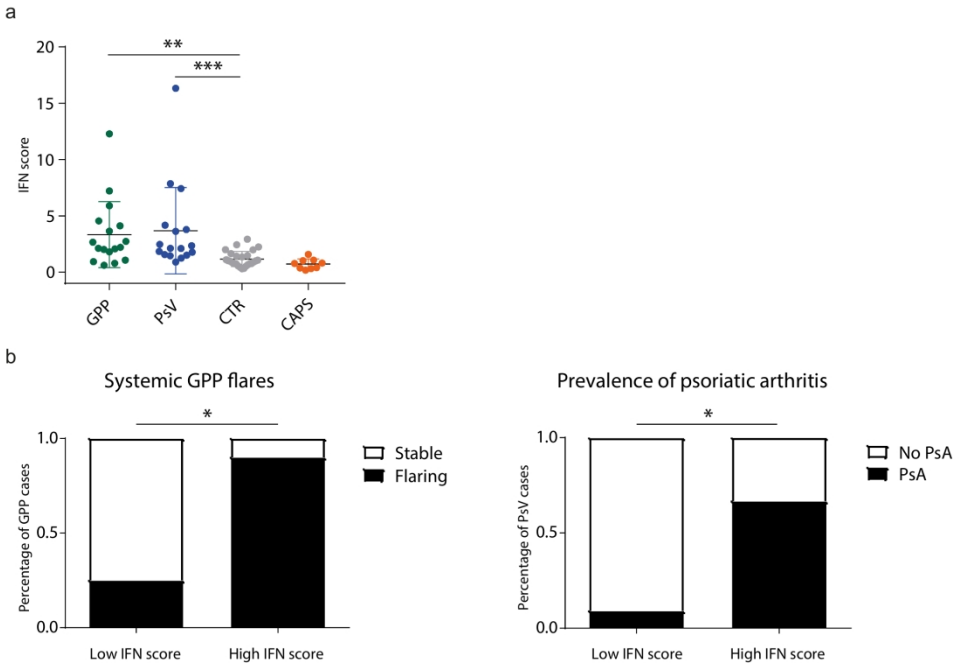

Figure 3

192x133mm (300 x 300 DPI)

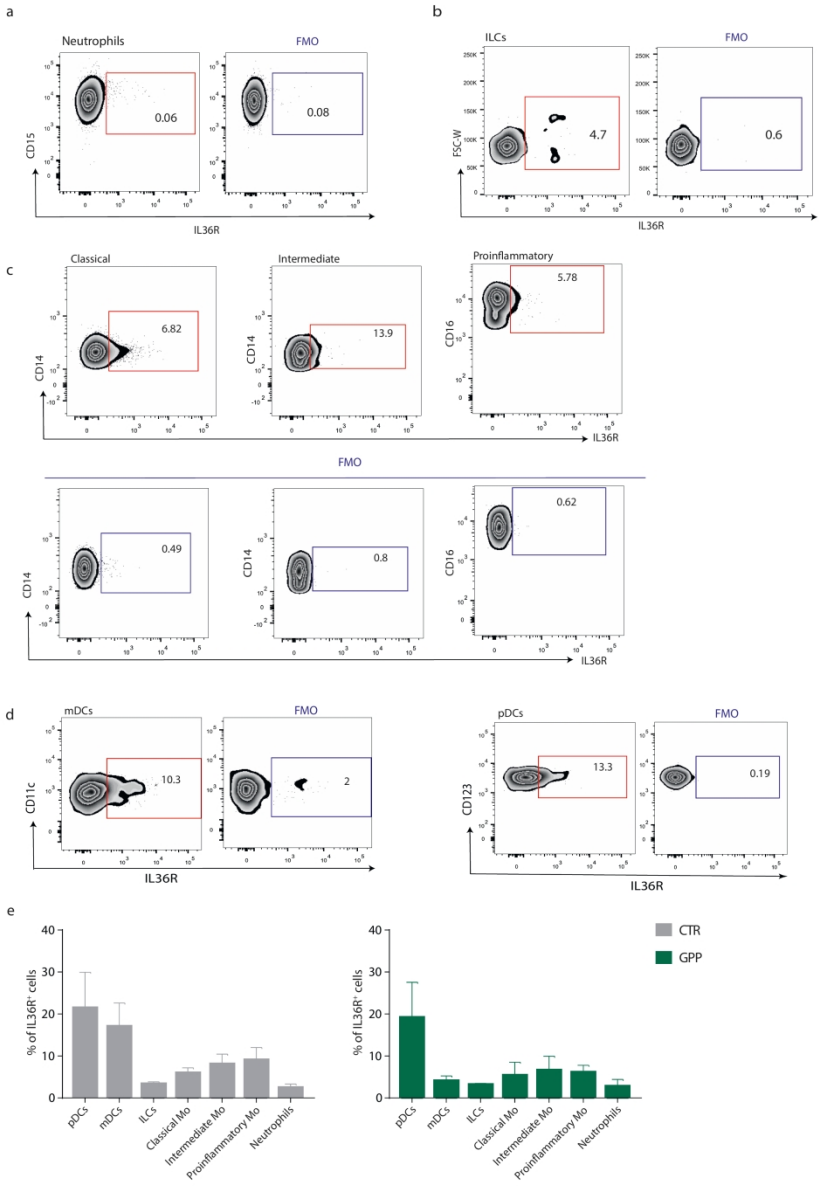

Figure 4

209x297mm (300 x 300 DPI)

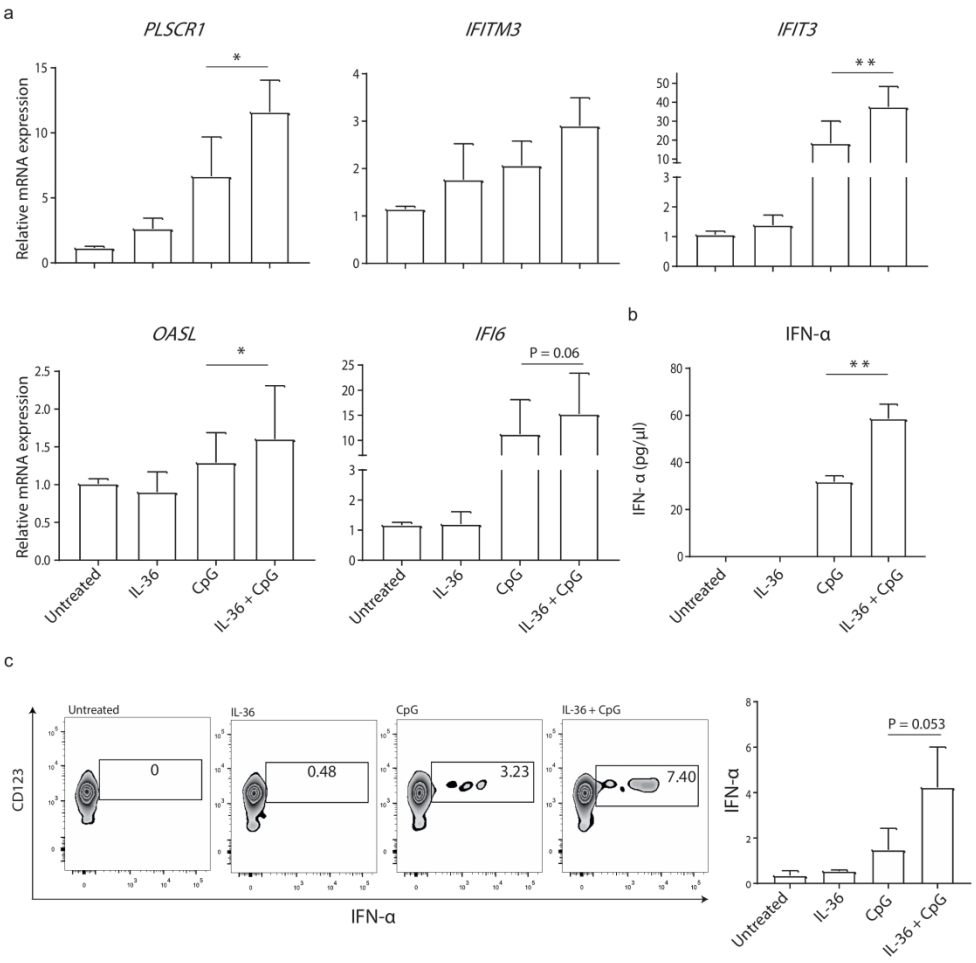

Figure 5

209x207mm (300 x 300 DPI)

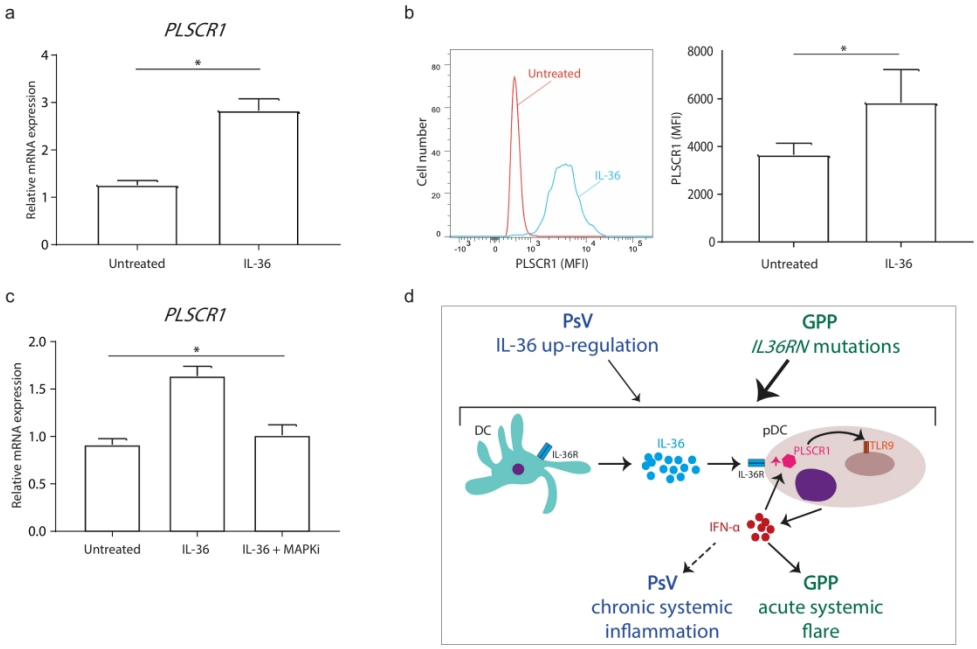

Figure 6

209x143mm (300 x 300 DPI)